Title
The role of tissue inhibitor of metalloproteinases-1 in epithelial carcinogenesis

Author
Rhee, Jin-Sae,

Publication Date
2003

Peer reviewed|Thesis/dissertation

The Role of Tissue Inhibitor of Metalloproteinases-1
in Epithelial Carcinogenesis

by

Jin-Sae Rhee

DISSERTATION

Submitted in partial satisfaction of the requirements for the degree of

DOCTOR OF PHILOSOPHY

in

Biomedical Sciences

in the

GRADUATE DIVISION

of the

UNIVERSITY OF CALIFORNIA, SAN FRANCISCO

Ap

Date University Librarian

Degree Conferred:.....

Dedication

To my family, in appreciation of their unconditional support.

Preface

Lisa M. Coussens, my mentor, by far deserves the greatest credit for this work: none of this would have been even remotely possible if not for her outstanding guidance, thoughtful wisdom, and especially her patience.

I am also grateful to the members, current and past, of the Coussens lab, for all of their experimental and personal help. The members of my thesis committee, Zena Werb and Kevin Shannon, have been extremely generous with their time and attention.

Finally, I am indebted to the people of the University of California, San Francisco, Medical Scientist Training Program, especially David Sretavan, Jana Toutolmin, and Catherine Norton for their help.

The Role of Tissue Inhibitor of Metalloproteinases-1

in Epithelial Carcinogenesis

Cancers are heterogeneous cellular networks that can be characterized by certain neoplastic hallmarks, including enhanced cellular proliferation, evasion of apoptosis, sustained angiogenesis, ectopic growth capacity and metastatic potential. Many of these neoplastic processes are regulated in part by a family of multifunctional proteins called the *T*issue *I*nhibitors of *M*etallo*P*roteinases (TIMPs). Originally characterized for their ability to inhibit the matrix metalloproteinase (MMP) family of enzymes, TIMPs were initially hypothesized to play a negative role in carcinogenesis based upon their ability to inhibit MMP activities believed to be necessary for the late-stage processes, e.g., invasion, during neoplastic progression. The realization that TIMPs, especially TIMP-1, are multifunctional molecules and can also induce cell proliferation as well as protect cells from apoptotic cell death led to a re-examinatiuon of the role of TIMP-1 during cancer developement. Thus, to determine the functional significance of TIMP-1 during epithelial carcinogenesis, we have used the K14-HPV16 transgenic mouse model of de novo carcinogenesis in the skin. In the studies reported here, we demonstrate that expression of TIMP-1 is incrementally increased throughout neoplastic progression and reaches maximum levels in the carcinoma stage. Furthermore, transgenic expression of TIMP-1 results in an increase in epidermal carcinomas, that can be correlated with earlier keratinocyte hyperproliferation and accelerated onset of keratinocyte aneuploidy. Loss of endogenous TIMP-1, however, does not alter the characteristics of neoplastic progression in K14-HPV16 mice, potentially due to functional redundancy resulting from expression

Table of Contents

List of Tables

List of Figures

List of Figures, continued

Chapter 1

Tissue Inhibitors of Metalloproteinases in Cancer

PROLOGUE

This chapter provides an introduction to the biological role of tissue inhibitors of metalloproteinases (TIMPs) in the context of cancer development. It also reviews the literature on the functional significance of matrix metalloproteinases and the development of synthetic inhibitors of MMP activity designed as anti-cancer therapeutics. Currently, components of this chapter are being prepared for submission as an invited review manuscript for the journal *Advances in Cancer Research.*

Abstract

*T*issue *I*nhibitors of *M*etallo*P*roteinases (TIMPs) are a family of multifunctional proteins originally characterized for their inhibitory activity against matrix metalloproteinases (MMPs) [1]. More recently, it has been appreciated that TIMPs possess other bioactivities in addition to MMP inhibition, including regulation of proliferation, apoptosis, angiogenesis and inflammation. Historically, TIMPs were believed to exert protective effects against cancer due to their ability to inhibit MMP activity; however, more recent studies including clinical trials with synthetic MMP inhibitors and examination of experimental models of de novo tumorigenesis have broadened our understanding into the diverse roles of TIMPs and MMPs as regulators of the neoplastic phenotype. The combined implication of these studies is that TIMPs and MMPs play multiple roles during the onset, development and progression of neoplastic cells that are concentration-, location- and context-dependent.

Introduction

Cancers, independent of type, exhibit certain hallmark characteristics, such as enhanced cellular proliferation, sustained angiogenesis, ability to evade cell death programs and ectopic tissue growth capacity [2]. What has become appreciated recently is that these characteristic neoplastic processes are regulated, not only by genetic alterations intrinsic to neoplastic cells themselves, but also by interactions of neoplastic cells with the dynamic extracellular matrix (ECM) and surrounding stromal cells. Many of these interactions are believed to be regulated, at least in part, by the actions of several types of secreted and/or cell surface proteases of several classes, e.g., serine, cysteine and matrix metalloproteinases (MMPs).

MMPs represent a diverse family of approximately 20 zinc-dependent endopeptidases, originally identified for their ability to cleave structural components of the ECM [3]. The structural and functional (*in vitro*) diversity amongst MMP family members suggested that their activities would include more than merely clearing barriers imposed by the ECM. Hence, more thorough investigation into the substrate repertoire of MMPs has expanded their known bioactivities to include liberation of ECM-sequestered growth factors [4], activation and inactivation of inflammatory chemoattractants [5] and ligands regulating apoptosis [6], as well as activation and inactivation of ligand-binding proteins modulating proliferation of a wide variety of cell types [7].

Involvement in degradative processes that facilitated the ability of malignant cells to cross ectopic tissue boundaries, invade ECM and metastasize to distant tissue sites prompted examination of the role of MMPs in the context of human cancer development [8]. Retrospective clinical studies demonstrated that MMP mRNA levels were elevated in

many types of cancers, and often could be associated with more advanced disease and shorter survival [9,10]; thus, interest in targeting the actions of MMPs as potential strategies for anti-cancer therapy expanded investigation into the biological mechanisms regulating MMP function [11].

TIMPs: Structure and Function

Tissue inhibitors of metalloproteinases (TIMPs) are a family of four secreted proteins ranging in size from 20 to 34 kDa that were named in order of their discovery [12]. TIMP-1 was originally identified (in rabbit bone) as a collagenase inhibitor also possessing activity against other type of metalloproteinases (MPs) [13]. The cDNA encoding TIMP-1 was cloned from human fibroblasts and revealed sequence encoding a secreted protein of 184 amino acids (Fig 1) [14]. TIMP-2 was later identified as a protein that copurified with MMP-2/gelatinase A that shared 40% sequence identity with TIMP-1 [15]. Identification and cloning of TIMP-3, from a human breast cancer cDNA library, revealed 30% identity with TIMP-1 [16]. TIMP-4 was found by molecular cloning from a human heart cDNA library and showed a 37% sequence identity with TIMP-1 [17]. Comparison of TIMP amino acid sequences revealed sites of conservation across the TIMP family, including twelve cysteine residues dispersed throughout their structures (Fig 1) suggesting perhaps functional significance of these residues for MMP inhibitory activity.

Structural analysis of TIMPs, first by multidimensional nuclear magnetic resonance (NMR) [18] and then by X-ray crystallography [19,20], revealed a two-domain protein structure, where each domain was stabilized by three disulfide linkages, formed

from the twelve cysteine residues. Based on functional studies, it was suggested that the N-terminal domain mediated MMP inhibition [21], a finding that was verified by X-ray crystallography of TIMP-1 in complex with MMP-3/stromelysin-1 and revealed residues Cys1-Thr2-Cys3-Val4 of TIMP-1 as those occupying the active site of MMP-3 analogous to P1-P1'-P2'-P3' interaction with a substrate [19]. Further sequence analysis has revealed that the N-terminal domain of TIMP-1 is homologous to the Netrin (NTR) module, a structure shared by the C-terminal domains of netrins, frizzled-related proteins and type I procollagen C-proteinase enhancer (PCPE) proteins [22], and also to the OB-fold module, a beta barrel Greek key motif found in oligonucleotide and oligosaccharide-binding proteins [23]. Furthermore, structural similarities for the TIMP N-terminal domain have been verified by NMR studies using the NTR domain of type I PCPE proteins [24]. Mutation analysis and removal of the TIMP-1 C-terminal domain was found to reduce the inhibitory activity of TIMP-1 against MMP-3, raising the K_i from 0.2 to 1.5 nM [25], suggesting that the C-terminal domain was involved in stabilizing MMP-TIMP interactions. Other structural studies demonstrated binding interaction of TIMP C-terminal domains to the C-terminal domains of MMPs [26] and to the ECM in the case of TIMP-3 [27].

Functional characterization studies of TIMP family members, that historically focused on TIMP-1, suggested that regulation of TIMP bioactivity occurred at both the gene transcription level as well as the post-translational level via specific and targeted degradation. It was determined that transcription of TIMP-1 was stimulated by various mitogens, including serum, phorbol esters, cytokines, growth factors and viruses [28].

Specifically, signaling molecules such as transforming growth factor beta (TGFβ), interleukin-1 (IL-1), interleukin-6 (IL-6), retinoic acid, tumor-necrosis-factor-alpha (TNF-α), epidermal growth factor (EGF) and glucocorticoids were all found to induce TIMP mRNA expression in a variety of cell types [29]. Consistent with this diverse spectrum of mitogenic regulators, TIMP-1 was found to be expressed in a variety of cell types, e.g. keratinocytes [30,31], fibroblasts [14], inflammatory cells [32,33] and to be widely distributed throughout vertebrate and reptilian anatomy, e.g. plasma, bone, skin, ovary, heart [11,34]. Studies examining post-translational regulation of mature TIMP-1 revealed that the protein could be specifically degraded by serine proteinases secreted from inflammatory cells, i.e. mast-cell chymase [35] and neutrophil elastase [36].

Biological Activities of TIMP-1

TIMPs and proliferation: Studies investigating the biological role of TIMPs suggested that they were multifunctional proteins with biological activities extending beyond MMP inhibition [1]. The ability of TIMP-1 to induce cellular proliferation *in vitro* was first realized with the discovery that its amino acid sequence was identical to that which had been previously described for erythroid-potentiating-activator (EPA) [37], a mitogen for erythroid cells. Subsequent studies have revealed that TIMP-1 exerts mitogenic activity toward a wide range of cell types in culture [38], including epidermal keratinocytes [39]. Mutational analysis demonstrated that mutations abrogating the MMP inhibitory activity of TIMP-1 preserved its ability to regulate proliferation, suggesting that its mitogenic properties were mediated by a mechanism distinct from MMP inhibition [40]. In order to

identify mechanisms for MMP-independent induction of proliferation, other studies revealed direct interaction of TIMP-1 with a cell-surface receptor [41]. Binding of TIMP-1 to this putative cell surface receptor triggers internalization of TIMP-1 and subsequent translocation to the nucleus during S-phase [42,43], the functional significance of which is presently unclear.

The search for additional non-MMP-inhibitory activities of TIMP-1 revealed that TIMP-1 also regulated apoptosis [44], angiogenesis [45,46], inflammation [47-49], differentiation [50] and cellular morphology [51]. Regarding apoptosis, TIMP-1 was shown to play a protective role independent of MMP inhibition [44]. These studies involved generating reduced and alkylated forms of TIMP-1 that had lost their ability to inhibit MMP activity but were still able to protect lymphoma cells from a variety of apoptotic signals [44].

TIMPs and angiogenesis: The known biological activity of several MMPs has recently been expanded to include regulating activation and organization of angiogenic vasculature during neoplastic progression [4,52,53]. As such, TIMP-1 has also been studied to examine if it exerts any biological role in regulating various parameters of angiogenesis and/or new vessel formation [45,46]. These studies have revealed that, depending on the context, TIMP-1 exerts either positive or negative effects on the proliferation and migration of capillary-associated cells. Based upon this range of effects for TIMP-1 on angiogenesis, *in vitro* assays with TIMP-1 protein sought to determine if this process was mediated by non-MMP-inhibitory mechanisms, as previously revealed

for proliferation and apoptosis [51]. These *in vitro* studies identified a 66 kDa aggregate form of TIMP-1 lacking MMP inhibitory activity retaining the ability to inhibit angiogenesis [51]. The implication of these studies supports a model of MMP-independent regulation of angiogenesis by TIMP-1.

TIMPs and Cancer

Cellular invasion is a hallmark of developing cancers [2]. Since MMPs were historically believed to be key mediators of cell invasion, many groups investigated the possibility that TIMP-1 might therefore inhibit neoplastic-associated invasive processes. Utilizing xenograft assays, non-tumorigenic Swiss 3T3 cells were transfected with antisense TIMP-1 cDNA and injected into nude mice [54]. Loss of TIMP-1 expression in these 3T3 cells resulted in primary subcutaneous tumor formation and lung metastasis, suggesting that TIMP-1 negatively regulated tumorigenesis and metastasis in this model [54]. Many such studies have shown similar results, the sum of which overwhelmingly suggested that TIMP-1 exerted an inhibitory effect on growth and migration of tumor cell lines (Table 1).

Based on their anti-cancer activity in *in vivo* studies (Table 1) as well as their potent anti-MMP activity and anti-invasive potential in *in vitro* studies [55,56], TIMPs were initially investigated as potential therapeutics [28]. Technical difficulties, however, were encountered in the production of recombinant TIMP proteins in sufficient quantities [57]. Furthermore, their suitability as therapeutics were mitigated by high dosing requirements necessary for efficacy (~50mg/kg body weight) due to their the rapid

clearance *in vivo* (~4 minutes $t_{1/2}$) [56], although it has been suggested that the problem of stability could be mitigated by glycosylation in the case of TIMP-1 [58]. Hence, in an attempt to bypass these issues, attention was shifted to the development of synthetic MMP inhibitors (MPIs) as alternatives to recombinant TIMPs as anti-cancer therapeutics.

Synthetic MMP Inhibitors

Given the early results from studies of MMPs and TIMPs suggesting that MMP inhibition could be protective against cancer, efforts were directed towards developing small-molecular weight synthetic MMP inhibitors (MPIs) [59,60]. Among this first round of candidate molecules were the collagen mimetics that mimicked the cleavage recognition sites of MMPs and functioned by chelating the zinc atoms by hydroxamate, thiol, carboxyl or phosphorous groups on the inhibitor [59].

Utilizing various transplantation models of tumorigenesis, early preclinical studies with MPIs sought to determine if they attenuated cancer development *in vivo* [8]. For example, in one study using human metastatic colon carcinoma cells transplanted orthotopically into the colon of nude mice [61], treatment with batimastat—one of the early hydroxamate-based MPIs—began seven days following transplantation and resulted in improved median survival and reduction of primary tumor growth, local spread and distant metastasis as compared to placebo [61]. These findings, in conjunction with similar studies [8], suggested that MPIs might have therapeutic efficacy as anticancer agents.

Development of MPIs for human clinical trials yielded a range of candidate molecules [57,62]. The first MPIs, such as batimastat (BB-94), were hampered by poor

bioavailability; thus, in order to achieve what was believed to be an efficacious dose, patience tolerance was limited due to severe musculoskeletal pain [57]. To circumvent the poor bioavailability issues encountered with BB-94, other compounds that could be administered orally such as marimastat (BB-2516) were developed [57]. In order to minimize the potential for rheumatoid side effects attributed to broad-spectrum inhibition, MPIs such as prinomastat (AG-3340) and tanomastat (BAY-12-9566) were designed to specifically target the "deeper-pocket" MMPs such as MMP-2 and –9 [57]. Clinical testing of these compounds, however, demonstrated similar musculoskeletal problems as earlier drugs [63], suggesting that the rheumatoid side effects involved more than just MMP inhibition. Hence, attempts to develop MPIs that did not inhibit tumor necrosis factor-alpha (TNF-α)-converting enzyme (TACE), which induced the shedding of TNF receptor that was found to mediate the rheumatoid side effects, led to the development of compounds such as BMS-275291, which have thus far failed to induce joint toxicity [64] (Table 2).

The use of MPIs in human Phase III Clinical trials, however, gave far less encouraging results than what had been anticipated based upon the experimental mouse studies utilizing xenograft models of tumorigenesis [8,60,65]. In general, phase III trials in which patients with late-stage cancers were treated with MPIs as the sole treatment, or as part of a multidrug regimen, failed to show any benefit compared to controls in terms of overall survival or time to progression [60]. For tanomastat, treatment of advanced pancreatic cancer resulted in shorter survival time when compared to the existing chemotherapeutic drug, gemicitabine [66]. Another study actually showed a detrimental

effect of MPIs, in which treatment with tanomastat for patients with advanced small-cell-lung-cancer led to shorter survival times than placebo [65] (Bayer press release [67]). A positive exception was reported in the treatment of patients with gastric cancer using either marimastat or placebo [68]. In this study, marimastat treatment resulted in statistically significant improvements for progression-free and overall survival in patients who most likely had less advanced disease (i.e. those who lacked distant metastases or who had already been treated with chemotherapy) [68]. Nevertheless, the overall lack of success from the early MPI clinical trials led to a critical reevaluation of the existing notions for how MMPs and their inhibitors might regulate cancer.

Recent insights into MMPs and TIMPs Role in Cancer Development

Realization of the need to reevaluate the role of MMP inhibition in cancer arose from the development and examination of de novo mouse models of tumorigenesis. For example, the assumption that the contribution of MMPs to cancer was limited to the late-stage events of invasion and metastasis was challenged by work with a spontaneous mammary carcinogenesis mouse model induced by expression of MMP-3 under the whey acidic protein (WAP) gene promoter [69,70]. Prompted by the finding that MMP-3 activity in the mammary glands of these mice initiated neoplastic progression in normal mouse mammary cells resulting in their eventual malignant conversion, Sternlicht and colleagues sought to determine the biological mechanisms involved following sustained MMP-3 expression in the mammary glands of otherwise normal mice. The study found that mice with the WAP-MMP-3 transgene developed spontaneous mammary tumors, suggesting that MMP-3 functioned early in the process of tumorigenesis and served as a

sufficient initiating stimulus for complete carcinogenesis [69,70]. One mechanism that has been suggested for these findings has been the realization that MMP-3 mediates cleavage of E-cadherin from the cell membrane and leads to upregulation of β-catenin pathway and cyclin D1 activity [67].

Another model that has provided great insight in evaluating the functional significance of MMP and TIMPs during epithelial carcinogenesis is the K14-HPV16 mouse model of epithelial carcinogenesis [71]. HPV16 transgenic mice express the early region oncogenes E6 and E7 of human papillomavirus type 16 (HPV16) under the control of the human keratin-14 promoter (K14) [52,72,73]. HPV16 mice are born phenotypically normal, develop premalignant hyperplastic lesions by 1 month of age with 100% penetrance that progress to broad angiogenic dysplasias by 6 months of age, and ultimately exhibit an ~60% incidence of various epithelial tumors, ~50% of which are squamous cell carcinomas (SCCs) that metastasize to regional lymph nodes with a frequency of ~20%. Prompted by findings that MMP-9 (Gelatinase B) was upregulated in many human cancers and to be correlated with worse clinical outcomes in many cases [9], Coussens and colleagues tested the functional significance of MMP-9 using the K14-HPV16 model, modified by homozygous deletion of the endogenous MMP-9 gene [74]. HPV16/MMP-9-deficient mice, while exhibiting a decreased incidence of SCCs, developed less differentiated carcinomas representative of more aggressive tumors. This implied a protective effect of MMP-9 against neoplastic progression toward less differentiated carcinomas. Similalry a recent study also using MMP-9-deficient mice serving as tumor recipients for transplantation of lung carcinoma [75] demonstrated that MMP-9-deficiency conferred an acceleration of tumor growth, attributed by the ability of

MMP-9 to cleave collagen type IV and generate tumstatin as an angiogenesis inhibitor [75]. Based upon these results in mouse models, MMP inhibition could potentially be contributing to neoplastic progression—an interpretation consistent with the exacerbation of human small-cell-lung cancer by tanomastat described earlier and with more recent studies of TIMP-1 (Chapter 3).

Similarly, the study of TIMP-1 in mouse models of spontaneous tumorigenesis has challenged the notion that TIMPs play a protective role against carcinogenesis by inhibiting MMPs. Prompted by previous studies correlating high levels of MMP expression to human gastrointestinal carcinogenesis, Heppner-Goss and colleagues used the APC^{min} spontaneous tumorigenesis model of intestinal neoplasia to compare the effects of batimastat and TIMP-1 on tumor growth [76,77]. In APC^{min} mice, in which a mutation of the adenomatous-polyposis-of-the-colon (APC) tumor suppressor gene leads to development of multiple premalignant tumors of the intestine [76], treatment with batimastat from 6 to 14 weeks after birth led to a reduction in tumor multiplicity [77]. Unexpectedly, however, APC^{min} mice that transgenically expressed human TIMP-1 under the control of a gastrointestinal promoter exhibited an increased tumor multiplicity in one line of mice [77]. This finding represented the first demonstration of a pro-cancer regulatory role for TIMP-1 on tumorigenesis within a spontaneous *in vivo* model, although other work with a transplantation model has demonstrated a contributory role in metastasis as well; in some clones of transformed cell lines, TIMP-1 expression led to an increased efficiency of lung colonization upon transplantation [78].

Though additional mouse models have yielded conflicting results on the nature of the role played by TIMP-1 (summarized in Table 3), studies of TIMP-1 in human cancers

have also suggested the possibility of a contributory role in carcinogenesis [9]. Correlational studies with retrospective human clinical specimens have shown that higher levels of TIMP mRNA and protein associated with more advanced disease and shorter median survival for several cancer types [79], including oral squamous cell carcinoma [80], lymphoma [50], non-small-cell lung carcinoma [81] and primary breast carcinoma [82]. Whether or not these correlations are the result of non-MMP-inhibitory effects of TIMP-1, such as induction of proliferation and protection against apoptosis [56,83], remains to be determined.

Conclusion

In summary, the prospects for the use of TIMPs as endogenous inhibitors in the treatment of cancer are limited, given the paradoxical discrepancies observed from studies among mouse models and human disease. It has been suggested that the multifunctional effects of TIMP-1, such as induction of proliferation and protection against apoptosis could actually contribute to carcinogenesis [56,83]. If so, clinical development of TIMPs towards a therapeutic application in cancer could potentially lead to a similar outcome as the early, unsuccessful trials with synthetic inhibitors. The advent of improved gene therapy techniques, that would eliminate the prior obstacle of large-scale manufacturing of TIMP proteins, has renewed interest in the pursuit of TIMPs as therapeutic molecules [28,84]. Hence, it will be imperative to identify the functional significance of TIMPs in relevant, preclinical *in vivo* models before any further development as a therapy for cancer is pursued.

REFERENCES

1. Baker, A.H., Edwards, D.R. & Murphy, G. Metalloproteinase inhibitors: biological actions and therapeutic opportunities. *J Cell Sci* **115**, 3719-3727 (2002).

2. Hanahan, D. & Weinberg, R.A. The hallmarks of cancer. *Cell* **100**, 57-70 (2000).

3. Brinckerhoff, C.E. & Matrisian, L.M. Matrix metalloproteinases: a tail of a frog that became a prince. *Nat.Rev.Mol.Cell Biol.* **3**, 207-214 (2002).

4. Bergers, G. *et al.* Matrix metalloproteinase-9 triggers the angiogenic switch during carcinogenesis. *Nat Cell Biol* **2**, 737-744 (2000).

5. McQuibban, G.A. *et al.* Inflammation dampened by gelatinase A cleavage of monocyte chemoattractant protein-3. *Science* **289**, 1202-1206 (2000).

6. Powell, W.C., Fingleton, B., Wilson, C.L., Boothby, M. & Matrisian, L.M. The metalloproteinase matrilysin proteolytically generates active soluble Fas ligand and potentiates epithelial cell apoptosis. *Curr Biol* **9**, 1441-1447. (1999).

7. Manes, S. *et al.* The matrix metalloproteinase-9 regulates the insulin-like growth factor-triggered autocrine response in DU-145 carcinoma cells. *J Biol Chem* **274**, 6935-6945 (1999).

8. Nelson, A.R., Fingleton, B., Rothenberg, M.L. & Matrisian, L.M. Matrix metalloproteinases: biologic activity and clinical implications. *J Clin Oncol* **18**, 1135-1149 (2000).

9. Curran, S. & Murray, G.I. Matrix metalloproteinases in tumour invasion and metastasis. *J Pathol* **189**, 300-308 (1999).

10. Sternlicht, M.D. & Bergers, G. Matrix metalloproteinases as emerging targets in anticancer therapy: status and prospects. *Emerg. Theurpeut. Targets* **4**, 609-633 (2000).

11. Woessner, J.F. & Nagase, H. *Matrix metalloproteinases and TIMPs*, (Oxford University Press, Oxford, UK, 2000).

12. Gomez, D.E., Alonso, D.F., Yoshiji, H. & Thorgeirsson, U.P. Tissue inhibitors of metalloproteinases: structure, regulation and biological functions. *Eur J Cell Biol* **74**, 111-122. (1997).

13. Sellers, A., Murphy, G., Meikle, M.C. & Reynolds, J.J. Rabbit bone collagenase inhibitor blocks the activity of other neutral metalloproteinases. *Biochem Biophys Res Commun* **87**, 581-587. (1979).

14. Carmichael, D.F. *et al.* Primary structure and cDNA cloning of human fibroblast collagenase inhibitor. *Proc Natl Acad Sci U S A* **83**, 2407-2411 (1986).

15. Stetler-Stevenson, W.G., Krutzsch, H.C. & Liotta, L.A. Tissue inhibitor of metalloproteinase (TIMP-2). A new member of the metalloproteinase inhibitor family. *J Biol Chem* **264**, 17374-17378 (1989).

16. Wick, M., Burger, C., Brusselbach, S., Lucibello, F.C. & Muller, R. A novel member of human tissue inhibitor of metalloproteinases (TIMP) gene family is regulated during G1 progression, mitogenic stimulation, differentiation, and senescence. *J Biol Chem* **269**, 18953-18960 (1994).

17. Greene, J. *et al.* Molecular cloning and characterization of human tissue inhibitor of metalloproteinase 4. *J Biol Chem* **271**, 30375-30380. (1996).

18. Williamson, R.A. *et al.* Solution structure of the active domain of tissue inhibitor of metalloproteinases-2. A new member of the OB fold protein family. *Biochemistry* **33**, 11745-11759 (1994).

19. Gomis-Ruth, F.X. *et al.* Mechanism of inhibition of the human matrix metalloproteinase stromelysin-1 by TIMP-1. *Nature* **389**, 77-81. (1997).

20. Fernandez-Catalan, C. *et al.* Crystal structure of the complex formed by the membrane type 1-matrix metalloproteinase with the tissue inhibitor of metalloproteinases-2, the soluble progelatinase A receptor. *Embo J* **17**, 5238-5248 (1998).

21. Murphy, G. *et al.* The N-terminal domain of tissue inhibitor of metalloproteinases retains metalloproteinase inhibitory activity. *Biochemistry* **30**, 8097-8102 (1991).

22. Banyai, L. & Patthy, L. The NTR module: domains of netrins, secreted frizzled related proteins, and type I procollagen C-proteinase enhancer protein are homologous with tissue inhibitors of metalloproteases. *Protein Sci* **8**, 1636-1642. (1999).

23. Brew, K., Dinakarpandian, D. & Nagase, H. Tissue inhibitors of metalloproteinases: evolution, structure and function. *Biochim.Biophys.Acta* **1477**, 267-283 (2000).

24. Liepinsh, E. *et al.* NMR Structure of the Netrin-like Domain (NTR) of Human Type I Procollagen C-Proteinase Enhancer Defines Structural Consensus of NTR Domains and Assesses Potential Proteinase Inhibitory Activity and Ligand Binding. *J Biol Chem* **278**, 25982-25989. (2003).

25. Huang, W. *et al.* Folding and characterization of the amino-terminal domain of human tissue inhibitor of metalloproteinases-1 (TIMP-1) expressed at high yield in E. coli. *FEBS Lett* **384**, 155-161 (1996).

26. Murphy, G. & Willenbrock, F. Tissue inhibitors of matrix metalloendopeptidases. *Methods Enzymol* **248**, 496-510 (1995).

27. Langton, K.P., Barker, M.D. & McKie, N. Localization of the functional domains of human tissue inhibitor of metalloproteinases-3 and the effects of a Sorsby's fundus dystrophy mutation. *J Biol Chem* **273**, 16778-16781 (1998).

28. Fassina, G. *et al.* Tissue inhibitors of metalloproteases: regulation and biological activities. *Clin Exp Metastasis* **18**, 111-120 (2000).

29. KËahËari, V.M. & Saarialho-Kere, U. Matrix metalloproteinases and their inhibitors in tumour growth and invasion. *Annals of Medicine* **31**, 34-45 (1999).

30. Kobayashi, T. *et al.* Immunolocalizations of human gelatinase (type IV collagenase, MMP-9) and TIMP (tissue inhibitor of metalloproteinases) in normal epidermis and some epidermal tumors. *Arch Dermatol Res* **288**, 239-244. (1996).

31. Sugita, Y., Morita, E., Tanaka, T., Nakamura, K. & Yamamoto, S. Production of tissue inhibitor of metalloproteinase-1 and -2 by cultured keratinocytes. *J Dermatol Sci* **22**, 107-116 (2000).

32. Price, B., Dennison, C., Tschesche, H. & Elliott, E. Neutrophil tissue inhibitor of matrix metalloproteinases-1 occurs in novel vesicles that do not fuse with the phagosome. *J Biol Chem* **275**, 28308-28315 (2000).

33. La Fleur, M., Underwood, J.L., Rappolee, D.A. & Werb, Z. Basement membrane and repair of injury to peripheral nerve: defining a potential role for macrophages, matrix metalloproteinases, and tissue inhibitor of metalloproteinases-1. *J Exp Med* **184**, 2311-2326 (1996).

34. Welgus, H.G. & Stricklin, G.P. Human skin fibroblast collagenase inhibitor. Comparative studies in human connective tissues, serum, and amniotic fluid. *J Biol Chem* **258**, 12259-12264. (1983).

35. Frank, B.T., Rossall, J.C., Caughey, G.H. & Fang, K.C. Mast cell tissue inhibitor of metalloproteinase-1 is cleaved and inactivated extracellularly by alpha-chymase. *J Immunol* **166**, 2783-2792 (2001).

36. Itoh, Y. & Nagase, H. Preferential inactivation of tissue inhibitor of metalloproteinases-1 that is bound to the precursor of matrix metalloproteinase 9 (progelatinase B) by human neutrophil elastase. *J Biol Chem* **270**, 16518-16521. (1995).

37. Docherty, A.J. *et al.* Sequence of human tissue inhibitor of metalloproteinases and its identity to erythroid-potentiating activity. *Nature* **318**, 66-69. (1985).

38. Hayakawa, T., Yamashita, K., Tanzawa, K., Uchijima, E. & Iwata, K. Growth-promoting activity of tissue inhibitor of metalloproteinases-1 (TIMP-1) for a wide range of cells. A possible new growth factor in serum. *FEBS Lett* **298**, 29-32. (1992).

39. Bertaux, B., Hornebeck, W., Eisen, A.Z. & Dubertret, L. Growth stimulation of human keratinocytes by tissue inhibitor of metalloproteinases. *J Invest Dermatol* **97**, 679-685 (1991).

40. Chesler, L., Golde, D.W., Bersch, N. & Johnson, M.D. Metalloproteinase inhibition and erythroid potentiation are independent activities of tissue inhibitor of metalloproteinases-1. *Blood* **86**, 4506-45015 (1995).

41. Avalos, B.R. *et al.* K562 cells produce and respond to human erythroid-potentiating activity. *Blood* **71**, 1720-1725 (1988).

42. Zhao, W.Q. *et al.* Cell cycle-associated accumulation of tissue inhibitor of metalloproteinases-1 (TIMP-1) in the nuclei of human gingival fibroblasts. *J Cell Sci* **111 (Pt 9)**, 1147-1153 (1998).

43. Ritter, L.M., Garfield, S.H. & Thorgeirsson, U.P. Tissue inhibitor of metalloproteinases-1 (TIMP-1) binds to the cell surface and translocates to the nucleus of human MCF-7 breast carcinoma cells. *Biochem Biophys Res Commun* **257**, 494-499. (1999).

44. Guedez, L. *et al.* In vitro suppression of programmed cell death of B cells by tissue inhibitor of metalloproteinases-1. *J Clin Invest* **102**, 2002-2010 (1998).

45. Yamada, E. *et al.* TIMP-1 promotes VEGF-induced neovascularization in the retina. *Histol Histopathol* **16**, 87-97. (2001).

46. Johnson, M.D. *et al.* Inhibition of angiogenesis by tissue inhibitor of metalloproteinase. *J Cell Physiol* **160**, 194-202. (1994).

47. Carmichael, D.F., Stricklin, G.P. & Stuart, J.M. Systemic administration of TIMP in the treatment of collagen-induced arthritis in mice. *Agents Actions* **27**, 378-379 (1989).

48. Kumagai, K. *et al.* Inhibition of matrix metalloproteinases prevents allergen-induced airway inflammation in a murine model of asthma. *J Immunol* **162**, 4212-4219 (1999).

49. Apparailly, F. *et al.* Paradoxical effects of tissue inhibitor of metalloproteinases 1 gene transfer in collagen-induced arthritis. *Arthritis Rheum* **44**, 1444-1454 (2001).

50. Guedez, L. *et al.* Tissue inhibitor of metalloproteinases 1 regulation of interleukin-10 in B-cell differentiation and lymphomagenesis. *Blood* **97**, 1796-1802 (2001).

51. Thorgeirsson, U.P., Yoshiji, H., Sinha, C.C. & Gomez, D.E. Breast cancer; tumor neovasculature and the effect of tissue inhibitor of metalloproteinases-1 (TIMP-1) on angiogenesis. *In Vivo* **10**, 137-144. (1996).

52. Coussens, L.M. *et al.* Inflammatory mast cells up-regulate angiogenesis during squamous epithelial carcinogenesis. *Genes Dev* **13**, 1382-1397 (1999).

53. Hamano, Y. *et al.* Physiological levels of tumstatin, a fragment of collagen IV alpha3 chain, are generated by MMP-9 proteolysis and suppress angiogenesis via alphaVbeta3 integrin. *Cancer Cell* **3**, 589-601 (2003).

54. Khokha, R. *et al.* Antisense RNA-induced reduction in murine TIMP levels confers oncogenicity on Swiss 3T3 cells. *Science* **243**, 947-950. (1989).

55. Alexander, C.M. & Werb, Z. Targeted disruption of the tissue inhibitor of metalloproteinases gene increases the invasive behavior of primitive mesenchymal cells derived from embryonic stem cells in vitro. *J Cell Biol* **118**, 727-739 (1992).

56. Blavier, L., Henriet, P., Imren, S. & Declerck, Y.A. Tissue inhibitors of matrix metalloproteinases in cancer. *Ann.N.Y.Acad.Sci.* **878**, 108-119 (1999).

57. Whittaker, M., Floyd, C.D., Brown, P. & Gearing, A.J. Design and therapeutic application of matrix metalloproteinase inhibitors. *Chem Rev* **99**, 2735-2776 (1999).

58. Caterina, N.C. *et al.* Glycosylation and NH2-terminal domain mutants of the tissue inhibitor of metalloproteinases-1 (TIMP-1). *Biochim Biophys Acta* **1388**, 21-34. (1998).

59. Hidalgo, M. & Eckhardt, S.G. Development of matrix metalloproteinase inhibitors in cancer therapy. *J Natl Cancer Inst* **93**, 178-193 (2001).

60. Coussens, L.M., B. Fingleton, B. & Matrisian, L.M. Matrix metalloproteinase inhibitors and cancer: trials and tribulations. *Science* **295**, 2387-2392 (2002).

61. Wang, X., Fu, X., Brown, P.D., Crimmin, M.J. & Hoffman, R.M. Matrix metalloproteinase inhibitor BB-94 (batimastat) inhibits human colon tumor growth and

spread in a patient-like orthotopic model in nude mice. *Cancer Res* **54**, 4726-4728. (1994).

62. Brown, P.D. Ongoing trials with matrix metalloproteinase inhibitors. *Expert Opin Investig Drugs* **9**, 2167-2177 (2000).

63. Wilding, G., Small, E., Collier, M., Dixon, M. & Pithavala, Y. A Phase I pharmacokinetic evaluation of the matrix metalloproteinase inhibitor AG-3340 in combination with mitoxantrone and prednisone in patients with advanced prostate cancer. *Proc. Am. Soc. Clin. Oncol.* **18**, Abstract 1244,1323a (1999).

64. Ferrante, K., Winograd, B. & Canetta, R. Promising new developments in cancer chemotherapy. *Cancer Chemother Pharmacol* **43**, S61-68. (1999).

65. Zucker, S., Cao, J. & Chen, W.T. Critical appraisal of the use of matrix metalloproteinase inhibitors in cancer treatment. *Oncogene* **19**, 6642-6650. (2000).

66. Moore, M.J. *et al.* A Comparison Between Gemcitabine (GEM) and the Matrix Metalloproteinase (MMP) Inhibitor BAY12-9566 (9566) in Patients (PTS) with Advanced Pancreatic Cancer. in *ASCO Online* Vol. http://www.asco.org/prof/me/html/00abstracts/gic/m_930.htm (, 2000).

67. Bayer Pharmaceutical Division, Press Release: Bayer Halts Clinical Trials Evaluating MMPI. , http://www.bayerpharma-na.com/news/co0221.asp (1999).

68. Fielding, J. *et al.* A Randomized Double-Blind Placebo-Controlled Study of Marimastat in Patients with Inoperable Gastric Adenocarcinoma. in *American Society of Clinical Oncology (ASCO)'s 36th Annual Meeting* http://www.asco.org/prof/me/html/00abstracts/gic/m_929.htm (, New Orleans, 2000).

69. Sternlicht, M.D. *et al.* The stromal proteinase MMP3/stromelysin-1 promotes mammary carcinogenesis. *Cell* **98**, 137-146 (1999).

70. Sternlicht, M.D., Bissell, M.J. & Werb, Z. The matrix metalloproteinase stromelysin-1 acts as a natural mammary tumor promoter. *Oncogene* **19**, 1102-1113 (2000).

71. Arbeit, J.M., Munger, K., Howley, P.M. & Hanahan, D. Progressive squamous epithelial neoplasia in K14-human papillomavirus type 16 transgenic mice. *J Virol* **68**, 4358-4368 (1994).

72. Coussens, L.M., Hanahan, D. & Arbeit, J. Genetic predisposition and parameters of malignant progression in K14-HPV16 transgenic mice. *Am J Path* **149**, 1899-1917 (1996).

73. van Kempen, L.C.L. *et al.* Epithelial carcinogenesis: dynamic interplay between neoplastic cells and their microenvironment. *Differentiation* **70**, 501-623 (2002).

74. Coussens, L.M., Tinkle, C.L., Hanahan, D. & Werb, Z. MMP-9 supplied by bone marrow-derived cells contributes to skin carcinogenesis. *Cell* **103**, 481-490 (2000).

75. Hamano, Y. *et al.* Physiological levels of tumstatin, a fragment of collagen IV alpha3 chain, are generated by MMP-9 protelysis and suppress angioenesis via alphaVbeta3 integrin. *Cancer Cell* **3**, 589-601 (2003).

76. Su, L.K. *et al.* Multiple intestinal neoplasia caused by a mutation in the murine homolog of the APC gene. *Science* **256**, 668-670. (1992).

77. Goss, K.J., Brown, P.D. & Matrisian, L.M. Differing effects of endogenous and synthetic inhibitors of metalloproteinases on intestinal tumorigenesis. *Int J Cancer* **78**, 629-635 (1998).

78. Soloway, P.D., Alexander, C.M., Werb, Z. & Jaenisch, R. Targeted mutagenesis of Timp-1 reveals that lung tumor invasion is influenced by Timp-1 genotype of the tumor but not by that of the host. *Oncogene* **13**, 2307-2314. (1996).

79. Egeblad, M. & Werb, Z. New functions for the matrix metalloproteinases in cancer progression. *Nat Rev Cancer* **2**, 161-174 (2002).

80. Kurahara, S. *et al.* Expression of MMPS, MT-MMP, and TIMPs in squamous cell carcinoma of the oral cavity: correlations with tumor invasion and metastasis. *Head Neck* **21**, 627-638 (1999).

81. Thomas, P., Khokha, R., Shepherd, F.A., Feld, R. & Tsao, M.S. Differential expression of matrix metalloproteinases and their inhibitors in non-small cell lung cancer. *J Pathol* **190**, 150-156 (2000).

82. Schrohl, A.S. *et al.* Tumor Tissue Concentrations of the Proteinase Inhibitors Tissue Inhibitor of Metalloproteinases-1 (TIMP-1) and Plasminogen Activator Inhibitor Type 1 (PAI-1) are complementary in determining prognosis in primary breast cancer. *Mol Cell Proteomics* **2**, 164-172. (2003).

83. Jiang, Y., Goldberg, I.D. & Shi, Y.E. Complex roles of tissue inhibitors of metalloproteinases in cancer. *Oncogene* **21**, 2245-2252 (2002).

84. Baker, A.H., Ahonen, M. & Kahari, V.M. Potential applications of tissue inhibitor of metalloproteinase (TIMP) overexpression for cancer gene therapy. *Adv Exp Med Biol* **465**, 469-483. (2000).

85. Kawamata, H. *et al.* Over-expression of tissue inhibitor of matrix metalloproteinases (TIMP1 and TIMP2) suppresses extravasation of pulmonary metastasis of a rat bladder carcinoma. *Int J Cancer* **63**, 680-687. (1995).

86. Watanabe, M. *et al.* Inhibition of metastasis in human gastric cancer cells transfected with tissue inhibitor of metalloproteinase 1 gene in nude mice. *Cancer* **77**, 1676-1680 (1996).

87. Kruger, A., Fata, J.E. & Khokha, R. Altered tumor growth and metastasis of a T-cell lymphoma in Timp-1 transgenic mice. *Blood* **90**, 1993-2000. (1997).

88. Kruger, A. *et al.* Host TIMP-1 overexpression confers resistance to experimental brain metastasis of a fibrosarcoma cell line. *Oncogene* **16**, 2419-2423. (1998).

89. Yoshiji, H. *et al.* Mammary carcinoma cells over-expressing tissue inhibitor of metalloproteinases-1 show enhanced vascular endothelial growth factor expression. *Int J Cancer* **75**, 81-87 (1998).

90. Guedez, L. *et al.* Tissue inhibitor of metalloproteinase-1 alters the tumorigenicity of Burkitt's lymphoma via divergent effects on tumor growth and angiogenesis. *Am J Pathol* **158**, 1207-1215. (2001).

91. Heppner-Goss, K.J., Brown, P.D. & Matrisian, L.M. Differing effects of endogenous and synthetic inhibitors of metalloproteinases on intestinal tumorigenesis. *Int J Cancer* **78**, 629-635 (1998).

92. Martin, D.C. *et al.* Transgenic TIMP-1 inhibits simian virus 40 T antigen-induced hepatocarcinogenesis by impairment of hepatocellular proliferation and tumor angiogenesis. *Lab Invest* **79**, 225-234 (1999).

93. Martin, D.C., Fowlkes, J.L., Babic, B. & Khokha, R. Insulin-like growth factor II signaling in neoplastic proliferation is blocked by transgenic expression of the metalloproteinase inhibitor TIMP-1. *J Cell Biol* **146**, 881-892. (1999).

94. Buck, T.B., Yoshiji, H., Harris, S.R., Bunce, O.R. & Thorgeirsson, U.P. The effects of sustained elevated levels of circulating tissue inhibitor of metalloproteinases-1 on the development of breast cancer in mice. *Ann N Y Acad Sci* **878**, 732-735 (1999).

FIGURE LEGENDS

Figure 1. TIMP family members.

Amino acid sequences for mature human TIMP-1, -2, -3, and –4 were aligned by the ClustalW Multiple Sequence Alignment and Boxshade programs via the Baylor College of Medicine website (http://searchlauncher.bcm.tmc.edu/multi-align/multi-align.html). Shading indicates residues conserved over all four family members and boxes indicate conserved cysteine residues.

Figure 1

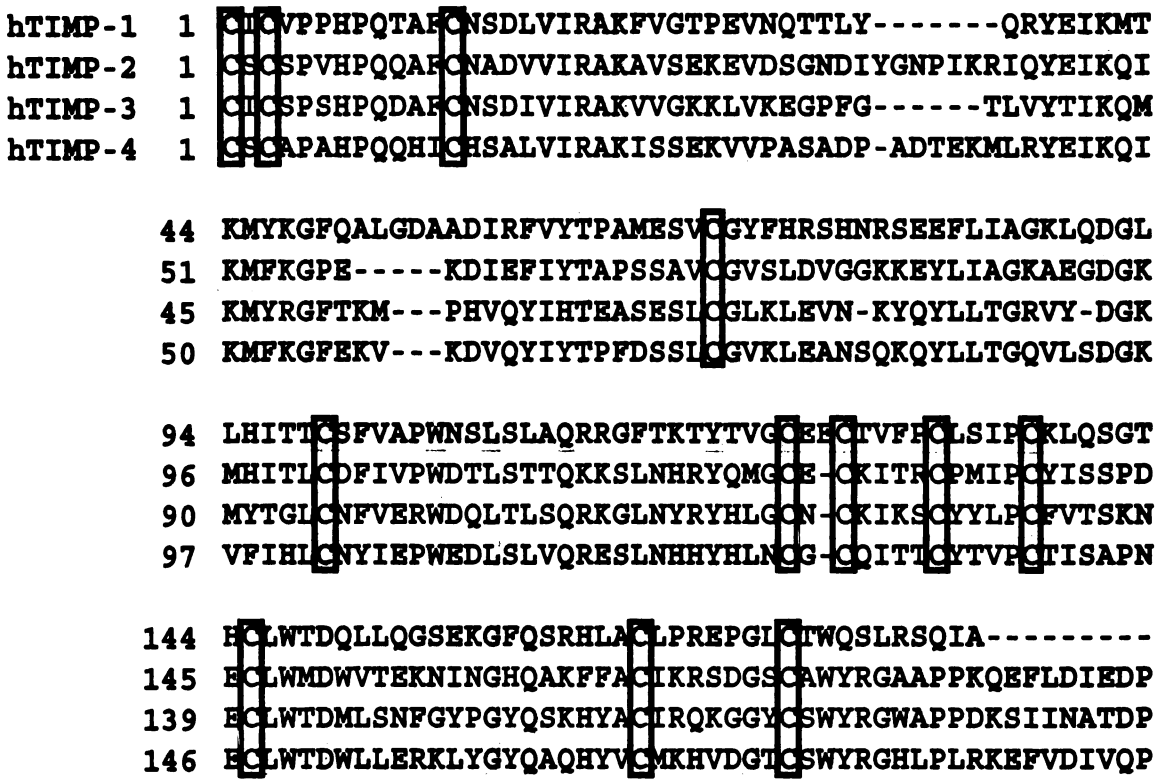
hTIMP-1 1 CTCVPPHPQTAHCNSDLVIRAKFVGTPEVNQTTLY-------QRYEIKMT
hTIMP-2 1 CSCSPVHPQQAHCNADVVIRAKAVSEKEVDSGNDIYGNPIKRIQYEIKQI
hTIMP-3 1 CTCSPSHPQDAHCNSDIVIRAKVVGKKLVKEGPFG------TLVYTIKQM
hTIMP-4 1 CSCAPAHPQQHICHSALVIRAKISSEKVVPASADP-ADTEKMLRYEIKQI
44 KMYKGFQALGDAADIRFVYTPAMESVCGYFHRSHNRSEEFLIAGKLQDGL
51 KMFKGPE-----KDIEFIYTAPSSAVCGVSLDVGGKKEYLIAGKAEGDGK
45 KMYRGFTKM---PHVQYIHTEASESLCGLKLEVN-KYQYLLTGRVY-DGK
50 KMFKGFEKV---KDVQYIYTPFDSSLCGVKLEANSQKQYLLTGQVLSDGK
94 LHITTCSFVAPWNSLSLAQRRGFTKTYTVGCEECTVFPCLSIPCKLQSGT
96 MHITLCDFIVPWDTLSTTQKKSLNHRYQMGCE-CKITRCPMIPCYISSPD
90 MYTGLCNFVERWDQLTLSQRKGLNYRYHLGCN-CKIKSCYYLPCFVTSKN
97 VFIHLCNYIEPWEDLSLVQRESLNHHYHLNCG-CQITTCYTVPCTISAPN
144 HCLWTDQLLQGSEKGFQSRHLACLPREPGLCTWQSLRSQIA---------
145 ECLWMDWVTEKNINGHQAKFFACIKRSDGSCAWYRGAAPPKQEFLDIEDP
139 ECLWTDMLSNFGYPGYQSKHYACIRQKGGYCSWYRGWAPPDKSIINATDP
146 ECLWTDWLLERKLYGYQAQHYVCMKHVDGTCSWYRGHLPLRKEFVDIVQP

Table 1. Examination of TIMP-1 function using transplantation mouse models of tumorigenesis

TIMP-1 Expression	Transplantation (delivery & site)	Result	Reference
Host vs. Donor KO	Transformed skin cells (i.v.)	↓ or ↑ lung metastasis if donor KO, No effect if host KO	78
Donor AS-TIMP1	3T3 cells (sc & i.v.)	↑Tumor growth, ↑Metastasis	54
Donor SV40-mTIMP1	Rat bladder carcinoma cells (orthotopic)	↓Metastasis to lung	85
Donor SV40-hTIMP1	Gastric carcinoma cells (orthotopic)	No effect primary growth, ↓Metastasis	86
Host MHC-TIMP1	Lymphoma cells (sc)	↓Tumor growth, ↓Metastasis	87
Host MT1-TIMP1	Fibrosarcoma cells (i.v.)	↓Metastasis to brain	88
Donor CMV-hTIMP1	Breast carcinoma cells (sc)	↑Growth	89
Donor LTR-hTIMP1	Lymphoma cells (sc)	↑Early growth, but ↓Late growth	90

Host vs. Donor KO, recipient host homozygous null TIMP-1 vs. transplant cell lines homozygous null TIMP-1; i.v., intravenous injection; Donor AS-TIMP1, cell-line transfection of anti-sense cDNA against mouse TIMP-1; 3T3 cells (sc. and i.v.), subcutaneous (sc) and i.v. injections for primary tumorigenesis and metastasis of Swiss 3T3 cells; Donor SV40-mTIMP1, cell-line-transfection of SV40 early promoter with mouse TIMP-1; Donor SV40-hTIMP1, cell-line-transfection of SV40 early promoter with human TIMP-1; MHC-TIMP1, major histocompatability class I promoter with mouse TIMP-1; sc inject., subcutaneous injection; MT1, metallothionein-1 promoter; CMV, cytomegalovirus immediate-early promoter; LTR, long terminal repeat promoter.

Table 2. Inhibitory concentrations of MPIs against specific MMPs

Inhibitor	MMP-1	MMP-2	MMP-3	MMP-7	MMP-9
Batimistat (IC_{50})	3	4	20	6	4
Marimastat (IC_{50})	5	6	200	20	3
Prinomastat (K_i)	8	0.08	0.27	54	0.26
Tanomastat (K_i)	>5000	11	134	-	301
BMS-275291 (IC_{50})	25	41	157	-	25

Modified from reviews by P. Brown [62] and Nelson et al. [8] (-) indicates, no data reported.

Table 3. Examination of TIMP-1 function using spontaneous mouse models of tumorigenesis.

TIMP-1 expression	Oncogenic stimulus	Result	Reference
LFABP-hTIMP1	APC^{min}	↑Tumor multiplicity in one case, No effect in others	91
MHC-TIMP1	Crp-Tag in liver	↓Onset, ↓Tumor growth	92,93
Albumin-hTIMP1	DMBA + MPA in breast	↓Tumor incidence	94
WAP-hTIMP1	WAP-MMP3 in breast	↓Hyperplasia	69,70

LFABP = liver fatty acid binding protein promoter; APC^{min}, adenomatous polyposis coli gene with multiple intestinal neoplasia mutation; host MHC-TIMP1, major histocompatability class I promoter with mouse TIMP-1; Crp-Tag, C-reactive protein gene promoter with SV40 T antigen; albumin-hTIMP1, albumin gene promoter with human TIMP-1; DMBA + MPA, dimethylbenzanthracene + medroxyprogesterone acetate; WAP, whey acidic protein gene promoter.

Chapter 2

RECKing MMP Function: Implications for Cancer Development

PROLOGUE

This chapter reviews the studies of an endogenous MMP inhibitor, RECK. It summarizes the significance of RECK (or REversion-inducing-Cysteine-rich protein with Kazal motifs), which is singular for its cell-surface localization and its ability to inhibit MMPs at multiple levels of regulation, in the contexts of cancer and embryonic development. This chapter was published as an invited review manuscript for the journal *Trends in Cell Biology*.

ABSTRACT

Cancer is a multi-stage process requiring progressive genetic and epigenetic changes in neoplastic and responding stromal cells. Many alterations that occur during the malignant progression process, are regulated by the matrix metalloproteinase (MMP) family of extracellular proteases and their endogenous inhibitors. Recent work has identified a new cell-surface inhibitor of MMPs – RECK. RECK regulates MMP-induced pericellular signaling cascades resulting in embryonic lethality and attenuated tumor development in adults; thus, providing further support for an efficacious role for protease inhibitors as anti-cancer therapeutics.

The development of cancer is a multi-stage process involving progressive genetic change in initiated cells (cells harboring activated oncogenes and/or inactivated tumor suppressor genes) and epigenetic change in the microenvironment (extracellular matrix (ECM) remodeling, inflammation, and angiogenesis) [1]. Taken together, these characteristics endow neoplastic cells with specific capabilities essential for their cancerous development – alterations rendering them self-sufficient for growth, insensitive to growth-inhibitory signals, resistant to programs of terminal differentiation, senescence, or apoptosis – as well as endowing them with unlimited self-renewal capacity, the ability to orchestrate and sustain angiogenesis, and the ability to invade and thrive in ectopic tissue environments [2]. The matrix metalloproteinase (MMP) family of zinc-dependent extracellular proteases and their endogenous inhibitors, have been implicated as regulators of several of these critical steps in carcinogenesis and as such, a great deal of research has focused on elucidating the intricacies of their regulation and their exact contributions to processes involved in tumor progression and metastasis [3]. MMPs are overexpressed in almost all human cancers, and in some instances, correlate with worse clinical outcomes [4]. In addition, vast preclinical data overwhelmingly implicates MMPs as functional contributors to malignant development [3,5]; thus, inhibition of MMP activity has been targeted as an anti-cancer therapeutic strategy. Recent Phase III clinical trials testing efficacy of several synthetic metalloprotease inhibitors (MPIs) has not however, borne out initial optimism [6]. Hence, at a time when interest in MPIs has waned in the pharmaceutical industry, a new MMP inhibitory molecule has been identified, e.g., RECK [7], whose multi-faceted MMP-inhibitory activities may provide insight into novel strategies for regulating MMP function during malignant processes.

Regulation of Matrix Metalloproteinases

The MMP family consists of ~24 members and the closely related ADAMS and ADAMTS proteases characterized in humans, rodents, and amphibians [3]. Initially classified as zinc-dependent proteases capable of cleaving all structural components of the ECM (*in vitro*), their specific proteolytic targets have since expanded to include other extracellular proteins. These include ECM molecules, other proteases, protease inhibitors, clotting factors, chemotactic molecules, latent growth factors, growth factor binding proteins, cell surface receptors, and cell-cell and cell-ECM adhesion molecules [3]. Regulation of MMP function occurs at multiple levels. MMP mRNA expression is under tight, cell-type dependent control, with expression of individual MMPs associated with specific inflammatory, connective tissue or epithelial cell types. MMP transcripts rise rapidly when tissues undergo remodeling, such as in inflammation, wound healing, and cancer. MMPs are synthesized as latent enzymes that can be stored in secretory granules in inflammatory cells, but are most often secreted and found anchored to or associated with the cell surface. Latent MMPs are proteolyticaly activated in multiple steps. Once active, MMPs are subject to inhibition by endogenous tissue inhibitors of metalloproteinases (TIMPs 1-4), a plasma inhibitor α2-macroglobulin, the carboxy-terminal fragment of procollagen C-terminal proteinase enhancer, tissue factor pathway inhibitor-2, proteolytic fragments of MMP substrates, and the recently characterized RECK, a novel plasma membrane-anchored MMP inhibitor [7-11].

RECK and MMP inhibition

RECK, originally discovered in an expression cloning screen attempting to isolate human cDNAs inducing flat reversion of v-Ki-*ras*-transformed NIH3T3 cells [12], encodes a secreted 110 kDa glycoprotein containing a serine-protease inhibitor-like domain, two domains containing EGF-like repeats, and a carboxy-terminal domain encoding a glycosylphosphatidylinositol (GPI)-modification anchoring RECK to the plasma membrane [13]. *RECK*, or REversion-inducing-Cysteine-rich protein with Kazal motifs, is widely expressed in mesenchymal tissues in E10.5 embryos, the marginal zone of the neural tube, and exhibits a high level of expression in vascular smooth muscle cells proximal to large blood vessels [7,13]. Whereas, *RECK* mRNA is abundant in many normal adult tissues, it is suppressed in malignant cell lines expressing various oncogenes, suggesting *RECK* is a target for oncogenic-induced signaling *in vitro* [13]. Restored expression of *RECK* in tumor-derived cell lines does not alter cell viability, growth, motility, or chemotactic activity of malignant cells *in vitro* or *in vivo*, but does attenuate *in vitro* invasive capacity and *in vivo* metastasis formation in experimental metastasis assays [13]. The ability to suppress matrix invasion is not limited to membrane-anchored RECK since a solubilized version containing a carboxy-terminal truncation demonstrates similar efficacy [13]. How then does RECK regulate *in vitro* invasion and experimental metastasis formation, and does RECK play a role in regulating these processes *in vivo*?

Through a series of elegant studies, Noda and colleagues have determined that RECK post-transcriptionally regulates at least three members of the MMP family, e.g., MMP-2/gelatinase A, MMP-9/gelatinase B, and MMP-14/MT1-MMP (membrane type 1-metalloproteinase), by various mechanisms [7,13]. Membrane-anchored RECK inhibits

secretion of proMMP-9, whereas both membrane-anchored and soluble RECK directly inhibits MMP-2, -9, and –14 catalytic activity. In addition, RECK inhibits both catalytic steps of proMMP-2 activation. By inhibiting MMP-14 activity, RECK inhibits processing of proMMP-2 to the intermediate species. RECK also inhibits the final processing step of proMMP-2 where the intermediate processed form is autolytically activated (Fig 1). While the exact molecular mechanisms involved in regulating MMP secretion and/or activity by RECK are yet to be resolved, direct protein-to-protein interactions are implicated, though the stoichiometry of these interactions is presently unknown. In addition, the functional significance of the GPI anchor of RECK is undetermined, but may simply be significant for positioning RECK at sites of robust pericellular proteolytic activity.

The implication of RECK as a critical regulator of MMP function at the cell surface is perhaps best understood by examination of RECK homozygous null (*RECK*$^{-/-}$) mouse embryos versus RECK-expressing tumors. *RECK*$^{-/-}$ embryos die by E10.5 and are distinct from RECK$^{+/-}$ littermates by their smaller body size, reduced structural integrity, and propensity for abdominal hemorrhage [7]. Histologically, *RECK*$^{-/-}$ embryos evidence disrupted organogenesis, disorganized mesenchymal tissue architecture, and whereas vascular networks are formed, vascular endothelial cells do not form tight tubules [7], as might be expected for over-expression or gain-of-function mutations of an MMP. These data suggest that RECK, either through its ability to regulate MMP activity or through an as of yet undescribed regulatory function, controls blood vessel maturation (vasculogenesis). In the context of tumor development, overexpression of RECK in HT1080 cells results in attenuated tumor formation in nude mice, as a consequence of

limited angiogenic sprouting [7]. Since the balance between ECM deposition and degradation is key for endothelial cell homeostasis, RECK likely functionally contributes to vasculogenesis and angiogenesis by attenuating MMP-substrate degradation. Thus, as would be predicted, in RECK$^{-/-}$ embryos where MMP activity is robust, MMP substrates are reduced, specifically, loss of collagen fibrils and a discontinuous basal lamina surrounding the neural tube [7].

Degradation of collagen fibrils requires the action of collagenolytic MMPs that cleave specific peptide bonds in interstitial collagen fibrils [14,15]. Four murine MMP collagenases are capable of initiating degradation of fibrillar collagen, i.e., MMP-8/neutrophil collagenase, MMP-13/interstitial collagenase, MMP-14, and mColA [14-16]. While type I collagen stabilizes MMP-2 and reduces its rate of autolytic inactivation, MMP-2 cleaves intact type I collagen poorly, if at all [17]. Thus, collagen fibril loss in RECK$^{-/-}$ embryos is likely the result of uninhibited MMP-14 activity, or perhaps other collagenolytic MMPs yet to be identified as RECK targets. Moreover, it is noteworthy that lethality in RECK$^{-/-}$ embryos is delayed, albeit by one day, by MMP-2-deficiency. These data suggest that collagen-fibril loss in RECK$^{-/-}$ embryos is not their sole impairment, but other substrates, regulated by MMP-2 and/or MMP-9 are also critical. The outstanding question of course is whether, RECK deficiency could be further rescued by either MMP-9, MMP-14 deficiency, or combinations thereof.

Therapeutic Implications for RECK in Neoplastic Progression

The combined demonstrations that *RECK* expression is low in many human tumors, and that *RECK* expression reduces invasive and metastatic behavior of neoplastic cells, in

combination with its demonstrated role as a multi-faceted MMP-inhibitor invite the speculation that RECK might have therapeutic utility. One observation in support of this is the effective MMP inhibitory activities of soluble RECK — pharmacologically appealing in that delivery would not be problematic if stability could be achieved without toxicity. Nevertheless, reasons for tempering initial optimism for RECK as a therapeutic agent are numerous. Lessons learned from Phase III MPI Clinical Trials suggest that our understanding of MMP biology during tumor development is still lacking. While great strides have recently been made, considerable gaps in our understanding of the events regulated by MMPs and their endogenous inhibitors during cancer development exist. That said, even with the limited data available regarding RECK, it is intriguing to speculate that an MMP-inhibitor harboring RECK characteristics may one day find therapeutic efficacy in the treatment of malignant diseases.

ACKNOWLEDGEMENTS

We thank Zena Werb and Leon van Kempen for helpful discussions. We apologize to authors whose work could not be cited owing to space limitations. LMC is supported by the NIH, AACR, the V Foundation for Cancer Research, the Edward G. Mallinckrodt Foundation, and the California Research Coordinating Committee.

REFERENCES

1. Bissell, M.J. & Radisky, D. Putting tumors in context. *Nat Rev Cancer* **1**, 46-54 (2001).

2. Hanahan, D. & Weinberg, R.A. The hallmarks of cancer. *Cell* **100**, 57-70 (2000).

3. Egeblad, M. & Werb, Z. New functions for the matrix metalloproteinases in cancer progression. *Nat Rev Cancer* **2**, 161-174 (2002).

4. Sternlicht, M.D. & Bergers, G. Matrix metalloproteinases as emerging targets in anticancer therapy: status and prospects. *Emerg. Theurpeut. Targets* **4**, 609-633 (2000).

5. McCawley, L.J. & Matrisian, L.M. Matrix metalloproteinases: they're not just for matrix anymore! *Curr Opin Cell Biol* **13**, 534-540. (2001).

6. Coussens, L.M., Fingleton, B. & Matrisian, L.M. Matrix metalloproteinase inhibitors and cancer: trials and tribulations. *Science* **295**, 2387-2392 (2002).

7. Oh, J. *et al.* Membrane-anchored MMP inhibitor RECK is a key regulator of extracellular matrix integrity and angiogenesis. *Cell* **107**, 789-800. (2001).

8. Sternlicht, M.D. & Werb, Z. How matrix metalloproteinases regulate cell behavior. *Annu Rev Cell Dev Biol* **17**, 463-516 (2001).

9. Herman, M.P. *et al.* Tissue factor pathway inhibitor-2 is a novel inhibitor of matrix metalloproteinases with implications for atherosclerosis. *J Clin Invest* **107**, 1117-1126. (2001).

10. Mott, J.D. *et al.* Post-translational proteolytic processing of procollagen C-terminal proteinase enhancer releases a metalloproteinase inhibitor. *J Biol Chem* **275**, 1384-1390. (2000).

11. Welm, B., Mott, J. & Werb, Z. Developmental Biology: Vasculogenesis is a wreck without RECK. *Current Biology* **12**, R1-R3 (2002).

12. Noda, M. *et al.* Detection of genes with a potential for suppressing the transformed phenotype associated with activared ras genes. *Proc. Nat. Acad. Sci. U.S.A.* **86**, 162-166 (1989).

13. Takahashi, C. *et al.* Regulation of matrix metalloproteinase-9 and inhibition of tumor invasion by the membrane-anchored glycoprotein RECK. *Proc. Nat. Acad. Sci. U.S.A.* **95**, 13221-13226 (1998).

14. Krane, S.M. *et al.* Different collagenase gene products have different roles in degradation of type I collagen. *J Biol Chem* **271**, 28509-28515. (1996).

15. Balbin, M. *et al.* Identification and enzymatic characterization of two diverging murine counterparts of human interstitial collagenase (MMP-1) expressed at sites of embryo implantation. *J Biol Chem* **276**, 10253-10262 (2001).

16. Ohuchi, E. *et al.* Membrane type 1 matrix metalloproteinase digests interstitial collagens and other extracellular matrix macromolecules. *J Biol Chem* **272**, 2446-2451. (1997).

17. Ellerbroek, S.M., Wu, Y.I. & Stack, M.S. Type I collagen stabilization of matrix metalloproteinase-2. *Arch Biochem Biophys* **390**, 51-56 (2001).

FIGURE LEGENDS

Figure 1. Regulation of MMP Function by RECK.

(A) Secretion of proMMP-9 is blocked by RECK. In addition, RECK, in either soluble or membrane-anchored form, inhibits catalytic activity of MMP-9 towards target substrates.

(B) The active form of MMP-14/MT1-MMP is also inhibited by soluble and membrane-anchored RECK; thus, limiting the initial processing step of proMMP-2 activation when proMMP-2 is in the ternary complex containing MMP-14 and TIMP-2.

(C) RECK inhibits catalytic activity of active MMP-2 as well as the final autolytic processing step in proMMP-2 activation.

Figure 1

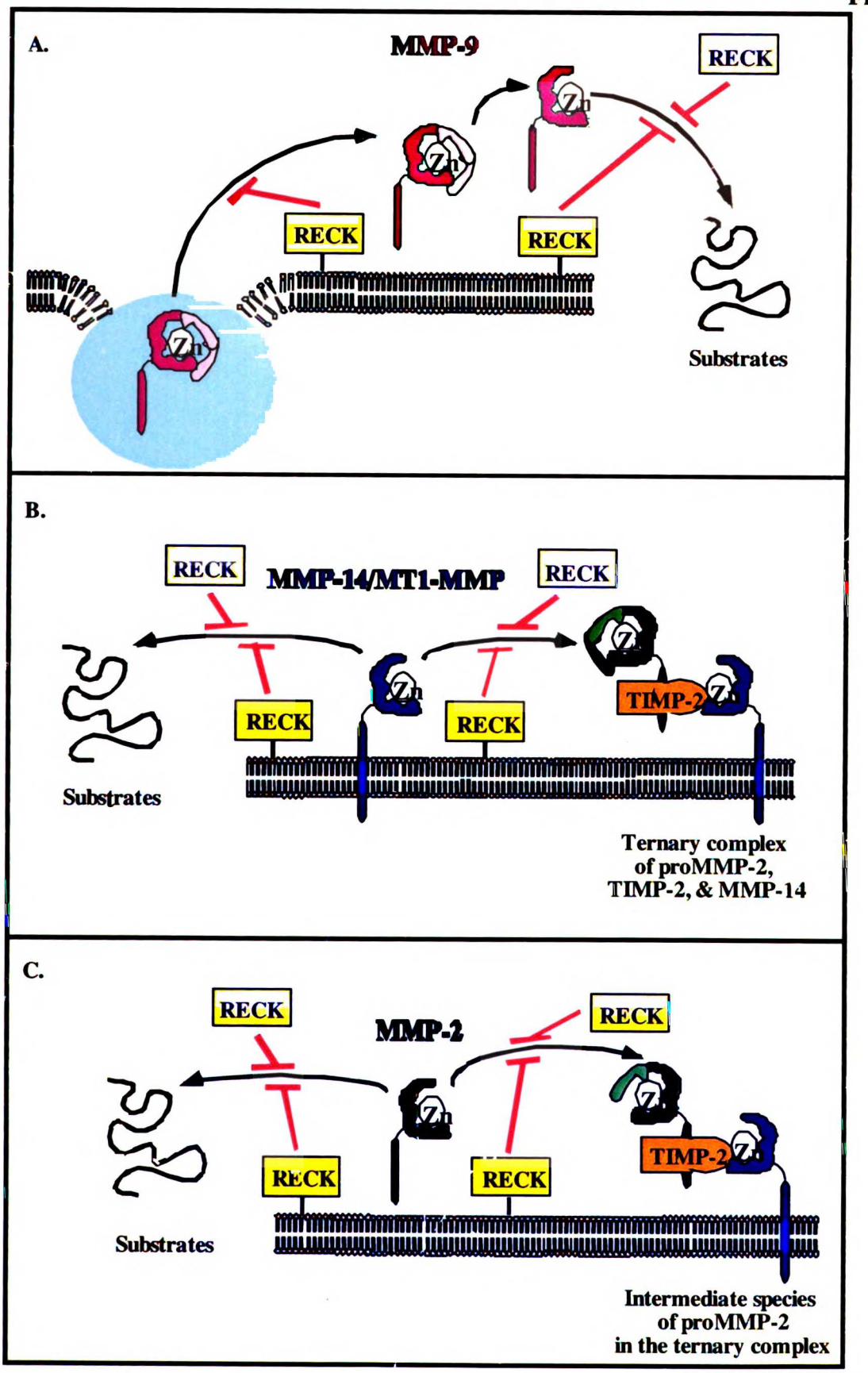
A.
MMP-9
RECK
RECK
RECK
Substrates
B.
RECK
MMP-14/MT1-MMP
RECK
RECK
RECK
TIMP-2
Substrates
Ternary complex
of proMMP-2,
TIMP-2, & MMP-14
C.
RECK
MMP-2
RECK
RECK
RECK
TIMP-2
Substrates
Intermediate species
of proMMP-2
in the ternary complex

Chapter 3

TIMP-1 Alters Susceptibility to Carcinogenesis

PROLOGUE

The studies in this chapter consist of work assessing the functional significance of TIMP-1 during neoplastic progression utilizing the K14-HPV16 transgenic mouse model of epithelial carciogenesis. Taking a genetic approach, we have generated HPV16 mice that express human TIMP-1 under the control of the β-actin promoter. Analyses described in this chapter include assays for tumor incidence, *in vivo* proliferation and apoptosis, proteolysis of matrix components and chromosomal copy number changes. Currently, this chapter is being prepared for submission to the journal *Cancer Research.*

ABSTRACT

*T*issue *I*nhibitors of *M*etallo*P*roteinases (TIMPs) are a family of multifunctional proteins known to possess a broad range of biological activities, including inhibition of matrix metalloproteinase (MMP) activity, regulation of proliferation and apoptosis of a variety of cell types, and, depending upon the context, differential regulation of angiogenic and inflammatory responses. Elevated mRNA expression of TIMP family members correlates with malignancy and clinical outcome in many human cancer types; however, a protective role for TIMPs has also been observed in various mouse models of human cancer. In the current study, we found distinct spatial-temporal expression patterns for the mRNA of TIMP family members in a mouse model of epithelial carcinogenesis, i.e. K14-HPV16 transgenic mice. To test the hypothesis that elevated expression of TIMP-1 functionally regulates epithelial carcinogenesis, we introduced a human TIMP-1 transgene into K14-HPV16 transgenic mice and assessed neoplastic progression. Results from these studies suggest that TIMP-1 enhances tumorgenicity by potentiating keratinocyte hyperproliferation and appearance of chromosomal aberrations in premalignant cells, thereby increasing their risk to undergo malignant conversion. In addition, TIMP-1 inhibits tissue gelatinolytic activity in tumor stroma, affects stabilization of collagen fibrils, but does not inhibit malignant conversion of dysplasias into carcinomas or development of metastases. The combined implications of these studies suggest that TIMP-1 is an important contributor to epithelial neoplastic progression and supports the concept that TIMP-1 exerts differential regulation on tissues in a stage-dependent manner.

INTRODUCTION

TIMPs are a family of four multifunctional proteins, numbered in order of their discovery and characterized by a conserved structure ranging from 20 to 30 kDa that inhibit metalloproteinase (MP) activity, specifically matrix metalloproteinase (MMP) activities in a one-to-one stoichiometry [1]. Though named for their ability to inhibit MMP activity, TIMPs also possess other important bioactivities [2,3]. TIMP-1, originally identified for its erythroid potentiating activity [4], induces proliferation in a wide range of cell types [5-7] by mechanisms that are independent of its MMP inhibitory activity [8]. In addition, TIMP-1 is known to promote activation of angiogenesis [9,10], regulate apoptosis [11], amplify inflammation [12] and regulate metastasis formation [13]. Similar pleiotropic activities have also been demonstrated for TIMP-2 [14], TIMP-3 [15] and TIMP-4 [16].

TIMP-1 mRNA expression is upregulated in many human cancer types and in some cases correlates with more severe clinical outcome, e.g., colorectal carcinoma, non-small cell lung carcinoma and breast carcinoma, [17]. Paradoxically, studies in experimental mouse models have revealed that TIMP-1 can exhibit pro- and anti-carcinogenic effects during primary and metastatic tumor development [13,18-23].

In the current study we have sought to critically examine the spatial-temporal expression patterns of TIMP mRNAs and to evaluate the functional significance of TIMP-1 expression during de novo epithelial carcinogenesis utilizing a transgenic mouse model of skin carcinoma development, e.g., K14-HPV16 transgenic mice [24-26]. In K14-HPV16 transgenic mice, the expression of human papillomavirus type 16 (HPV16) early region genes has been targeted to basal keratinocytes [27]; animals are born phenotypically

normal, and by one month of age with 100% penetrance, transgenic skin becomes uniformly hyperplastic. These benign lesions advance focally into broad hyperproliferative dysplastic lesions present in 100% of mice between 4-6 months of age. By one year of age, ~60% of mice develop tumors, 50% of which are squamous cell carcinomas (SCCs) that metastasize to regional lymph nodes with an ~30% frequency, and 10% of which are locally invasive non-metastatic microcystic adnexal carcinomas (MACs). Results from the current study suggest that TIMP mRNAs are not coordinately regulated during the development and progression of skin carcinogenesis in HPV16 mice, and that sustained TIMP-1 expression functionally promotes epithelial carcinogenesis during the early stages of neoplastic progression, while in later stages, it inhibits tissue gelatinolytic activity and stabilizes ECM matrices without affecting primary tumor development or their metastatic spread.

MATERIALS AND METHODS

Animal husbandry, genotype and histopathologic analyses

K14-HPV16 transgenic mice [27], the preparation of tissue sections for histologic examination and the characterization of neoplastic stages based on hematoxylin-eosin histopathology and keratin intermediate filament expression have been described previously [25,26,28,29]. Tissue samples were fixed by immersion in 10% neutral-buffered formalin, dehydrated through graded ethanol and xylenes, embedded in paraffin, cut by a Leica 2135 microtome into 5-μm-thick sections and histopathologically examined following hematoxylin and eosin staining and immunoreactivity of keratin intermediate filaments. Hyperplastic lesions were identified by a two-fold increase in epidermal thickness and an intact granular cell layer with keratohyalin granules; dysplastic lesions were characterized based on basal and spinous cell layers with hyperchromatic nuclei representing greater than half of the total epidermal thickness and incomplete terminal differentiation of keratinocytes, SCC lesions by an abundance of abnormal mitotic figures and an invasive loss of integrity in the basement membrane with clear development of malignant cell clusters proliferating in the dermis. Characterization of infundibular (MACs) and sebaceous lesions (sebaceous adenomas) was as previously described [26].

The βA-hT1 transgenic mice have been described previously [30]. Briefly, these mice contain a transgene where the human β-actin promoter directs expression of a human TIMP-1 cDNA, initially generated in the CD1 mouse strain. To minimize the effect of background strain differences in susceptibility to carcinogenesis, βA-hT1 mice were backcrossed a minimum of six generations into the FVB/n strain prior to

intercrossing with K14-HPV16 mice (FVB/n, N15). The βA-hT1 transgene was followed by PCR genotyping of tail DNA using oligonucleotide primers (5'-TGT GGG ACA CCA GAA GTC AAC-3' and 5'-CTA TCT GGG ACC GCA GGG ACT-3'). DNA was amplified for 30 cycles at 95°C 60 seconds, 59°C 30 seconds, and 72°C 120 seconds, to generate a 480-bp product corresponding to a region within the human TIMP-1 cDNA. In all analyses, HPV16/βA-hT1$^+$ double transgenic mice were compared to littermate controls lacking the βA-hT1 transgene (HPV16/βA-hT1$^-$). P values ≤ 0.05 were considered to be statistically significant.

RNA analysis

Real-time PCR analysis was performed as described previously [26]. Total RNA was extracted with TRIzol reagent™ (Invitrogen) according to the manufacturers recommendations and the method of Chomczynski [31] by powdering fresh-frozen tissue samples in liquid nitrogen, homogenizing with a microtube pestle (USA Scientific), shearing by multiple passages through a syringe and 21-gauge needle (Becton Dickinson), followed by phenol-chloroform extraction and isopropanol precipitation. Quantification of TIMP-1 mRNA levels was performed on three mice per category as previously described [26].

In situ hybridization was performed as described previously [28], using ^{35}S-labelled riboprobes generated from cDNA containing plasmid templates for mouse TIMP-1 [32], mouse TIMP-2 [33], mouse TIMP-3 [34], mouse TIMP-4 [35] and human TIMP-1 [30]. As negative controls, hybridization using sense probes was performed and showed no signal (data not shown).

Protein analysis

Protein lysates were prepared by grinding fresh-frozen tissue samples from ear, tumor or lymph nodes in liquid nitrogen and homogenizing in Tris buffer (25 mM Tris pH 7.6, 5 mM $CaCl_2$, 0.25% Triton X-100) in a 2 ml tissue grinder (Fisher). After centrifugation at 13,000xg at 4°C for 30 minutes, supernatants were measured for protein concentration by the DC protein assay™ (Bio-Rad). Serum samples were prepared by extraction of whole blood, coagulation overnight at 4°C, followed by centrifugation at 700xg at 4°C for 30 minutes to remove cells. ELISA was performed in 96-well Costar plates (Corning), prepared by precoating with a mouse monoclonal anti-human-TIMP-1 antibody (Oncogene Research Products) diluted 1:250 in 50 mM carbonate buffer pH 9.6 at 4°C overnight, followed by blocking in 1% bovine serum albumin in phosphate-buffered saline (BSA/PBS) at room temperature for one hr. Plates were washed with buffer (0.1% BSA, 0.05% Tween-20, in PBS) and incubated with either 10 µl serum or 25 µg protein lysate diluted in wash buffer for 3 hrs. Plates were washed and then processed by incubation with a rabbit polyclonal anti-human TIMP-1 antibody (Biogenesis) diluted 1:1,000 in wash buffer, goat anti-rabbit biotinylated secondary antibody (Pierce) diluted 1:10,000 in wash buffer and ExtrAvidin peroxidase conjugate™ (Sigma) diluted 1:1,000 in blocking buffer. Assays were performed with the Quantikine detection system™ (R&D Systems) by the manufacturers recommendations and quantified at 650 nm on a SpectraMax 340 spectrophotomoter™ (Molecular Devices). Samples were assayed from three mice per category and all experiments were repeated three times.

Gelatinase assay

Protein lysates were generated from fresh-frozen tissue samples, as described above for the ELISA assay. 3.0 μg of protein lysate was incubated at 37°C in reaction buffer (50 mM Tris, pH 7.6, 150 mM NaCl, 5 mM $CaCl_2$, 0.2 mM NaN_3, 0.05% Brij-35) with 400 ng DQ-gelatin (Molecular Probes) in a total volume of 200 μl/well in a 96-well black tissue culture microtitre plate (Falcon). Reactions were incubated for up to 5 hr at 37°C and fluorescence measured (excitation 485 nm, emission 530 nm) every 3 minutes on a SpectraMax Gemini™ spectrophotometer (Molecular Devices) operated by SoftMax Pro 4.3 software (Molecular Devices). MMP inhibition was performed by incubation in the presence of 4 mM 1,10-phenanthroline (Sigma). Tissue lysates from four mice were assayed per category and all experiments were repeated three times.

Substrate zymography

Tissue samples from negative littermate or neoplastically-staged transgenic mice were weighed and then homogenized (1:8 weight to volume) in lysis buffer containing 50 mM Tris-HCl (pH 8.0), 150 mM NaCl, 0.1% NP-40, 0.5% deoxycholate, 0.1% SDS. Soluble and insoluble extracts were separated by centrifugation (10,000xg) and subsequently stored at –80°C. Equivalent amounts of soluble extract were analyzed by gelatin zymography [36] on 10% SDS-polyacrylamide gels copolymerized with substrate (1 mg/ml of gelatin) in sample buffer (2% SDS, 50 mM Tris-HCl, 10% Glycerol, 0.1% Bromophenol Blue, pH 6.8). After electrophoresis, gels were washed 3 times for 30 min in 2.5% Triton X-100, 3 times for 15 min in ddH_2O, incubated overnight at 37°C in 50 mM Tris-HCl, 10 mM $CaCl_2$ (pH 8.2), and then stained in 0.5% Coomassie Blue and

destained in 20% methanol, 10% acetic acid. Negative staining indicates the location of active protease bands. Exposure of proenzymes within tissue extracts to SDS during gel separation procedure leads to activation without proteolytic cleavage [37]. Assays were performed in duplicate.

Picro-Sirius Red staining

Staining of collagen in tissues by Picro-Sirius Red was performed as described previously [38,39]. 5-μm-thick paraffin sections were deparaffinized in xylenes, rehydrated in graded ethanol and stained for one hr in 0.1% (w/v) solution of Sirius Red F3B dissolved in saturated aqueous picric acid. Sections were rinsed in 0.5% glacial acetic acid, dehydrated in graded ethanol and xylenes, and mounted in Cytoseal 60™ (Fisher Scientific). Images were captured at high-magnification under normal illumination and polarized light on a Leica DM-RXA microscope attached to a Leica digital camera operated by OpenLab software™. Presence of mature fibrillar type-I-collagen was assessed from captured images [40,41], using the morphometric quantification technique described previously [42]. Briefly, for each field, an image taken under polarized light was quantified for pixel density using a set threshold for detection of the strongly-birefringent signal indicative of fibrillar collagen. For the same field, an image under brightfield was quantified for exclusion of regions not to be evaluated, i.e. vessel lumen, ear cartilage and epithelial compartments. Calculated values represent the percentage of fibrillar collagen, normalized for stromal area, averaged from four fields per mouse, with six mice per category.

Immunohistochemistry

Immunohistochemical detection of antigens was performed as described previously [28]. To simultaneously detect keratin-5 and bromodeoxyuridine (BrdU)-positive cells in tissues, animals received intraperitoneal injections of BrdU (Roche) dissolved in phosphate-buffered saline (PBS) at 50 μg/g total body weight, 90 minutes before sacrifice and preparation of tissue samples. 5-μm-thick paraffin sections were deparaffinized in xylenes, rehydrated in graded ethanol, boiled in Citra™ antigen retrieval solution (BioGenex), washed in PBS, blocked in 1X Blocking buffer (5% normal goat serum/2.5% bovine serum albumin/PBS), and incubated in a 1:10,000 dilution of a rabbit polyclonal antibody against mouse keratin 5 (Babco) in 0.5X blocking buffer overnight at 4°C, followed by a series of PBS washes, incubation of slides with a biotinylated donkey secondary antibody against rabbit (Pierce), blocking in 0.6% hydrogen peroxide in methanol, conjugation by ABC-Elite™ (Vector) and development in Fast-DAB™ (Sigma). BrdU-positive cells were detected essentially as described by the manufacturers recommendations using the BrdU Labeling Kit II™ (Roche), developed by Vector Red Alkaline Phosphatase Kit™ (Vector), counterstaining by hematoxylin and eosin, dehydrating by graded ethanol and xylenes, and mounted in Cytoseal 60™ (Richard-Allan Scientific). Five fields per mouse were captured at high-magnification (40X) on a Leica DM-RXA microscope attached to a Leica digital camera operated by OpenLab software™ (Improvision). Proliferative index was quantified from five high-power (40X) images per tissue and included five mice per category as the percentage of the BrdU-positive nuclei in keratin-5-positive keratinocytes over the total number of keratin-5-positive keratinocytes.

Apoptotic frequency was assayed on 5-μm-thick paraffin sections, deparaffinized as described above and processed for the TUNEL reaction using the Fluorescein-FragEL DNA fragmentation detection kit (Oncogene Research Products) by the manufacturer's recommendations. Apoptotic index was quantified from five high-power (40X) images per tissue and included five mice per category as the percentage of the TUNEL-positive keratinocytes over the total number of DAPI-stained keratinocytes.

Neutrophils were detected using immunohistochemistry as described previously [2643]. 5-μm-thick paraffin sections were deparaffinized in xylenes, rehydrated in graded ethanol and PBS, digested for three minutes in Proteinase K (DAKO), washed in PBS, blocked in 1X Blocking buffer (5% normal goat serum/2.5% bovine serum albumin/PBS), and incubated in a 1:1,000 dilution of a rat monoclonal antibody against mouse neutrophils (Cedarlane) in 0.5X blocking buffer for two hours. This was followed by a series of PBS washes, incubation of slides with a biotinylated secondary antibody against rat (Vector), conjugation by ABC-AP™ (Vector) and development in NTB/X-phosphate substrate (Roche). Slides were counterstained in eosin, dehydrated by graded ethanol and xylenes, and mounted in Cytoseal 60™ (Richard-Allan Scientific). Five fields per mouse were analyzed at high-magnification (40X) on a Leica DM-RXA microscope attached to a Leica digital camera operated by OpenLab software™ (Improvision). Neutrophil density was quantified for five mice per category as the number of neutrophils per unit stromal area of 1,000 μm^2.

Proliferation assay *in vitro*

Proliferation assays were performed using an immortalized keratinocyte cell line derived from mouse skin, BMK-2 [44] (generously provided by Dr. Stuart Aaronson), and recombinant, bacterially-expressed protein representing the N-terminal domain of human TIMP-1, N-TIMP-1 [45] (generously provided by Dr. Kenneth Brew). BMK-2 cells were cultured in EMEM (BioWhittaker) supplemented with 0.06 mM $CaCl_2$, 8% dialyzed fetal bovine serum (dFBS; Invitrogen), and 10 ng/ml mouse epidermal growth factor (mEGF; Invitrogen), plated at a density of 50,000 cells per well of a 96-well Costar plates (Corning), and allowed to recover for 48 hours in complete medium. Synchronization was performed by serum deprivation in EMEM containing only 0.06 mM $CaCl_2$ and 0.5% dFBS for 48 hours. Induction of proliferation was performed by treatment with increasing concentrations of N-TIMP-1 (0, 8, 20 μg/ml) in EMEM with 0.06 mM $CaCl_2$ and supplemented either with 8% dFBS by itself or with 0.5% dFBS plus 10 ng/ml mEGF. DNA synthesis was quantified at induction and at 18 hours post-induction by incubation in 2 μCi/ml ^{3}H-labelled thymidine (Perkin-Elmer) in EMEM with 0.06 mM $CaCl_2$ and 0.5% dFBS for 2 hours, followed by harvesting on a 96-well cell harvester (Tomtec) and counting on a 1205 Betaplate™ liquid scintillation counter (Wallac). Assays were performed in triplicate.

Confocal fluorescent angiography

Vascular structure was visualized as described previously [26 46]. Mice were injected with 100 μl fluorecein isothiocyanate conjugated *Lycopersicon esculentum* (tomato) lectin (2 mg/ml, Vector Laboratories, FL-1171) via the tail vein followed by cardiac perfusion through the aorta with 30 ml PBS-buffered 4% paraformaldehyde (pH 7.4). Ears were

harvested and the ventral aspect of the ear separated from cartilage, immersion-fixed in PBS-buffered 4% paraformaldehyde (pH 7.4) for 4 hr at 4°C, rinsed briefly in PBS and whole-mounted in Vectashield mounting medium (Vector Laboratories) for fluorescence visualization using a laser scanning confocal Zeiss LSM510 META microscope and analyzed with a Zeiss LSM Image Examiner. Images were captured from three fields per mice, and three mice per category.

Chloroacetate-esterase histochemistry

Enzyme histochemistry to reveal the presence of serine esterase activity in mast cells was performed as described previously [47,48]. 5-μm-thick paraffin sections were deparaffinized in xylenes, rehydrated in graded ethanol and water, and incubated in buffer (0.1 M Veronal acetate, 1% Triton-X100, 0.2% hexazotized pararosanilin, 40 mM NaF, pH 6.3) containing 1 mM Naphthol-chloroacetate (Sigma) for two hours. Slides were washed in water, dehydrated by graded ethanol and xylenes, and mounted in Cytoseal 60™ (Richard-Allan Scientific). Mast cells were quantified as described for neutrophils, from five fields per mouse, five mice per category, as the number of mast cells per unit stromal area of 1,000 μm^2.

Dual-Color Fluorescent In Situ Hybridization (FISH) on Paraffin Sections

Preparation of paraffin sections: Neoplastically staged tissue sections were deparaffinized by incubating slides at 65°C for 30 minutes on a heating block followed by three incubations in xylene for 15 minutes at 50°C. Xylene was removed by three washes in 100% ethanol for 5 minutes at room temperature. After rehydration (two minute

washes in 85%, 70% and 50% ethanol), slides were rinsed in 1X PBS at room temperature, incubated in 1M NaSCN for 8 minutes at 80°C and washed two times in 1X PBS for 5 minutes at room temperature. The sections were digested with 0.1 mg/ml pepsin (Worthington Biochemicals) for 4 minutes at 37°C, rinsed with 1X PBS at 4°C, washed in 1X PBS/0.1% Tween-20 for 5 minutes at room temperature and rinsed in ice cold 1X PBS. The sections were then dehydrated (2 minutes each in 70%, 85% and 100% ethanol), air dried for 15 minutes at 37°C, fixed in Carnoy's solution (3:1 methanol:acetic acid) and air dried for 30 minutes at 37°C. In preparation for hybridization, sections were rehydrated, incubated in 2X SSC for 30 minutes at 37°C, denatured in 50% formamide/2X SSC for 5 minutes at 37°C, dehydrated and then placed on a 37°C slide warmer until the hybridization mixture was added. Once FISH probes were placed on sections, the sections were covered with plastic cover strips and placed in plastic slide holders (American Scientific) containing a strip of Whatman paper (3MM) soaked in 750 µl of 50% formamide/2X SSC pH 7.0. After hybridizing for 48-72 hr at 37°C, the slides were washed in three 10 minute washes consisting of 50% formamide/2X SSC at 45°C, one 10 minute wash in 2X SSC at 45°C, one 10 minute wash in 2X SSC at room temperature, one 10 minute wash in 4X SSC/0.1 % Trition X-100 at room temperature and two 5 minute washes in ddH_20 at room temperature. The sections were then counterstained with 1.0 µM DAPI (Sigma) in 90% glycerol/1X PBS mounting solution.

Preparation of hybridization probes: Probes mapping to consistently amplified regions of chromosome 5 (clone RP23-451L8, coordinates 74787760bp – 74991110bp and clone RP23-118A6, coordinates 17908843bp – 18113246bp; BAC PAC Resource Center at the

Children's Hospital Oakland Research Institute, Oakland, CA) and unchanged regions (chromosome 10 clone CITB-CJ7B-047K7 containing marker D10MIT49 at coordinates 6066401bp - 6066505bp, and clone RP23-421E11, coordinates 81701304bp – 81701622bp; BAC PAC Resource Center at the Children's Hospital Oakland Research Institute, Oakland, CA) as determined by array comparative genomic hybridization (CGHa) analyses were selected. All coordinates are based on the February 2003 freeze of the mouse genome assembly at http://genome.ucsc.edu. DNA templates for FISH probes (200 ng) were digested with Dpn 2 (New England Biolabs), purified with QiaQuick™ PCR purification columns (Qiagen), and random-prime-labeled using the BioPrime™ DNA Labeling kit (Invitrogen) with either Cy3-dUTP (Amersham) or Alexa 488-dUTP (Molecular Probes). The labeled samples were purified separately using G-50 mini spin columns (Amersham), co-precipitated with 50 μg of mouse Cot-1 DNA (Invitrogen) and re-suspended in 20 μl of hybridization buffer (50% formamide/2X SSC/10% dextran sulfate/2% SDS) before denaturation at 72°C for 15 min.

Analysis: Quantification was performed using a Zeiss Axioplan microscope, at 100X magnification, under oil immersion. From the ventral ear leaflet of each animal fifty labeled nuclei were counted from a minimum of four mice per time-point. The data shown reflect the percentage of an average copy number ratio of chromosome 5 (Cy3 signals) to chromosome 10 (Alexa 488 signals) for each animal. To optimize the sensitivity for the low-copy number changes in hyperplasias, scoring was limited to nuclei of basal keratinocytes that were within the first two cell layers adjacent to the basement membrane and that demonstrated hybridization signals for both fluorochromes.

RESULTS

TIMP-1 mRNA expression increases during neoplastic progression in HPV16 transgenic mice.

In studies of human cancer, many groups have documented increased expression of human TIMP-1 mRNA as compared to adjacent premalignant and/or distal normal control tissue [32,49,50]. Using K14-HPV16 transgenic mice [27,28], we sought to examine the spatial and temporal expression patterns of TIMP family members during epithelial neoplastic progression and to determine the functional significance of TIMP-1 during that progression. We utilized real-time PCR to quantify the amount of TIMP-1 mRNA in tissue samples representing distinct stages of neoplastic development, i.e. hyperplastic, dysplastic and SCCs as compared to normal skin (Fig. 1A). These data revealed an incremental increase in TIMP-1 mRNA at each neoplastic stage similar to reports for human carcinoma development [32,49,50].

To determine the spatial and temporal expression patterns of TIMP-1 mRNA expression in neoplastic skin, we utilized *in situ* hybridization analysis on neoplastically staged paraffin-embedded tissue sections (Fig 1B-G). Whereas TIMP-1 mRNA was not observed in non-neoplastic normal skin (Fig 1B), it was detected diffusely within the epidermis and focally in discrete areas of the dermal stroma in hyperplasias and dysplasias (Fig 1C-D). In contrast to the diffuse expression in premalignant tissue, expression of TIMP-1 mRNA was focally increased in malignant keratinocytes at the invasive edges of Grade I and Grade III SCCs with persistent low-level expression in tumor-associated stromal cells (Fig 1E-F). TIMP-1 mRNA was not observed in lymph nodes with or without SCC metastases (Fig 1G).

TIMP mRNAs are not coordinately regulated during squamous carcinogenesis

mRNA expression of TIMP family members is known to be differentially regulated during embryonic development [3] and in some pathologic disease states [51]. To determine if the mRNAs for TIMP-2, –3 or -4 were coordinately expressed with TIMP-1 (spatially and/or temporally), mRNA expression of TIMP-2, -3, and -4 was examined on adjacent tissue sections by *in situ* hybridization analysis (Fig 2). In non-neoplastic normal skin, TIMP-2 and -3 mRNA was present in follicular epithelial cells and peri-cartilage cells (in ear skin) (Fig 2A and G). In hyperplastic and dysplastic skin from HPV16 mice, TIMP-2 mRNA persisted in follicular epithelial cells and was also broadly expressed in interfollicular suprabasal terminally differentiating keratinocytes (Fig 2B-C). In SCCs, mRNA expression of TIMP-2 persisted in stromal cells distal to the epithelial-stromal interface, was highest in keratinocytes of Grade I Well-Differentiated SCCs (Fig 2D), and was also expressed, albeit to a lower degree, in Grade III Poorly-Differentiated SCCs (Fig 2E). Diffuse expression was observed throughout lymph nodes but was not notably altered in metastatic areas (Fig 2F).

In hyperplastic and dysplastic skin, TIMP-3 mRNA expression was observed in the matrix cells at the base of the follicles and in the inner root sheath cells near the axis of the follicles, but was not detected in any other epithelial or stromal cells (Fig 2H-I). In Grade I SCCs, TIMP-3 mRNA was present in keratinocytes at the leading edge of carcinomas but was more abundant in less differentiated Grade III SCCs (Fig 2J-K). In lymph nodes, TIMP-3 was expressed diffusely throughout the nodal tissue (Fig 2L). Expression of TIMP-4 mRNA was not observed in either wildtype skin or any of the

neoplastic stages from HPV16 mice (Fig 2 M-R). These data suggest that TIMP-2, -3 and –4 mRNAs are not coordinately expressed with TIMP-1 mRNA.

TIMP-1 enhances epithelial carcinogenesis

The progressive increase and distinctive spatial expression pattern of TIMP-1 mRNA observed during neoplastic progression in HPV16 mice suggested that TIMP-1 might functionally contribute to neoplastic development by mechanisms distinct from those regulated by TIMP-2 or -3. To test this hypothesis and to assess the functional significance of increased TIMP-1 mRNA expression during neoplastic progression, we took a genetic approach utilizing TIMP-1 transgenic mice where a human TIMP-1 cDNA is regulated by the human beta-actin promoter, i.e. βA-hT1$^+$ transgenic mice [30]. K14-HPV16 transgenic mice were intercrossed with βA-hT1$^+$ mice to generate two cohorts, e.g., single transgenic control (HPV16/βA-hT1$^-$, n = 83) and double transgenic mice (HPV16/βA-hT1$^+$, n = 129).

Histopathologically, HPV16/βA-hT1$^-$ control mice were not significantly different from historic HPV16 transgenic cohorts (n = 297) [26]. With 100% penetrance, HPV16/βA-hT1$^-$ mice developed hyperplastic skin that was visually discernible at weaning, followed by development of focal dysplasias between 4 - 6 months of age (Fig 3B). HPV16/βA-hT1$^-$ mice exhibited a 55% incidence of SCC development and 10% of MAC development by 12 months of age , with the earliest cancers arising by ~4 months of age (Fig 3A-B). Any differences with historic HPV16 transgenic cohorts [26] were most likely the consequence of background strain differences of the original βA-hT1$^+$ strain (CD1) persisting after six generations of backcrossing into the FVB/n strain.

While not altering the latency of progression between neoplastic stages, expression of hTIMP-1 in HPV16/βA-hT1$^+$ mice (Fig. 4A-B) resulted in a significantly increased incidence of tumors (83.0% versus 65.1% in HPV16/βA-hT1$^-$ mice, p = 0.0048, Log-rank analysis; Fig 3A-B), while anatomic location (ear: 35.3% vs. 25.5%; trunk: 49.0% vs. 49.4%; appendages: 25.5% vs. 21.6%) and tumor multiplicity (1.22 vs. 1.10 per mouse) were unchanged. Histopathological analysis of HPV16/βA-hT1$^+$ tumors (papillomas, sebaceous adenomas, SCCs and MACs) revealed that their increased tumorgenicity was due to an increased incidence of SCCs (64.3% vs. 55.4%; p = 0.0342, Log-rank analysis) and MACs (21.7% vs. 10.8%, p = 0.0131, Log-rank analysis), while SCC grade (Fig. 3C) and frequency of lymphatic metastases were similar to the historical HPV16 and single transgenic HPV/βA-hT1$^-$ cohorts (Fig. 3B).

Decreased MMP activity and increased matrix stability in HPV16/βA-hT1$^+$ mice

The observed increase of SCCs and MACs in HPV16/βA-hT1$^+$ mice suggested that TIMP-1 potentiated the frequency of malignant conversion; however, the underlying biological mechanisms involved in this potentiation were not clear. We next assessed how increased TIMP-1 expression might differentially regulate malignant conversion and perhaps distinct biological pathways (Fig. 4 - 7).

To determine how presence of hTIMP-1 protein correlated with altered neoplastic progression in HPV16/βA-hT1$^+$ mice, we first utilized an ELISA to determine the amount of hTIMP-1 in (non-HPV16) βA-hT1$^+$ serum (Fig, 4A) as well as in neoplastically-staged tissue lysates from HPV16/βA-hT1$^+$ mice and found that hTIMP-1 protein increased from ~0.5 ng/mg in hyperplastic skin to ~1.5 ng/mg in carcinomas (Fig.

4B). Since the most notable bioactivity (at high concentrations) of TIMP-1 is its ability to inhibit metalloproteinase (MP) activity [1], we asked whether the increased levels of hTIMP-1 in dysplasias and/or SCCs altered MP activity in those tissues. To test this, we utilized an *in vitro* gelatinase assay to determine total gelatinolytic activity in HPV16/βA-hT1$^+$ and HPV16/βA-hT1$^-$ tissues derived from distinct stages of neoplastic progression (Fig 4C). In early hyperplastic and dysplastic tissues, gelatinolytic activity was not significantly different between lysates derived from the two cohorts (Fig. 4C). In contrast, carcinoma tissue lysates derived from HPV16/βA-hT1$^-$ had an increase in total gelatinolytic activity compared to lysates from histopathologically similar HPV16/βA-hT1$^+$ carcinomas (89.5 vs. 51.1 RFU/minute/μg, $p = 0.0392$, Mann-Whitney two-tailed analysis; Fig 4C), while not demonstrating any changes in abundance of either pro- or active forms of MMP-2 and MMP-9 (Fig. 4D). In combination, these data suggested that increased hTIMP-1 levels in HPV16/βA-hT1$^+$ carcinomas (~1.5 ng/mg) was sufficient to inhibit gelatinolytic activity present in SCCs by post-translational inhibition of gelatinolytic MMPs.

To functionally assess whether ECM architecture was altered in HPV16/βA-hT1$^+$ dysplasias and/or carcinomas resulting from decreased gelatinolytic activity *in vivo*, we examined the status of collagen fibrils *in situ* histologically by Picro-Sirius Red staining [38,39], an analysis that allows distinction between thinner reticular collagen versus thicker collagen fibrils, based on colored birefringence differences (Fig. 5) [40,41]. Qualitatively, polarization microscopic analysis of the Picro-Sirius Red staining in dysplasias and carcinomas from HPV16/βA-hT1$^-$ mice suggested that stroma adjacent to dysplasias (Fig. 5A) and tumor nests (Fig. 5 C) contained a combination of thick and thin collagen fibers

that were predominately weakly birefringent. In contrast, in HPV16/βA-hT1$^+$ mice, stroma adjacent to dysplastic epidermis (Fig. 5B) and within carcinomas (Fig. 5D) was almost devoid of thin weakly birefringent collagen fibers, but was instead composed predominately of more intensely-birefringent, thicker fibers. Quantitative morphometric analysis of the Picro-Sirius Red staining between the two cohorts was significantly different at both the dysplastic and carcinoma stages, with a greater than 2-fold increase in the percentage of the intensely-birefringent collagen fibers in the HPV16/βA-hT1$^+$ carcinomas (6.5% vs. 15.0%; p = 0.0317, Mann-Whitney two-tailed analysis) and an ~1.8-fold increase at the dysplastic stage (37.0% vs. 69.1%; p = 0.0043, Mann-Whitney two-tailed analysis). Taken together, these data suggest that although elevated levels of TIMP-1 in dysplasias and carcinomas stabilizes collagenous ECM in HPV16/βA-hT1$^+$ mice, it does not impede conversion of premalignant dysplasias into carcinomas, invasion of carcinomas into ectopic stroma or, metastatic spread of primary carcinomas.

TIMP-1 potentiates keratinocyte hyperproliferation

Acquisition of a hyperproliferative state is an intrinsic property of many neoplastic cell types [52]. Accordingly, we have previously reported that keratinocyte hyperproliferation incrementally increases during neoplastic progression in HPV16 mice and, in part, characterizes progression between premalignant stages [27,28]. In addition, we have shown that keratinocyte hyperproliferation can be attenuated by ablating MMP-9 activity in HPV16 mice, and in so doing decreases the incidence of SCCs [25]. Since TIMP-1 regulates MMP-9 activity *in vivo* and *in vitro* [1] and inhibits tissue gelatinase activity *in vivo* (Fig 4C), while also demonstrating mitogenicity towards keratinocytes, albeit

indirectly [6,53], we sought to determine if the increased tumor incidence in HPV16/βA-hT1$^+$ mice was associated with either an enhanced keratinocyte proliferation index or alternatively if increased expression of TIMP-1 in HPV16 mice phenocopied our previous results with HPV16/MMP-9 homozygous null mice and attenuated keratinocyte proliferation [25]. To test these hypotheses, we examined keratinocyte proliferative indices in hyperplastic, dysplastic, SCCs and their lymphatic metastases in HPV16/βA-hT1$^+$ and control mice (Fig 6). Qualitatively, BrdU-immunoreactivity of tissue sections suggested that in hyperplastic and dysplastic tissues of HPV16/βA-hT1$^+$ mice, a higher percentage of keratinocytes were proliferating (BrdU-positive, red staining) as compared to histopathologically-matched HPV16/βA-hT1$^-$ littermates at all neoplastic stages (Fig. 6A-H). Quantification of BrdU-positive keratinocytes *in situ* supported this observation and suggested that HPV16/βA-hT1$^+$ keratinocytes in early hyperplastic tissue (1-mo of age) attained a hyperproliferative state (23.9% in HPV16/βA-hT1$^+$ vs. 16.3% in HPV16/βA-hT1$^-$, $p = 0.023$, Mann-Whitney; compare Fig. 6B and 6F) more commonly associated with later dysplastic tissue characteristic of 6-mo old transgenic HPV16/βA-hT1$^-$ animals (Fig. 6I; compare Fig. 6F with 6C). At the later time point in dysplastic HPV16/βA-hT1$^+$ skin, hyperproliferation indices more resembled carcinomas than dysplastic epidermis (24.1% in HPV16/βA-hT1$^+$ vs. 18.5% in HPV16/βA-hT1$^-$, $p = 0.014$, Mann-Whitney; compare Fig. 6C and 6G); however, following malignant conversion, differences between the two genotypes were indistinguishable (Fig. 6I).

To determine how transgenic expression of hTIMP-1 regulates the observed keratinocyte hyperproliferation *in vivo* in premalignant HPV16/βA-hT1$^+$ skin, we sought to determine if hTIMP-1 regulated proliferation of mouse keratinocytes in culture

directly. Previous reports have revealed that human TIMP-1 protein can induce proliferation in primary cultures of epidermal keratinocytes [6,53], and that this mitogenic ability is contained within the N-terminal domain of the protein [8]. To test the hypothesis that TIMP-1 protein would induce proliferation *in vitro* in mouse keratinocytes, we assayed the mitogenic effects of the N-terminal domain of human TIMP-1 protein (N-TIMP-1), [45] on BMK-2 cells—an immortalized cell line derived from primary mouse epidermal keratinocytes that are dependent on mouse epidermal growth factor (mEGF) for proliferation [44]. In agreement with previous reports [6,53] our analyses revealed that human TIMP-1 protein alone was insufficient to induce proliferation in non-transformed keratinocytes, but potentiated keratinocyte proliferation and entry into S-phase in a dose-dependent fashion when provided in the presence of mEGF (Fig 6J). These data suggest that TIMP-1 induces keratinocyte hyperproliferation *in vitro* (and *in vivo*) by indirect mechanisms.

Cell number in tissues increases only when the proliferative index is not balanced by an increased apoptotic index. Since TIMP-1 may regulate apoptosis in some contexts [54,55], we asked if the increased proliferative index observed in HPV16/βA-hT1$^+$ mice was due to an altered apoptotic frequency. Accordingly, keratinocyte apoptotic index was quantified utilizing the TUNEL assay on staged neoplastic tissue sections adjacent to those previously utilized to assess proliferation, and revealed that apoptotic indices were similar in HPV16/βA-hT1$^+$ mice and their littermate controls at all stages of neoplastic development in histopathologically-matched sections (Fig 6K). Taken together, these data imply that the increased proliferation index observed during early neoplastic

progression in HPV16/βA-hT1$^+$ was the result of the mitogenic properties, direct or indirect, of TIMP-1 and independent of apoptotic cell death by TIMP-1 in this system.

No effect of transgenic TIMP-1 on vascular architecture or inflammation in HPV16/βA-hT1$^+$ mice.

Since TIMP-1 can regulate activation of angiogenesis and recruitment of inflammatory cells in some contexts [32] and since we have previously reported angiogenesis and inflammation to be rate-limiting stage-specific characteristics of neoplastic progression in HPV16 transgenic mice [25,26,48], we also assessed the onset and organization of angiogenic vasculature during neoplastic progression and the profile of inflammatory cells infiltrating neoplastic tissue (Fig 7) . The overall density and structure of the vasculature, visualized by confocal fluorescent angiography, increased incrementally during premalignant progression, as previously demonstrated [26], but without any significant differences between HPV16/βA-hT1$^-$ and HPV16/βA-hT1$^+$ mice (compare Fig 7 A-C with D-F). Furthermore, we found no quantifiable differences in terms of infiltration by mast cells (Fig 7G) or neutrophils (Fig 7H) between the two cohorts. Our interpretation of these data is that the increased tumorigenicity in HPV16/βA-hT1$^+$ mice most likely does not result from TIMP-1-induced alterations in vascular structure or inflammatory infiltration.

Accelerated onset of genomic instability in hyperplastic HPV16/βA-hT1$^+$ mice

Recurrent genome copy number aberrations in proliferating neoplastic cells are a common feature of human and murine cancers and are believed to contribute to tumor

evolution by copy-number-induced alterations in gene expression [56-58]. Utilizing array-based comparative genomic hybridization (CGH) analysis [57] to examine the complexity of genomic copy number changes associated with epithelial carcinogenesis in HPV16 mice, we found recurrent copy number gains on Chromosome (Ch.) 5 in 55 % of SCCs, while copy number changes on Ch. 10 are rare and occur in less than 1% of carcinomas examined (n = 22) (Diaz et al., manuscript submitted). Since low-level expression of TIMP-1 in early premalignant tissue potentiates keratinocyte hyperproliferation, we determined if it might also potentiate appearance of an aneuploid genotype and thereby enhance malignant risk. We utilized dual-color fluorescent *in situ* hybridization (FISH) analysis with markers for Ch. 5 and Ch.10 on hyperplastic and dysplastic tissue sections from 1-mo old and 6-mo old HPV16/βA-hT1$^+$ and HPV16/βA-hT1$^-$ mice (Fig 7). A total of 50 FISH measurements were taken from each tissue, four to six tissues were examined for each histopathologic stage, and two independent loci were examined for each chromosome.

Chromosome 5 and 10 FISH analysis of nuclei in 1-mo old hyperplastic HPV16/βA-hT1$^-$ keratinocytes showed a negligible increase in Ch. 5 signals relative to Ch. 10 compared to nuclei in negative littermate diploid control tissue, whereas nuclei of 6-mo old dysplastic keratinocytes in HPV16/βA-hT1$^-$ tissue showed a significant relative increase in Ch. 5 signals ($p = 0.0095$, Mann-Whitney two-tailed) compared to the same negative littermate control tissue (Fig 7A and C). In contrast, Ch. 5 and 10 FISH analysis of 1-mo old HPV16/βA-hT1$^+$ hyperplasias revealed a significant relative increase of Ch. 5 signals ($p = 0.0286$, Mann-Whitney two-tailed) that became more pronounced in later dysplastic keratinocytes ($p = 0.0159$, Mann-Whitney two-tailed) (Fig 7C). The increased

copy number level of Ch. 5 in hyperplastic HPV16/βA-hT1$^+$ epidermis ranged from three to seven copies, suggesting that chromosomal aberrations, more typically observed in dysplastic keratinocytes of older HPV16 transgenic mice (6-mo), occur at an earlier age and stage in HPV16/βA-hT1$^+$ mice coincident with increased keratinocyte hyperproliferation in 1-mo hyperplastic epidermis.

DISCUSSION

The present study reveals that TIMP-1 functionally contributes to epithelial cancer development in tumor-prone transgenic mice by MMP-dependent and MMP-independent mechanisms and is not coordinately regulated with other TIMP family members. We found that TIMP-1 enhanced keratinocyte hyperproliferation and accelerated appearance of genomic copy number abnormalities in early premalignant cells, thereby enhancing their susceptibility to undergo malignant conversion. In addition, in fully malignant tissue TIMP-1 effectively inhibited (MMP) gelatinolytic activity, stabilized collagen matrices *in vivo*, but did not inhibit invasion of malignant cells into ectopic tissue compartments or metastatic spread of primary carcinomas. The combined implications of these data are that, dependent upon its level of expression and the stage of neoplastic progression, TIMP-1 can enhance neoplastic risk while simultaneously stabilizing tumor stroma, and provides additional evidence that late-stage therapies mimicking TIMP-1 inhibition of MMP activity will have limited clinical efficacy.

TIMP-1 and inhibition of metalloproteinase activity

Enzymes that initiate remodeling of the ECM have long been viewed as being essential for tumor development [59-61]. Neoplastic cells were initially thought to produce these enzymes, thus permitting invasion into ectopic tissues, entry and exit from vasculature and metastasis to distant organs. MMPs were prime candidates for these activities since MMP family members collectively degrade all structural components of the ECM (*in vitro*) and were found to have increased expression and activity in tissues undergoing various types of pathologic remodeling including cancer [62]. Further evidence supporting the hypothesis that MMPs were critical regulators of invasion and metastasis came from studies of their natural tissue inhibitors, TIMPs. Several groups demonstrated that either overexpression of TIMPs or intraperitoneal injection of recombinant TIMP-1 reduced experimental metastasis formation [63-68], while functional studies exploiting transgenic technology further revealed TIMP/MMP significance during carcinogenesis, e.g., TIMP-1 overproduction slowed chemical carcinogenesis in skin [69] and inhibited SV40 large T antigen (T-Ag)-induced liver [70] and MMP-3/stromelysin-induced mammary carcinogenesis [19,71]. Paradoxically however, elevated TIMP-1 mRNA expression was also reported to correlate with malignant progression and poor clinical prognosis of several human cancers [11,72,73].

To determine if increased TIMP-1 expression would slow de novo carcinogenesis as initially hypothesized, or alternatively, potentiate carcinogenesis as suggested by observations associating TIMP-1 with poor clinical outcome, we took a genetic approach using a mouse model of epithelial carcinogenesis harboring a TIMP-1 transgene. Results from the current study provide insight into the duality of TIMP-1 as a modifier of neoplastic progression and highlight the irrelevance of inhibiting MMP activity once

solid tumors have already formed. Expression of TIMP-1 in malignant lesions of HPV16 mice is an efficacious inhibitor of gelatinase activity (Fig 4) and effectively stabilizes collagen matrices in neoplastic tissue—effects that are consistent with TIMP-1 acting as an MP-inhibitor. Nevertheless, some MMP proteolytic activity is detectable in the SCCs of HPV16/βA-hT1$^+$ mice (Fig 4), indicating that MMP activity is not completely abrogated in these mice and that perhaps higher levels of MMP inhibition may be necessary to attenuate neoplastic progression—a possibility which could be tested by the use of HPV16/βA-hT1$^+$ mice with an additional copy of the TIMP-1 transgenic allele. However, the net effect of these bioactivities, given the level of MMP inhibition in HPV16/βA-hT1$^+$ mice, is without consequence in limiting malignant conversion, malignant growth or metastatic spread of carcinomas - results that are remarkably similar to those reported for human clinical trials testing the efficacy of MPIs in patients with late-stage neoplastic disease [74,75]. In these trials, treatment with synthetic MP inhibitors generally failed to show any benefit compared to placebos in terms of overall survival or time to progression in cancer patients presenting with late-stage disease [76,77].

Matrisian and colleagues compared the effects of transgenic TIMP-1 expression in a mouse model of intestinal neoplasia [78] and similarly found that TIMP-1 enhanced tumor multiplicity; however, when those same mice were treated throughout neoplastic progression with batimastat, a broad spectrum MPI [79], there was a reduction in tumorgenicity [78]. This seeming paradox can be explained by the fact that TIMP-1 is a multifunctional protein whose activities include inhibition of MP activity at high concentration as opposed to mitogenic activities at lower concentrations [2,45], in contrast to batimastat which primarily functions as an MP inhibitor. One interpretation of these

data is that inhibiting MP activity might be more efficacious if performed prior to the emergence of malignant disease. This hypothesis in fact has been born out by Bergers and colleagues [80]: treatment of pancreatic islet carcinomas with batimastat was without effect on the persistence or continued growth of malignant tumors, whereas treatment of precursor hyperplastic lesions reduced their progression into more advanced angiogenic dysplasias, suggesting that the effective window for targeting MP activity as an anti-cancer strategy is early in the neoplastic cascade. When combined with functional studies examining transgenic mouse models of de novo carcinogenesis harboring homozygous null mutations in individual MMP genes [25,81,82], the implication is that targeting MMPs with synthetic inhibitors would yield more desirable outcomes if performed prior to overt tumor formation.

Pro-cancer activities of TIMP-1: Proliferation and chromosome instability

If TIMP-1 effectively inhibits MP activity *in vivo*, why then is enhanced expression of TIMP-1 pro-tumorigenic? Our findings suggest that induction of hyperproliferation versus inhibition of proteolytic activity are stage-dependent responses to TIMP-1 in HPV16 transgenic mice and represent *in vivo* evidence separating MMP-dependent from MMP-independent pro-cancer roles for TIMP-1 during carcinogenesis.

Previous reports utilizing *in vitro* cell culture assays have demonstrated (indirect) mitogenic properties of TIMP-1 in a wide range of cell types [5,7] including keratinocytes [6,53]. *In vitro* proliferation experiments using altered, non-inhibitory versions of TIMP-1 [8,11] revealed that TIMP-1's mitogenic properties are separate and distinct from its MMP inhibitory capabilities. Structurally, the first three loops of TIMP-1, being defined by the

disulfide linkages and constituting the N-terminal domain of the protein, have been shown to be crucial for MMP inhibition [83,84]. The mitogenic properties, on the other hand, have not been mapped to specific residues [8] and appears resistant to gross structural alterations such as reduction and alkylation of the protein [11]. Moreover, in addition to interacting with MMPs, TIMP-1 binds to a non-MMP cell surface protein with high-affinity (K_d = 100 pM), that is believed to mediate its erythroid potentiating activity [7].

Diverse mechanisms have been suggested for how TIMP-1 might regulate proliferation *in vivo* in addition to its indirect mitogenic properties [6,7,11,53,85]. In a mammary carcinoma transplantation model, TIMP-1 expression correlated with enhanced epithelial proliferation largely due to increased expression of VEGF-A mRNA and enhanced angiogenesis [86]. In contrast, using lymphoma cells, TIMP-1 was found to stimulate tumor growth by reciprocally decreasing apoptotic indices [87]. Paradoxically, in a mouse model of intestinal neoplasia, e.g., *min* mice, enhanced TIMP-1 expression resulted in increased tumor multiplicity [23]; however, changes in the proliferative status of neoplastic cells and angiogenesis were not examined. Our data suggest that in HPV16 mice, TIMP-1 expression can enhance epithelial proliferation, while not affecting epithelial apoptosis (Fig. 6) or development of angiogenic vasculature (Fig. 7).

How does increased hyperproliferative activity due to TIMP-1 translate into increased tumorgenicity in HPV16 mice or in mice predisposed to intestinal neoplasia? Mechanisms linking cell division and aneuploidy have been well characterized [88,89] and include, for example, errors in chromosome segregation during mitosis due to aberrant

centrosome duplication [90,91]. Regarding mechanisms of carcinogenesis resulting from HPV-induced tumorgenicity, it has been reported that the HPV oncoprotein E7 induces cell-division-associated aneuploidy by enhancing the activity of cdk2/cyclin E and cdk2/cyclin A complexes, both of which are involved in regulating centrosome duplication *in vivo* [92]. Thus, when the potential for chromosomal instability has been primed (by E7-induced centrosome errors), our data support a model in which low-level expression of TIMP-1 enhances keratinocyte hyperproliferation and results in a higher fraction of aneuploid cells at risk to undergo malignant conversion due to earlier accumulation of E7-induced chromosomal aberrations. Perhaps in human cancers, as in the HPV16 and *min* mouse models, late-stage MMP inhibition is not sufficient to block neoplastic cells that have already been genomically "de-programmed" resulting in loss of cell cycle check point control, hyperproliferation, and other events involved in malignant conversion. Premalignant chromosomal aberrations have been detected in a number of human malignancies [93-95] and notably, in early head and neck squamous cell carcinoma provide a predictive value for malignant conversion [96,97]. Taken together, and in conjunction with results from the present study, we suggest that of the many events that must take place in order to produce a bone fide tumor, intrinsic genomic changes involved in manifesting cancer likely occur at a very early stage in the evolutionary process, and in part, set the stage for further deregulation of cell intrinsic events involved in carcinogenesis. In HPV16 mice at least, genomic aberrations could represent one of these intrinsic neoplastic events subject to regulation by TIMP-1-induced hyperproliferation. Given the observation that TIMP-1 assumes a nuclear localization following plasma membrane binding in some cell types [98,99], we cannot rule out the

possibility that TIMP-1 may also directly (or indirectly) affect chromosome integrity in E6/E7-positive keratinocytes in HPV16 mice; however, examining this possibility awaits generation of reagents capable of detecting TIMP-1 protein localization *in situ*.

Multiplicity of pathways in HPV16 mice

If increased TIMP-1 potentiates neoplastic risk, does homozygous loss of TIMP-1 attenuate that same risk? We addressed this question by intercrossing HPV16 mice into a TIMP-1 homozygous null background [100], and found no discernible difference between HPV16/T1$^{-/-}$ (n = 51) and HPV16/T1$^{+/-}$ (n = 109) cohorts (Rhee and Coussens, unpublished observations; Chapter 4). Our interpretation of this seeming disparity illuminates the functional contribution of TIMP-1 as a modifier of carcinogenesis that is sufficient, but is not necessary for promoting the multiplicity of changes occurring during tumor development. We hypothesize that these data support a model reflecting the fact that multiple, discrete pathways must be altered and/or activated for full progression to the tumor state, and furthermore, that a minimal number or combination of these pathways must be compromised in order to exert a detectable attenuation in tumorigenesis. Hence, one implication of this is that factors such as MMP-9 would participate in multiple pathways (Chapter 5) whereas TIMP-1 on the other hand, exerts regulatory pressure on fewer pathways necessary for manifesting a tumor. In conclusion, the findings described here suggest that during *de novo* epithelial carcinogenesis, TIMP-1 functionally enhances neoplastic progression irrespective of its ability to inhibit MMP activity. Hence, therapeutic strategies based upon exploiting

ACKNOWLEDGEMENTS

We extend thanks to Zena Werb for generously providing βA-hT1$^+$ transgenic mice, Jake Lee and Andre Whitkin for technical assistance, Joe Gray, Zena Werb, Koei Chin, and members of the Coussens laboratory for fruitful discussion and critical comments. JSR was supported by the UCSF Medical Scientist Training Program and a UC Regents Fellowship. LMC was supported by grants from the National Cancer Institute, The Hellman Family and the American Association for Cancer Research.

REFERENCES

1. Woessner, J.F. & Nagase, H. *Matrix metalloproteinases and TIMPs*, (Oxford University Press, Oxford, UK, 2000).

2. Brew, K., Dinakarpandian, D. & Nagase, H. Tissue inhibitors of metalloproteinases: evolution, structure and function. *Biochim.Biophys.Acta* **1477**, 267-283 (2000).

3. Fassina, G. *et al.* Tissue inhibitors of metalloproteases: regulation and biological activities. *Clin Exp Metastasis* **18**, 111-120 (2000).

4. Docherty, A.J. *et al.* Sequence of human tissue inhibitor of metalloproteinases and its identity to erythroid-potentiating activity. *Nature* **318**, 66-69. (1985).

5. Hayakawa, T., Yamashita, K., Tanzawa, K., Uchijima, E. & Iwata, K. Growth-promoting activity of tissue inhibitor of metalloproteinases-1 (TIMP-1) for a wide range of cells. A possible new growth factor in serum. *FEBS Lett* **298**, 29-32. (1992).

6. Bertaux, B., Hornebeck, W., Eisen, A.Z. & Dubertret, L. Growth stimulation of human keratinocytes by tissue inhibitor of metalloproteinases. *J Invest Dermatol* **97**, 679-685 (1991).

7. Avalos, B.R. *et al.* K562 cells produce and respond to human erythroid-potentiating activity. *Blood* **71**, 1720-1725 (1988).

8. Chesler, L., Golde, D.W., Bersch, N. & Johnson, M.D. Metalloproteinase inhibition and erythroid potentiation are independent activities of tissue inhibitor of metalloproteinases-1. *Blood* **86**, 4506-45015 (1995).

9. Yamada, E. *et al.* TIMP-1 promotes VEGF-induced neovascularization in the retina. *Histol Histopathol* **16**, 87-97. (2001).

10. Thorgeirsson, U.P., Yoshiji, H., Sinha, C.C. & Gomez, D.E. Breast cancer; tumor neovasculature and the effect of tissue inhibitor of metalloproteinases-1 (TIMP-1) on angiogenesis. *In Vivo* **10**, 137-144. (1996).

11. Guedez, L. *et al.* Tissue inhibitor of metalloproteinases 1 regulation of interleukin-10 in B-cell differentiation and lymphomagenesis. *Blood* **97**, 1796-1802 (2001).

12. Apparailly, F. *et al.* Paradoxical effects of tissue inhibitor of metalloproteinases 1 gene transfer in collagen-induced arthritis. *Arthritis Rheum* **44**, 1444-1454 (2001).

13. Kruger, A. *et al.* Host TIMP-1 overexpression confers resistance to experimental brain metastasis of a fibrosarcoma cell line. *Oncogene* **16**, 2419-2423. (1998).

14. Valente, P. *et al.* TIMP-2 over-expression reduces invasion and angiogenesis and protects B16F10 melanoma cells from apoptosis. *Int J Cancer* **75**, 246-253 (1998).

15. Smith, M.R., Kung, H., Durum, S.K., Colburn, N.H. & Sun, Y. TIMP-3 induces cell death by stabilizing TNF-alpha receptors on the surface of human colon carcinoma cells. *Cytokine* **9**, 770-780 (1997).

16. Jiang, Y. *et al.* Stimulation of mammary tumorigenesis by systemic tissue inhibitor of matrix metalloproteinase 4 gene delivery. *Cancer Res* **61**, 2365-2370. (2001).

17. Curran, S. & Murray, G.I. Matrix metalloproteinases in tumour invasion and metastasis. *J Pathol* **189**, 300-308 (1999).

18. Martin, D.C. *et al.* Transgenic TIMP-1 inhibits simian virus 40 T antigen-induced hepatocarcinogenesis by impairment of hepatocellular proliferation and tumor angiogenesis. *Lab Invest* **79**, 225-234 (1999).

19. Sternlicht, M.D. *et al.* The stromal proteinase MMP3/stromelysin-1 promotes mammary carcinogenesis. *Cell* **98**, 137-146 (1999).

20. Buck, T.B., Yoshiji, H., Harris, S.R., Bunce, O.R. & Thorgeirsson, U.P. Overexpression of tissue inhibitor of matrixmetalloproteinases-1 (TIMP-1) in metastatic MDCK cells transformed by v-src. *Ann N Y Acad Sci* **878**, 732-735 (1999).

21. Kawamata, H. *et al.* Over-expression of tissue inhibitor of matrix metalloproteinases (TIMP1 and TIMP2) suppresses extravasation of pulmonary metastasis of a rat bladder carcinoma. *Int J Cancer* **63**, 680-687. (1995).

22. Watanabe, M. *et al.* Inhibition of metastasis in human gastric cancer cells transfected with tissue inhibitor of metalloproteinase 1 gene in nude mice. *Cancer* **77**, 1676-1680 (1996).

23. Heppner-Goss, K.J., Brown, P.D. & Matrisian, L.M. Differing effects of endogenous and synthetic inhibitors of metalloproteinases on intestinal tumorigenesis. *Int J Cancer* **78**, 629-635 (1998).

24. Coussens, L.M., Hanahan, D. & Arbeit, J.M. Genetic predisposition and parameters of malignant progression in K14- HPV16 transgenic mice. *Am J Path* **149**, 1899-1917 (1996).

25. Coussens, L.M., Tinkle, C.L., Hanahan, D. & Werb, Z. MMP-9 supplied by bone marrow-derived cells contributes to skin carcinogenesis. *Cell* **103**, 481-490 (2000).

26. van Kempen, L.C.L. *et al.* Epithelial carcinogenesis: dynamic interplay between neoplastic cells and their microenvironment. *Differentiation* **70**, 501-623 (2002).

27. Arbeit, J.M., Munger, K., Howley, P.M. & Hanahan, D. Progressive squamous epithelial neoplasia in K14-human papillomavirus type 16 transgenic mice. *J Virol* **68**, 4358-4368 (1994).

28. Coussens, L.M., Hanahan, D. & Arbeit, J. Genetic predisposition and parameters of malignant progression in K14-HPV16 transgenic mice. *Am J Path* **149**, 1899-1917 (1996).

29. Daniel, D. *et al.* Immune enhancement of skin carcinogenesis by CD4+ T cells. *J Exp Med* **197**(2003).

30. Alexander, C.M., Howard, E.W., Bissell, M.J. & Werb, Z. Rescue of mammary epithelial cell apoptosis and entactin degradation by a tissue inhibitor of metalloproteinases-1 transgene. *J Cell Biol* **135**, 1669-1677 (1996).

31. Chomczynski, P. A reagent for the single-step simultaneous isolation of RNA, DNA and proteins from cell and tissue samples. *Biotechniques* **15**, 532-534, 536-537 (1993)..

32. Edwards, D.R. The tissue inhibitors of metalloproteinases (TIMPs). in *Matrix Metalloproteinase Inhibitors in Cancer Therapy* (eds. Clendeninn, N.J. & Appelt, K.) 67-84 (Humana Press, Totowa, New Jersy, 2000).

33. Shimizu, S. *et al.* Cloning and sequencing of the cDNA encoding a mouse tissue inhibitor of metalloproteinase-2. *Gene* **114**, 291-292 (1992).

34. Apte, S.S. *et al.* Gene encoding a novel murine tissue inhibitor of metalloproteinases (TIMP), TIMP-3, is expressed in developing mouse epithelia, cartilage, and muscle, and is located on mouse chromosome 10. *Dev Dyn* **200**, 177-197 (1994).

35. Leco, K.J. *et al.* Murine tissue inhibitor of metalloproteinases-4 (Timp-4): cDNA isolation and expression in adult mouse tissues. *FEBS Lett* **401**, 213-217. (1997).

36. Herron, G.S., Werb, Z., Dwyer, K. & Banda, M.J. Secretion of metalloproteinases by stimulated capillary endothelial cells. I. Production of procollagenase and prostromelysin exceeds expression of proteolytic activity. *J Biol Chem* **261**, 2810-2813 (1986).

37. Herron, G.S., Banda, M.J., Clark, E.J., Gavrilovic, J. & Werb, Z. Secretion of metalloproteinases by stimulated capillary endothelial cells. II. Expression of collagenase and stromelysin activities is regulated by endogenous inhibitors. *J Biol Chem* **261**, 2814-2818. (1986).

38. Canham, P.B., Finlay, H.M., Kiernan, J.A. & Ferguson, G.G. Layered structure of saccular aneurysms assessed by collagen birefringence. *Neurol Res* **21**, 618-626 (1999).

39. Junqueira, L.C., Bignolas, G. & Brentani, R.R. Picrosirius staining plus polarization microscopy, a specific method for collagen detection in tissue sections. *Histochem J* **11**, 447-455. (1979).

40. Puchtler, H., Waldrop, F.S. & Valentine, L.S. Polarization microscopic studies of connective tissue stained with piscro-sirius red FBA. *Peitr. Path. Bd.* **150**, 174-187 (1973).

41. Junqueira, L.C., Cossermelli, W. & Brentani, R. Differential staining of collagens type I, II and III by Sirius Red and polarization microscopy. *Arch Histol Jpn* **41**, 267-274 (1978).

42. Malkusch, W., Rehn, B. & Bruch, J. Advantages of Sirius Red staining for quantitative morphometric collagen measurements in lungs. *Exp Lung Res* **21**, 67-77. (1995).

43. Ducharme, A. *et al.* Targeted deletion of matrix metalloproteinase-9 attenuates left ventricular enlargement and collagen accumulation after experimental myocardial infarction. *J Clin Invest* **106**, 55-62 (2000).

44. Coffey, R.J., Jr. *et al.* Growth modulation of mouse keratinocytes by transforming growth factors. *Cancer Res* **48**, 1596-1602 (1988).

45. Huang, W. *et al.* Folding and characterization of the amino-terminal domain of human tissue inhibitor of metalloproteinases-1 (TIMP-1) expressed at high yield in E. coli. *FEBS Lett* **384**, 155-161 (1996).

46. Thurston, G., Baluk, P., Hirata, A. & McDonald, D.M. Permeability-related changes revealed at endothelial cell borders in inflamed venules by lectin binding. *Am J Physiol* **271**, 2547-2562 (1996).

47. Leder, L.D. The chloroacetate esterase reaction. A useful means of histological diagnosis of hematological disorders from paraffin sections of skin. *Am J Dermatopathol* **1**, 39-42. (1979).

48. Coussens, L.M. *et al.* Inflammatory mast cells up-regulate angiogenesis during squamous epithelial carcinogenesis. *Genes Dev* **13**, 1382-1397 (1999).

49. Polette, M., Clavel, C., Birembaut, P. & De Clerck, Y.A. Localization by in situ hybridization of mRNAs encoding stromelysin 3 and tissue inhibitors of metallo-proteinases TIMP-1 and TIMP-2 in human head and neck carcinomas. *Pathol Res Pract* **189**, 1052-1057. (1993).

50. Charous, S.J., Stricklin, G.P., Nanney, L.B., Netterville, J.L. & Burkey, B.B. Expression of matrix metalloproteinases and tissue inhibitor of metalloproteinases in head and neck squamous cell carcinoma. *Ann Otol Rhinol Laryngol* **106**, 271-278 (1997).

51. Vaalamo, M., Leivo, T. & Saarialho-Kere, U. Differential expression of tissue inhibitors of metalloproteinases (TIMP-1, -2, -3, and -4) in normal and aberrant wound healing. *Hum Pathol* **30**, 795-802 (1999).

52. Hanahan, D. & Weinberg, R.A. The hallmarks of cancer. *Cell* **100**, 57-70 (2000).

53. Buisson-Legendre, N., Emonard, H., Bernard, P. & Hornebeck, W. Relationship between cell-associated matrix metalloproteinase 9 and psoriatic keratinocyte growth. *J Invest Dermatol* **115**, 213-218 (2000).

54. Guedez, L. *et al.* In vitro suppression of programmed cell death of B cells by tissue inhibitor of metalloproteinases-1. *J Clin Invest* **102**, 2002-2010 (1998).

55. Li, G., Fridman, R. & Kim, H.R. Tissue inhibitor of metalloproteinase-1 inhibits apoptosis of human breast epithelial cells. *Cancer Res* **59**, 6267-6275 (1999).

56. Pinkel, D. *et al.* High resolution analysis of DNA copy number variation using comparative genomic hybridization to microarrays. *Nat Genet* **20**, 207-211 (1998).

57. Hodgson, G. *et al.* Genome scanning with array CGH delineates regional alterations in mouse islet carcinomas. *Nat Genet* **29**, 459-464 (2001).

58. Snidjers, A.M. *et al.* Genome-wide-array-based comparative genomic hybridization reveals genetic homogeneity and frequent copy number increases encompassing CCNE1 in fallopian tube carcinoma. *Oncogene* , in press (2003).

59. Brinckerhoff, C.E. & Matrisian, L. Matrix metalloproteinases: a tail of a frog that became a prince. *Nature Reviews* **3**, 207-214 (2002).

60. Ala-aho, R. *et al.* Inhibition of collagenase-3 (MMP-13) expression in transformed human keratinocytes by interferon-gamma is associated with activation of extracellular signal-regulated kinase-1,2 and STAT1. *Oncogene* **19**, 248-257 (2000).

61. Deryugina, E.I., Luo, G.X., Reisfeld, R.A., Bourdon, M.A. & Strongin, A. Tumor cell invasion through matrigel is regulated by activated matrix metalloproteinase-2. *Anticancer Res* **17**, 3201-3210. (1997).

62. Egeblad, M. & Werb, Z. New functions for the matrix metalloproteinases in cancer progression. *Nat Rev Cancer* **2**, 161-174 (2002).

63. DeClerck, Y.A. & Imren, S. Protease inhibitors: role and potential therapeutic use in human cancer. *Eur J Cancer* **14**, 2170-2180 (1994).

64. Montgomery, A.M., Mueller, B.M., Reisfeld, R.A., Taylor, S.M. & DeClerck, Y.A. Effect of tissue inhibitor of the matrix metalloproteinases-2 expression on the growth and spontaneous metastasis of a human melanoma cell line. *Cancer Res* **54**, 5467-5473. (1994).

65. Khokha, R. Suppression of the tumorigenic and metastatic abilities of murine B16-F10 melanoma cells in vivo by the overexpression of the tissue inhibitor of the metalloproteinases-1. *J Natl Cancer Inst* **86**, 299-304. (1994).

66. Koop, S. *et al.* Overexpression of metalloproteinase inhibitor in B16F10 cells does not affect extravasation but reduces tumor growth. *Cancer Res* **54**, 4791-4797. (1994).

67. Schultz, R.M., Silberman, S., Persky, B., Bajkowski, A.S. & Carmichael, D.F. Inhibition by human recombinant tissue inhibitor of metalloproteinases of human amnion

invasion and lung colonization by murine B16-F10 melanoma cells. *Cancer Res* **48**, 5539-5545. (1988).

68. Alvarez, O.A., Carmichael, D.F. & DeClerck, Y.A. Inhibition of collagenolytic activity and metastasis of tumor cells by a recombinant human tissue inhibitor of metalloproteinases. *J Natl Cancer Inst* **82**, 589-595 (1990).

69. Buck, T.B., Yoshiji, H., Harris, S.R., Bunce, O.R. & Thorgeirsson, U.P. The effects of sustained elevated levels of circulating tissue inhibitor of metalloproteinases-1 on the development of breast cancer in mice. *Ann N Y Acad Sci* **878**, 732-735 (1999).

70. Martin, D.C., Rüther, U., Sanchez-Sweatman, O.H., Orr, F.W. & Khokha, R. Inhibition of SV40 T antigen-induced hepatocellular carcinoma in TIMP-1 transgenic mice. *Oncogene* **13**, 569-576 (1996).

71. Sternlicht, M.D., Bissell, M.J. & Werb, Z. The matrix metalloproteinase stromelysin-1 acts as a natural mammary tumor promoter. *Oncogene* **19**, 1102-1113 (2000).

72. Murashige, M. *et al.* Enhanced expression of tissue inhibitors of metalloproteinases in human colorectal tumors. *Jpn J Clin Oncol* **26**, 303-309. (1996).

73. Schrohl, A.S. *et al.* Tumor Tissue Concentrations of the Proteinase Inhibitors Tissue Inhibitor of Metalloproteinases-1 (TIMP-1) and Plasminogen Activator Inhibitor Type 1 (PAI-1) Are Complementary in Determining Prognosis in Primary Breast Cancer. *Mol Cell Proteomics* **2**, 164-172 (2003).

74. Whittaker, M., Floyd, C.D., Brown, P. & Gearing, A.J. Design and therapeutic application of matrix metalloproteinase inhibitors. *Chem Rev* **99**, 2735-2776 (1999).

75. Hidalgo, M. & Eckhardt, S.G. Development of matrix metalloproteinase inhibitors in cancer therapy. *J Natl Cancer Inst* **93**, 178-193 (2001).

76. Zucker, S., Cao, J. & Chen, W.T. Critical appraisal of the use of matrix metalloproteinase inhibitors in cancer treatment. *Oncogene* **19**, 6642-6650. (2000).

77. Coussens, L.M., B. Fingleton, B. & Matrisian, L.M. Matrix metalloproteinase inhibitors and cancer: trials and tribulations. *Science* **295**, 2387-2392 (2002).

78. Goss, K.J., Brown, P.D. & Matrisian, L.M. Differing effects of endogenous and synthetic inhibitors of metalloproteinases on intestinal tumorigenesis. *Int J Cancer* **78**, 629-635. (1998).

79. Wang, X., Fu, X., Brown, P.D., Crimmin, M.J. & Hoffman, R.M. Matrix metalloproteinase inhibitor BB-94 (batimastat) inhibits human colon tumor growth and spread in a patient-like orthotopic model in nude mice. *Cancer Res* **54**, 4726-4728. (1994).

80. Bergers, G., Javaherian, K., Lo, K.M., Folkman, J. & Hanahan, D. Effects of angiogenesis inhibitors on multistage carcinogenesis in mice. *Science* **284**, 808-812 (1999).

81. Wilson, C.L., Heppner, K.J., Labosky, P.A., Hogan, B.L. & Matrisian, L.M. Intestinal tumorigenesis is suppressed in mice lacking the metalloproteinase matrilysin. *Proc Natl Acad Sci U S A* **94**, 1402-1407. (1997).

82. Bergers, G. *et al.* Matrix metalloproteinase-9 triggers the angiogenic switch during carcinogenesis. *Nat Cell Biol* **2**, 737-744 (2000).

83. Walther, S.E. & Denhardt, D.T. Directed mutagenesis reveals that two histidines in tissue inhibitor of metalloproteinase-1 are each essential for the suppression of cell migration, invasion, and tumorigenicity. *Cell Growth Differ* **7**, 1579-1588 (1996).

84. Huang, W., Meng, Q., Suzuki, K., Nagase, H. & Brew, K. Mutational study of the amino-terminal domain of human tissue inhibitor of metalloproteinases 1 (TIMP-1) locates an inhibitory region for matrix metalloproteinases. *J Biol Chem* **272**, 22086-22091 (1997).

85. Martin, D.C., Fowlkes, J.L., Babic, B. & Khokha, R. Insulin-like growth factor II signaling in neoplastic proliferation is blocked by transgenic expression of the metalloproteinase inhibitor TIMP-1. *J Cell Biol* **146**, 881-892. (1999).

86. Yoshiji, H. *et al.* Mammary carcinoma cells over-expressing tissue inhibitor of metalloproteinases-1 show enhanced vascular endothelial growth factor expression. *Int J Cancer* **75**, 81-87 (1998).

87. Guedez, L. *et al.* Tissue inhibitor of metalloproteinase-1 alters the tumorigenicity of Burkitt's lymphoma via divergent effects on tumor growth and angiogenesis. *Am J Pathol* **158**, 1207-1215. (2001).

88. Doxsey, S. Duplicating dangerously: linking centrosome duplication and aneuploidy. *Mol Cell* **10**, 439-440 (2002).

89. Jallepalli, P.V. & Lengauer, C. Chromosome segregation and cancer: cutting through the mystery. *Nat Rev Cancer* **1**, 109-117 (2001).

90. D'Assoro, A.B., Lingle, W.L. & Salisbury, J.L. Centrosome amplification and the development of cancer. *Oncogene* **21**, 6146-6153 (2002).

91. Kramer, A., Neben, K. & Ho, A.D. Centrosome replication, genomic instability and cancer. *Leukemia* **16**, 767-775 (2002).

92. Duensing, S. & Munger, K. Human papillomaviruses and centrosome duplication errors: modeling the origins of genomic instability. *Oncogene* **21**, 6241-6248 (2002).

93. Doak, S.H. *et al.* Chromosome 4 hyperploidy represents an early genetic aberration in premalignant Barrett's oesophagus. *Gut* **52**, 623-628 (2003).

94. Duensing, S. & Munger, K. Centrosomes, genomic instability, and cervical carcinogenesis. *Crit Rev Eukaryot Gene Expr* **13**, 9-23 (2003).

95. Sugai, T. *et al.* Analysis of genetic alterations, classified according to their DNA ploidy pattern, in the progression of colorectal adenomas and early colorectal carcinomas. *J Pathol* **200**, 168-176 (2003).

96. Bockmuhl, U. & Petersen, I. DNA ploidy and chromosomal alterations in head and neck squamous cell carcinoma. *Virchows Arch* **441**, 541-550 (2002).

97. Sudbo, J. & Reith, A. Which putatively pre-malignant oral lesions become oral cancers? Clinical relevance of early targeting of high-risk individuals. *J Oral Pathol Med* **32**, 63-70 (2003).

98. Zhao, W.Q. *et al.* Cell cycle-associated accumulation of tissue inhibitor of metalloproteinases-1 (TIMP-1) in the nuclei of human gingival fibroblasts. *J Cell Sci* **111 (Pt 9)**, 1147-1153 (1998).

99. Ritter, L.M., Garfield, S.H. & Thorgeirsson, U.P. Tissue inhibitor of metalloproteinases-1 (TIMP-1) binds to the cell surface and translocates to the nucleus of human MCF-7 breast carcinoma cells. *Biochem Biophys Res Commun* **257**, 494-499. (1999).

100. Soloway, P.D., Alexander, C.M., Werb, Z. & Jaenisch, R. Targeted mutagenesis of Timp-1 reveals that lung tumor invasion is influenced by Timp-1 genotype of the tumor but not by that of the host. *Oncogene* **13**, 2307-2314. (1996).

FIGURE LEGENDS

Figure 1. TIMP-1 mRNA expression during squamous carcinogenesis in HPV16 transgenic mice.

(A) Real-time PCR analysis of TIMP-1 mRNA. Total RNA was obtained from ears of negative-littermates (-LM), premalignant hyperplastic (H) and dysplastic (D) epidermis, and SCCs from K14-HPV16 mice (T). Real-time PCR for endogenous mouse TIMP-1 mRNA was performed and calculated as a ratio over 18S rRNA as a standard. Error bars represent standard errors of the mean.

(B-G) Spatial-temporal expression of TIMP-1 mRNA during neoplastic progression. An antisense riboprobe specific for mouse TIMP-1 mRNA was hybridized to paraffin-embedded neoplastically staged tissue sections from negative-littermate ears (B) and ears from HPV16 mice with hyperplastic (C), dysplastic (D), and SCC pathologies, Grade I SCC (E) and Grade III SCC (F), and axillary lymph nodes containing metastases (G). Arrowheads indicate silver grains corresponding to epithelial cells expressing TIMP-1 mRNA; arrows indicate silver grains corresponding to stromal cells expressing TIMP-1 mRNA; dashed lines denote the epidermal-dermal or keratinocyte-stromal boundaries; e, epidermis; d, dermis; f, hair follicle; t, tumor; s, stroma; *, keratin pearl; m, metastasis; l, lymphoid tissue. Scale bar: 100 μm (B), 160 μm (C, D, G), 256 μm (E, F).

Figure 2. Distinct expression patterns for TIMP family members in HPV16 transgenic mice.

In situ hybridization for mouse TIMP-2 (A-F), TIMP-3 (G-L), and TIMP-4 (M-R) mRNA. Antisense riboprobes specific for mouse TIMP-2, -3, and -4 mRNA were hybridized to paraffin-embedded neoplastically-staged tissue sections from the ears of negative-littermate (-LM) mice (A, G, M), ears from HPV16 mice with hyperplasia (B, H, N), dysplasia (C, I, O), Grade I SCCs (D, J, P), Grade III SCCs (E, K, Q), and axillary lymph nodes with metastases (F, L, R). Arrows (suprabasal keratinocytes) and arrowheads (basal and spinous keratinocytes) indicate silver grains corresponding to mRNA presence, dashed lines denote the epidermal-dermal or keratinocyte-stromal boundaries; e, epidermis; d dermis; f, follicle; t, tumor; s, stroma; *, keratin pearl; m, metastasis; l, lymphoid tissue; c, cartilage. Scale bar: 100 μm (A, G, M), 160 μm (B, C, F, H, I, L, N, O, R), 256 μm (D, E, J, K, P, Q).

Figure 3. Increased tumorgenicity in HPV16/βA-hT1$^+$ mice.

(A) TIMP-1 increases tumorgenicity in HPV16 mice. Cohorts of HPV16/βA-hT1$^-$ (n = 83) and HPV16/βA-hT1$^+$ mice (n = 129) were aged 12 months or until appearance of tumors as found by gross examination, whereupon tissues were assessed histopathologically by hematoxylin and eosin staining and keratin intermediate filament immunoreactivity to detect the presence and nature of malignant lesions. Curves reflect the percentage of tumor-free mice in each cohort, where mice developing papillomas, sebaceous adenomas, SCCs or MACs were counted as tumor-bearing. A statistically significant difference was found when comparing the two cohorts ($p = 0.0048$, Log-rank analysis).

(B) Incidence of specific epithelial neoplasms. Tissue sections from the two cohorts were analyzed by hematoxylin-eosin staining and keratin intermediate filament immunoreactivity to determine the incidence of mice developing hyperplastic skin by one month of age (Hyp), dysplasia by six months of age (Dys), and the lifetime incidences of tumors, e.g., papillomas, sebaceous adenomas (SA), SCCs and microcystic adnexal carcinomas (MAC); and the incidence of mice with metastatic tumors in sentinel lymph nodes (LN mets). Values represent percentages of mice with that particular neoplastic phenotype and statistically significant differences between the two cohorts are shown.

(C) Distribution of SCCs by Grade. Tissue sections of SCCs from the two cohorts were analyzed by hematoxylin-eosin histopathology and keratin intermediate filament immunoreactivity to determine the grade of each carcinoma based upon its relative differentiation characteristics. Values represent the percentage for each SCC grade as a fraction of the total number of SCCs within each cohort.

Figure 4. Increased TIMP-1 expression decreases tissue gelatinolytic activity

(A) Serum levels of human TIMP-1 protein in transgenic mice. ELISA was performed on serum from βA-hT1$^-$ (grey bar) and βA-hT1$^+$ (black bar) mice using antibodies specific for human TIMP-1. Values represent human TIMP-1 protein (hTIMP-1) in serum (ng/ml), compared to recombinant human TIMP-1 as a control and averaged for three mice per category. Error bars represent standard error of the mean.

(B) Tissue levels of transgenic human TIMP-1 protein in HPV16 transgenic mice. ELISA was performed on tissue extracts from ears of negative-littermate (-LM) mice, premalignant ears with hyperplasia (Hyp) or dysplasia (Dys), SCCs (SCC) and lymph

nodes (LN) from HPV16/βA-hT1$^-$ and HPV16/βA-hT1$^+$ mice, as described in panel A. Values represent human TIMP-1 protein in tissue (ng/mg), averaged for three mice per time-point. Error bars represent standard error of the mean

(C) Gelatinase activity in neoplastic tissues. Enzymatic solution assays were performed on tissue extracts representing the same categories as in panel B. Gelatinolytic activities in tissue extracts were measured by incubation with fluorescein-conjugated gelatin, in the absence or presence of the metalloproteinase inhibitor 1,10 phenanthroline (4 mM). Values represent the change in relative fluorescence units (RFU) per minute per μg tissue protein, averaged for four mice per time-point. Error bars represent standard error of the mean, and asterisks (*) denote statistically significant differences between the HPV16/βA-hT1$^-$ and HPV16/βA-hT1$^+$ categories ($p = 0.0392$, Mann-Whitney test).

(D) Gelatin substrate zymography of neoplastic tissue lysates. Tissue lysates were prepared from (-)LM and HPV16/βA-hT1$^-$ and HPV16/βA-hT1$^+$ mice with distinct neoplastic development and assessed for relative differences in levels of pro and/or active molecular weight forms of MMP-2 and MMP-9, which were not found to vary between the two genotypes. Hyperplasia (Hyp); dysplasia (Dys); SCC (SCC).

Figure 5. High levels of TIMP-1 stabilize collagenous matrices.

(A-D) Stabilization of collagen matrix in HPV16/βA-hT1$^+$ mice. Picro-Sirius Red staining was performed on tissue sections from premalignant ears with dysplasia (A-B), and SCC Grade II pathologies (C-D) from HPV16/βA-hT1$^-$ (A, C) and HPV16/βA-hT1$^+$ (B, D) mice. Brightfield (BF) images indicate histological structure, whereas polarized light (PL) images reveal mature collagen as bright orange fibers, denoted by green

arrows. Dashed lines indicate the epidermal-dermal boundaries; e, epidermis; d, dermis; t, tumor; s, stroma. Scale bar: 100 μm (A-D).

Figure 6. Low level TIMP-1 expression potentiates keratinocyte hyperproliferation in HPV16/βA-hT1$^+$ mice.

(A-H) Proliferation of keratinocytes during neoplastic progression. Keratinocyte proliferation was assessed in paraffin-embedded ear and SCC tissue sections from negative-littermate ((-)LM; panels A and E), HPV16/βA-hT1$^-$ (panels B-D) and HPV16/βA-hT1$^+$ (panels F-H) mice at distinct stages of neoplastic progression, e.g., 1-month old mice with hyperplastic ears (B, F), 6-month old mice with dysplastic ears (C, G) and in SCCs (D, H). Dual-color immunohistochemistry for immunoreactivity of BrdU (red staining) and keratin intermediate filaments (brown staining) was performed on tissue sections. Scale bar: 100 μm (A-H).

(I) Keratinocyte proliferative index. The keratinocyte proliferative index was determined as the percentage of BrdU-positive keratinocytes as a fraction of total keratinocytes (% BrdU(+) keratinocytes), averaged from five high-power fields per mouse, and five mice per category. Error bars represent standard error of the mean, and asterisks (*) indicate statistically significant differences between HPV16/βA-hT1$^-$ and HPV16/βA-hT1$^+$ categories (*, $p = 0.0228$; **, $p = 0.0140$, Mann-Whitney).

(J) Keratinocyte proliferation *in vitro* in response to TIMP-1 protein. BMK-2 cells were synchronized and growth-arrested by serum-deprivation in 0.5% dialyzed fetal bovine serum (dFBS) without mouse epidermal growth factor (mEGF), then induced by increasing concentrations of the N-terminal domain of human TIMP-1 protein (0, 8, or 20

μg/ml N-TIMP-1) in the presence of either 8% dFBS or 10 ng/ml mEGF. Entry into S-phase was measured by incorporation of ^{3}H-thymidine, assayed at the time of induction ("0 hrs.") and 18 hours after induction ("18 hrs. post-induction") in triplicate. Error bars represent standard errors of the mean.

(K) Keratinocyte apoptotic index. The TUNEL reaction was performed on adjacent tissue sections to those used in panels A-H to determine the percentage of TUNEL-positive keratinocytes at distinct stages of neoplastic development in the two cohorts of mice. Apoptotic index was quantified as the percentage of TUNEL-positive keratinocytes over total keratinocytes, averaged from five high-power fields per mouse, and five mice per category and no statistically significant differences were found between the respective categories.

Figure 7. Transgenic TIMP-1 expression does not alter vascular architecture or inflammatory infiltration in HPV16/βA-hT1^{+} mice.

(A-F) Vascular architecture during neoplastic progression. Blood vessels were labelled by intravenous injection of a fluorescein-conjugated lectin probe, and visualized by confocal microscopy of whole-mounted ears of (A, D) negative-littermate mice ((-)LM), and of (B, C) HPV16/βA-hT1^{-} and (E, F) HPV16/βA-hT1^{+} mice at distinct stages of premalignant neoplastic progression, e.g., 1-month old mice with hyperplastic ears (B, E), and 6-month old mice with dysplastic ears (C, F). Scale bar: 200 μm (A-F).

(G) Mast cell infiltration. Mast cells were visualized by chloroacetate enzyme histochemistry and quantified by microscopy on sections of ears from negative-littermate mice ((-)LM), and HPV16/βA-hT1^{-} and HPV16/βA-hT1^{+} mice at distinct stages of

neoplastic progression. Mast cell density was quantified as the number of mast cells per unit stromal area of 1,000 μm^2, averaged from five high-power fields per mouse, and five mice per category. Error bars represent standard error of the mean.

(H) Neutrophil infiltration. Neutrophils were visualized by immunohistochemistry and quantified by microscopy on sections of ears from the same mice as in (G). Neutrophil density was quantified as was performed for the mast cells, as the number of cells per unit stromal area of 1,000 μm^2, averaged from five high-power fields per mouse, and five mice per category. Error bars represent standard error of the mean.

Figure 8. TIMP-1 expression induces early onset of chromosomal aberrations in hyperplastic HPV16/βA-hT1$^+$ keratinocytes.

(A-B) Dual color Fluorescence *in situ* hybridization (FISH) using DNA probes specific for either chromosome 5 (red staining) or chromosome 10 (green staining) was performed on 1-month old hyperplastic and 6-month old dysplastic ear tissue sections from (A) HPV16/βA-hT1$^-$ and (B) HPV16/βA-hT1$^+$ mice. Inset in panel B shows a magnified image (from panel B) of one nucleus containing seven FISH spots for chromosome 5 and three FISH spots for chromosome 10. Scale bar: 50 μm (A-B).

(C) Quantification of FISH was performed on tissue sections of neoplastic ears (1-month and 6-month old) and compared to skin from negative-littermates ((-)LM), respectively. Values represent the ratio of the copy number for chromosome 5 over the copy number for chromosome 10, assessed from fifty nuclei per mouse, averaged from four to six mice per category. Error bars represent standard error of the mean, and asterisks denote statistically significant differences (*, (-)LM βA-hT1$^-$ vs. 6-month old HPV16/βA-hT1$^-$, p

= 0.0095, Mann-Whitney; **, (-)LM βA-hT1$^+$ vs. 1-month old HPV16/βA-hT1$^+$, p = 0.0286, Mann-Whitney; ***, (-)LM βA-hT1$^+$ vs. 6-month old HPV16/βA-hT1$^+$, p = 0.0159, Mann-Whitney).

Figure 1

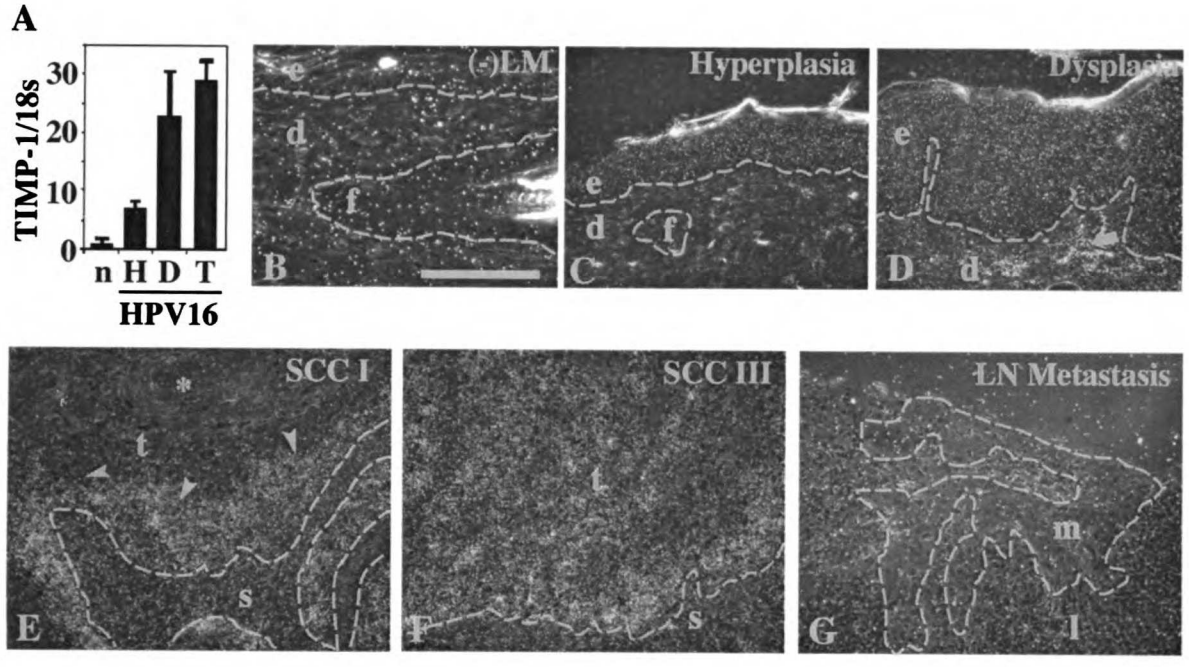
A
TIMP-1/18s
30
20
10
0
n H D T
HPV16
(-)LM
Hyperplasia
Dysplasia
SCC I
SCC III
LN Metastasis
B
C
D
E
F
G

Figure 2

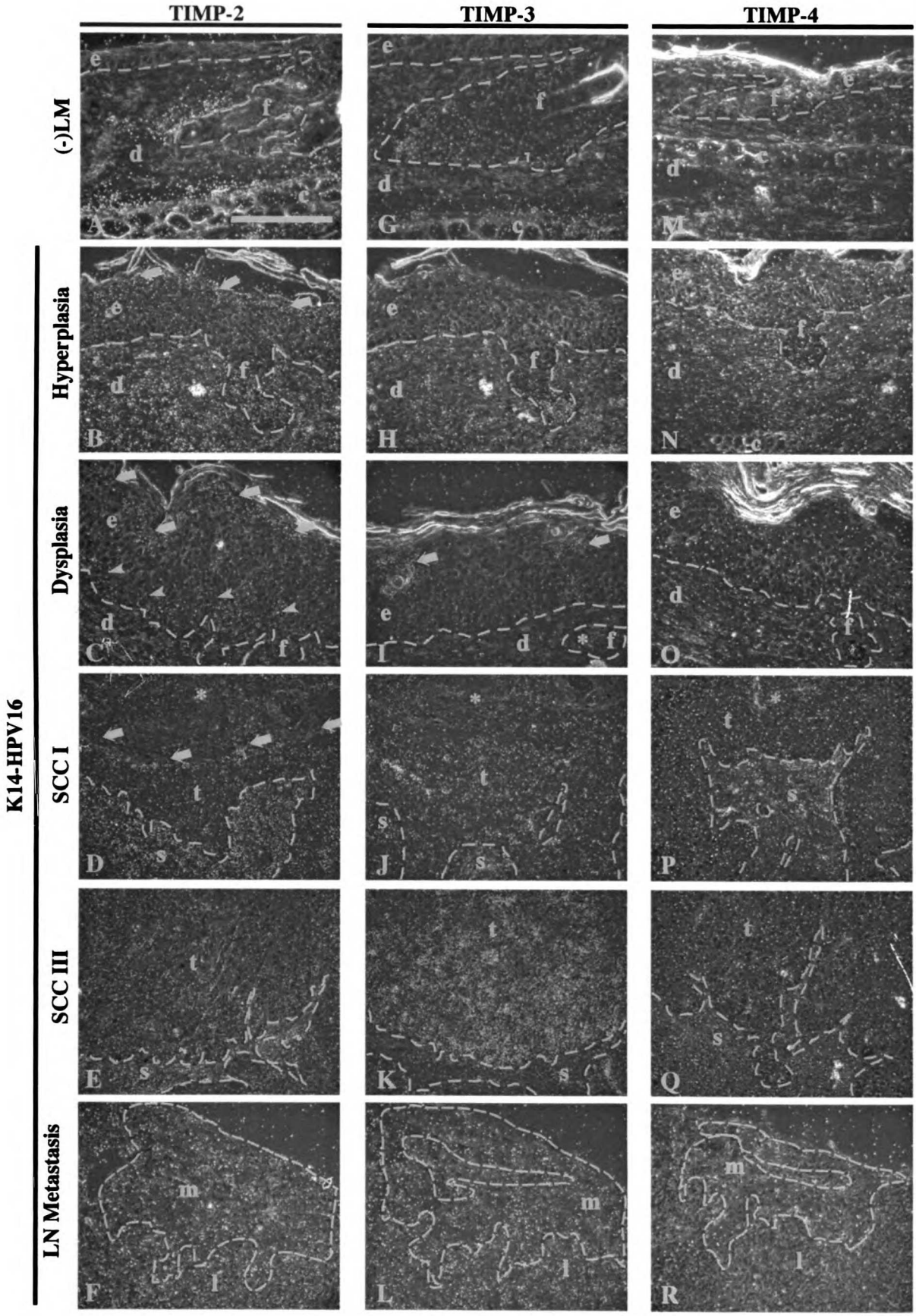
TIMP-2
TIMP-3
TIMP-4
K14-HPV16
(-)LM
Hyperplasia
Dysplasia
SCC I
SCC III
LN Metastasis
A
B
C
D
E
F
G
H
I
J
K
L
M
N
O
P
Q
R

A

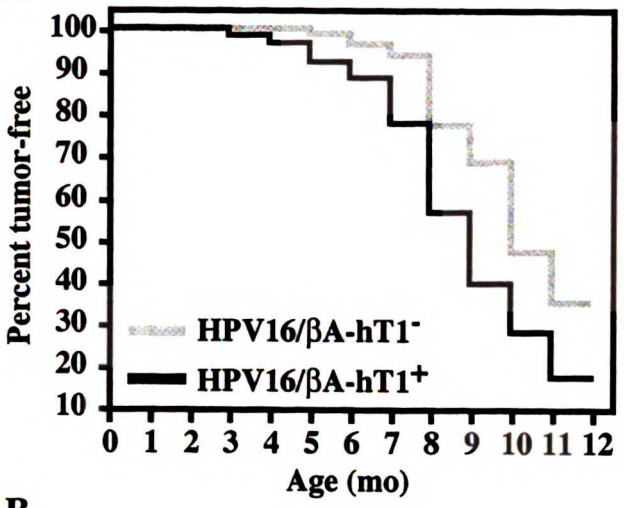

B

Histopathology	HPV16/βA-hT1⁻ n = 83	HPV16/βA-hT1⁺ n = 129	p value (log rank)
Hyp (by 1-mo)	100	100	
Dys (by 6-mo)	100	100	
Papilloma	13.2	12.4	
SA	6.0	5.4	
SCC	55.4	64.3	0.0342
MAC	10.8	21.7	0.0131
LN mets	23.2	17.2	

C

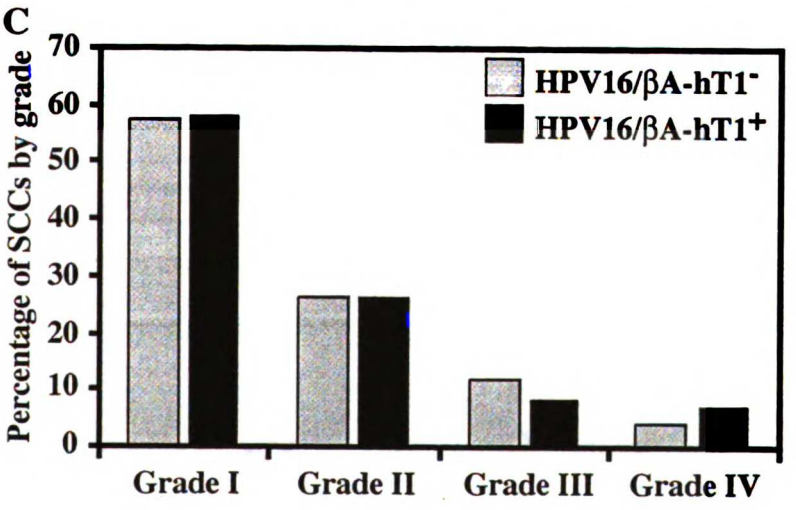

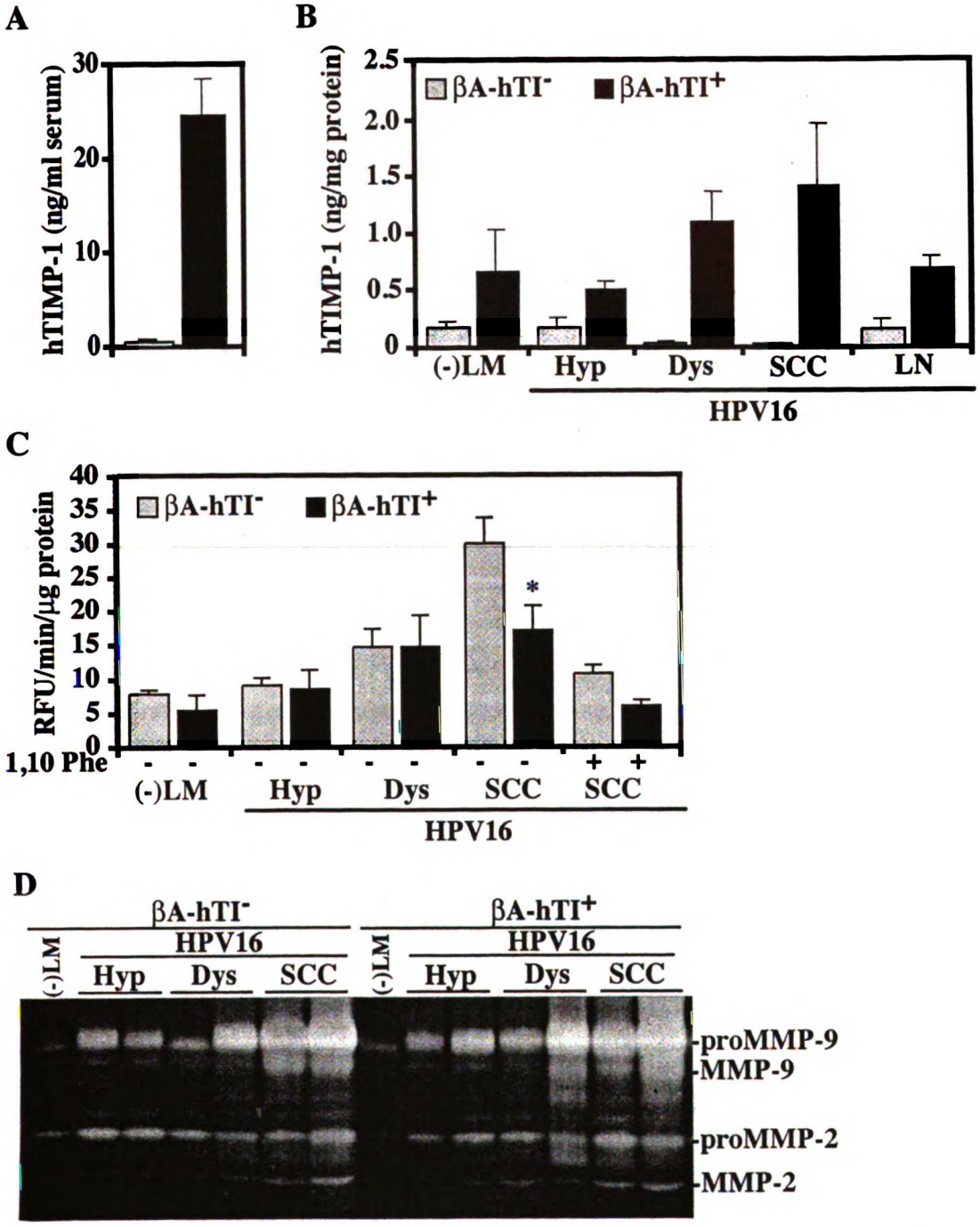
A
hTIMP-1 (ng/ml serum)
30
20
10
0
B
hTIMP-1 (ng/mg protein)
2.5
2.0
1.5
1.0
0.5
0
βA-hTI-
βA-hTI+
(-)LM
Hyp
Dys
SCC
LN
HPV16
C
RFU/min/μg protein
40
35
30
25
20
15
10
5
0
βA-hTI-
βA-hTI+
*
1,10 Phe
- - - - - - - - + +
(-)LM
Hyp
Dys
SCC
SCC
HPV16
D
βA-hTI-
βA-hTI+
HPV16
HPV16
(-)LM
Hyp
Dys
SCC
(-)LM
Hyp
Dys
SCC
proMMP-9
MMP-9
proMMP-2
MMP-2

Figure 5

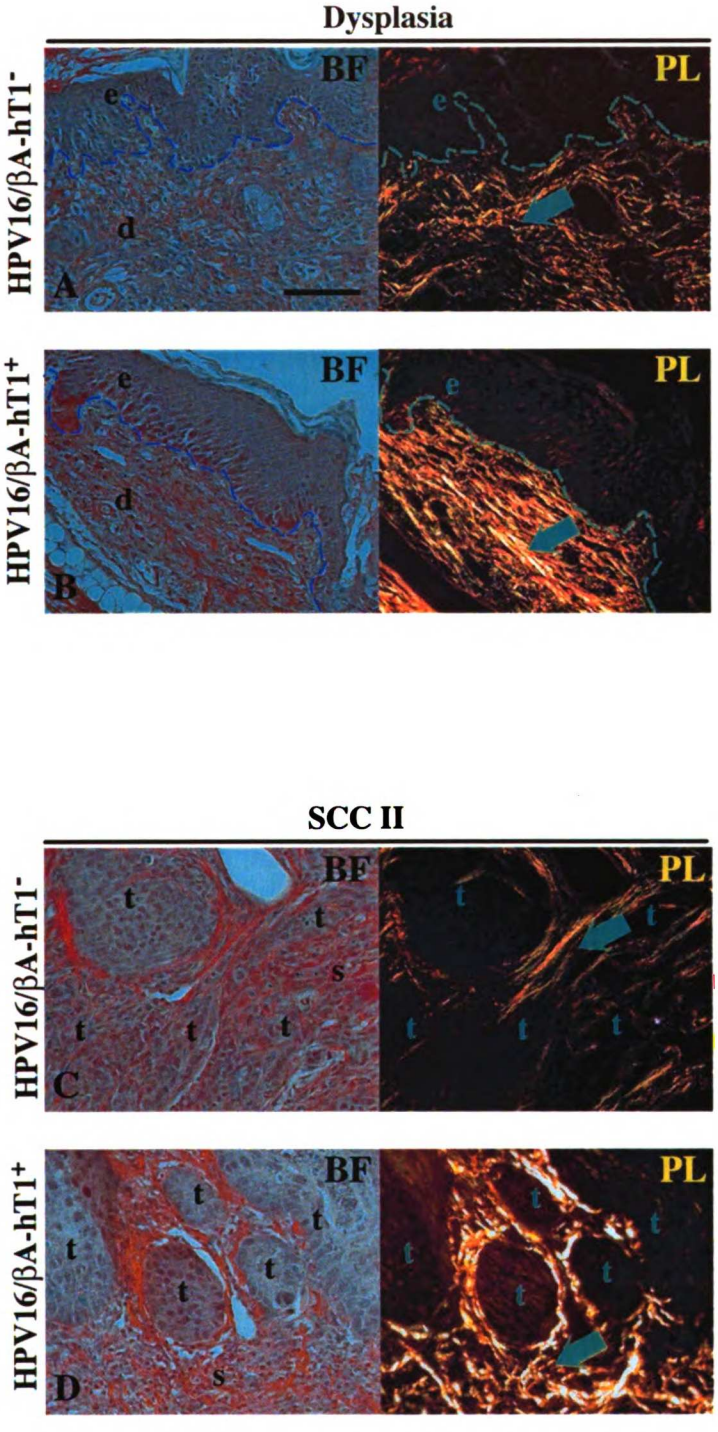

Figure 6

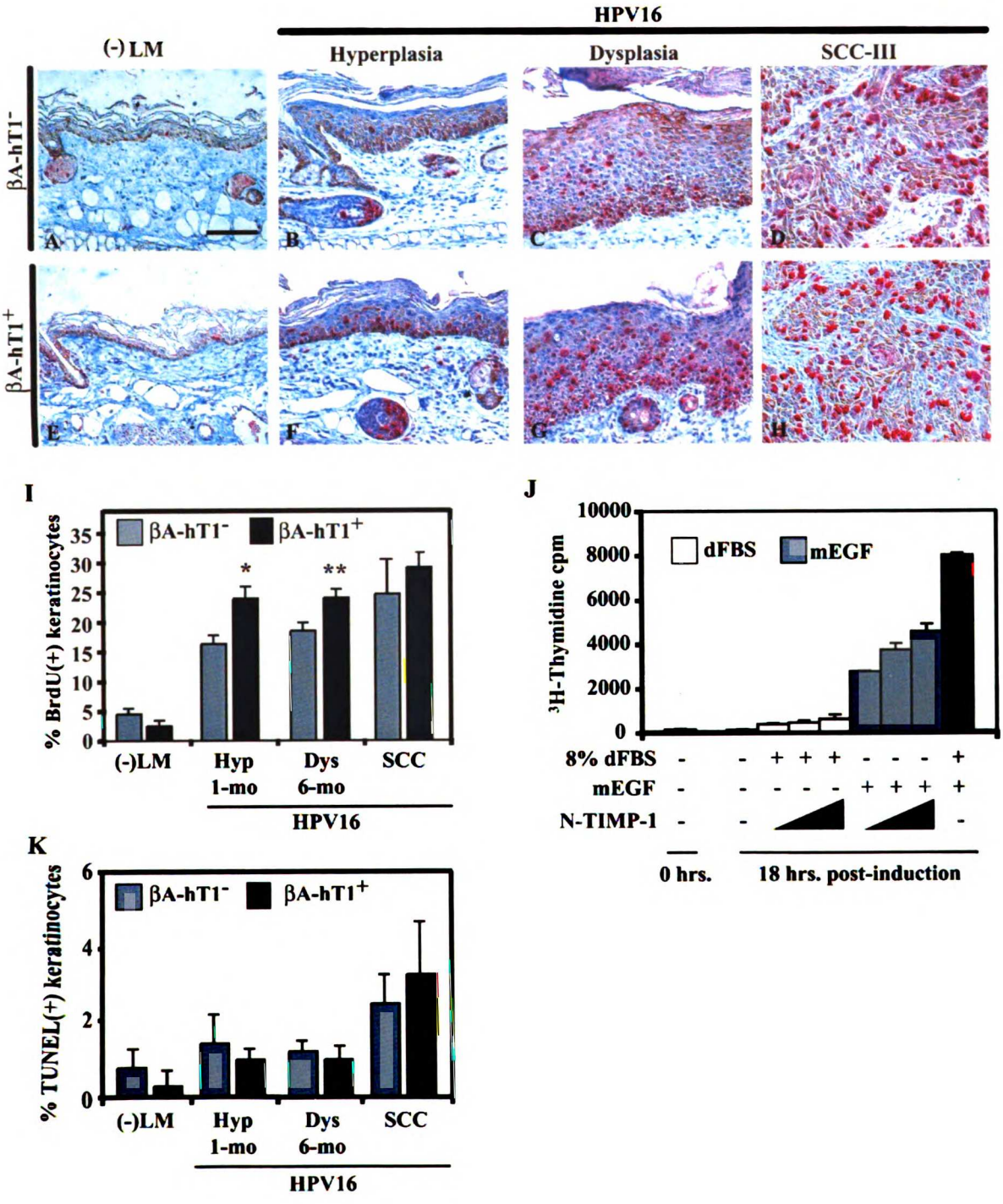
HPV16
(-) LM
Hyperplasia
Dysplasia
SCC-III
βA-hT1-
βA-hT1+
A
B
C
D
E
F
G
H
I
βA-hT1-
βA-hT1+
% BrdU(+) keratinocytes
35
30
25
20
15
10
5
0
*
**
(-)LM
Hyp 1-mo
Dys 6-mo
SCC
HPV16
J
10000
8000
6000
4000
2000
0
dFBS
mEGF
3H-Thymidine cpm
8% dFBS - - + + + - - - +
mEGF - - - - - + + + +
N-TIMP-1 - -
0 hrs.
18 hrs. post-induction
K
βA-hT1-
βA-hT1+
% TUNEL(+) keratinocytes
6
4
2
0
(-)LM
Hyp 1-mo
Dys 6-mo
SCC
HPV16

Figure 7

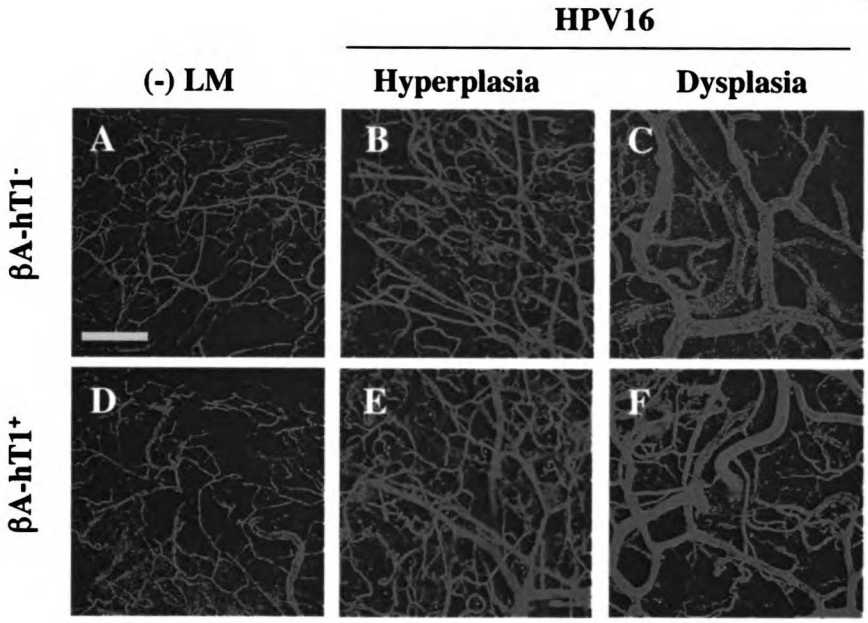
HPV16
(-) LM
Hyperplasia
Dysplasia
βA-hT1-
βA-hT1+
A
B
C
D
E
F

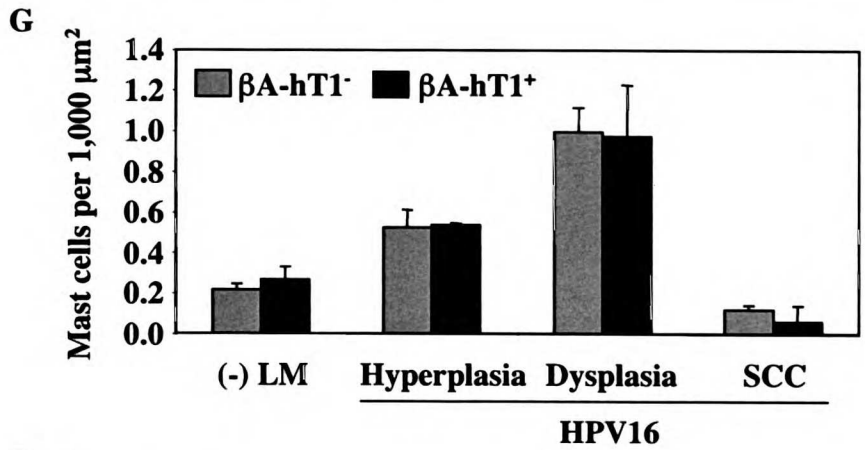
G
Mast cells per 1,000 μm²
βA-hT1-
βA-hT1+
1.4
1.2
1.0
0.8
0.6
0.4
0.2
0.0
(-) LM
Hyperplasia
Dysplasia
SCC
HPV16

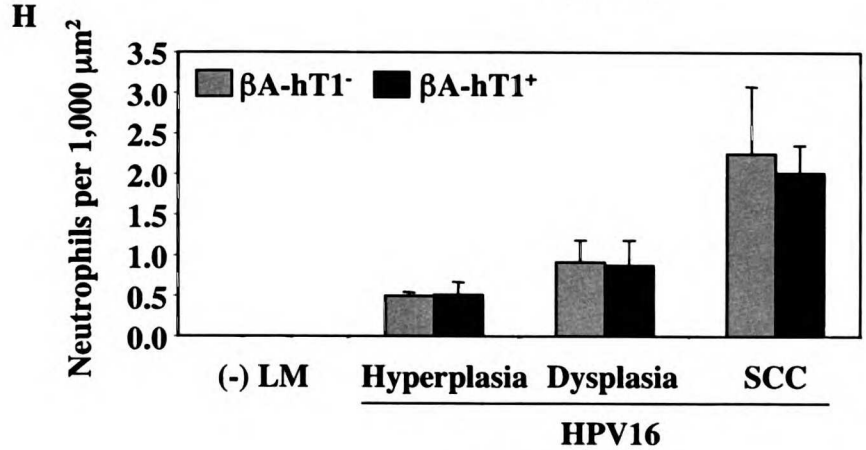
H
Neutrophils per 1,000 μm²
βA-hT1-
βA-hT1+
3.5
3.0
2.5
2.0
1.5
1.0
0.5
0.0
(-) LM
Hyperplasia
Dysplasia
SCC
HPV16

Figure 8

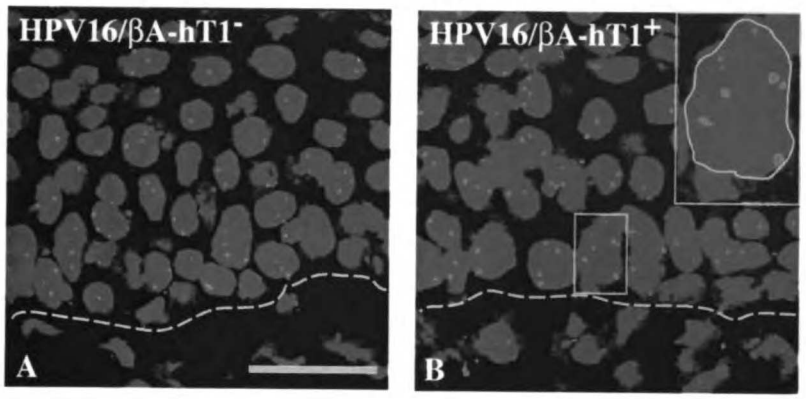
HPV16/βA-hT1⁻
HPV16/βA-hT1⁺
A
B

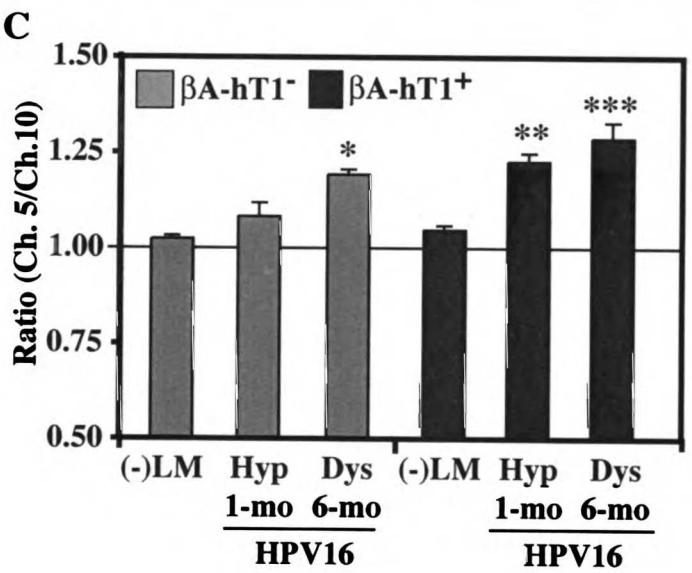
C
1.50
1.25
1.00
0.75
0.50
Ratio (Ch. 5/Ch.10)
βA-hT1⁻
βA-hT1⁺
*
**
***
(-)LM
Hyp
Dys
(-)LM
Hyp
Dys
1-mo
6-mo
1-mo
6-mo
HPV16
HPV16

Chapter 4

Characterization of HPV16 Mice Lacking Endogenous TIMP-1

PROLOGUE

The studies in this chapter consist of work assessing the functional significance of TIMP-1 expression during neoplastic progression utilizing the K14-HPV16 transgenic mouse model of epithelial carciogenesis. Taking a genetic approach, we have generated HPV16/TIMP-1-deficient mice to determine the functional significance of TIMP-1 expression by assessing the characteristics of neoplastic progression in its absence. The work described herein represents a complementary approach to that taken in Chapter 3, where the functional significance of TIMP-1 expression during neoplastic progression was assessed via a gain-of-function transgenic approach.

Note: Quantification of the *in situ* proliferation experiments shown in Figure 2C was done by a summer intern (Andre Witkin) working under my supervision. The neutrophil profiling studies shown in Figure 4 contributed to a publication in the journal *Differentiation* [1].

ABSTRACT

The significance of TIMP-1 mRNA expression during neoplastic progression has been studied in several experimental models of carcinogenesis as well as in primary human tumors and their derived cell lines; however, to date, studies examining the specific contributions of TIMP-1 during de novo carcinogenesis have revealed paradoxical results suggesting that TIMP-1 may play dual roles during cancer development depending upon the organ involved and stage of cancer progression being evaluated. We have previously reported that specific loss of MMP-9 significantly alters the characteristics of neoplastic progression in HPV16 transgenic mice [2]. Since TIMP-1 is a potent inhibitor of MMP-9 activity, we asked whether TIMP-1 was also a functionally significant contributor to neoplastic evolution and hypothesized that carcinogenesis might be enhanced when progressing in the absence of TIMP-1 expression. To test this hypothesis, we took a genetic approach and utilized TIMP-1 homozygous null mice intercrossed with HPV16 transgenic mice and generated two cohorts in which to study, e.g., HPV16/TIMP1$^{-/-}$ and HPV16/TIMP1$^{+/-}$ controls. Our data revealed that, unlike MMP-9 deficiency in HPV16 mice, singular loss of TIMP-1 was insufficient to alter the characteristics of epithelial neoplastic progression in HPV16 mice by numerous parameters tested, e.g., keratinocyte proliferation and apoptotic index, tissue gelatinolytic activity and overt tumorigenesis (multiplicity, incidence, phenotype or metastasis). Our conclusion from these studies is that TIMP-1 may functionally contribute to carcinogenesis, but its absence alone is insufficient to alter the development and progression of epithelial cancers initiated by HPV16 oncogenes in K14-HPV16 transgenic mice.

INTRODUCTION

*T*issue *I*nhibitors of *M*etallo*P*roteinases (TIMPs) are a family of multifunctional proteins known to possess a broad range of biological activities, including inhibition of matrix metalloproteinases (MMPs), and regulation of proliferation and apoptosis in a variety of cell types [3-5]. As the first of the family members to be identified, TIMP-1 was characterized initially for its role in inhibiting MMPs, but more recently has been implicated for its role in positively contributing to carcinogenesis, as reviewed in Chapter 1. In order to elucidate the role of TIMP-1 during epithelial carcinogenesis, we previously exploited TIMP-1 transgenic mice intercrossed with K14-HPV16 mice (Chapter 3). Briefly, enhanced expression of TIMP-1 in HPV16 mice, e.g., HPV16/βA-hT1$^+$ mice increased the incidence of epithelial cancers, specifically squamous cell carcinomas (SCCs) and microcystic adnexal carcinomas (MACs) (Rhee at al, manuscript submitted). Increased tumorgenicity in HPV16/βA-hT1$^+$ mice correlated with an increased keratinocyte proliferation index, decreased latency and increased presence of chromosomal aberrations in premalignant mice, and decreased matrix proteolysis and increased matrix stability in carcinomas (Rhee et al, manuscript submitted). One limitation to this transgenic gain-of-function genetic approach, however, is that it does not address the functional significance of endogenous TIMP-1 expression, which was shown in the K14-HPV16 mice to be incrementally increased throughout progression and to originate predominantly in the neoplastic epithelial cells (Chapter 3).

In this study, we have sought to determine if endogenous TIMP-1, expressed predominantly by premalignant and malignant keratinocytes, represents a functionally-significant regulator of epithelial carcinogenesis in HPV16 transgenic mice. To address

the role of endogenous TIMP-1, a genetic loss-of-function approach was taken utilizing K14-HPV16 mice homozygous-null for the endogenous TIMP-1 gene (HPV16/T1$^{-/-}$). Analysis of the HPV16/T1$^{-/-}$ mice showed no significant changes in tumorigenesis, as assessed by overall tumor incidence, frequency of papillomas, sebaceous adenomas, squamous cell carcinomas (SCCs) or microcystic adnexal carcinomas (MACs), onset of premalignant lesions or the multiplicity, anatomic location and lymph node metastases. Furthermore, loss of endogenous TIMP-1 expression did not alter proliferation, apoptosis or gelatinase activity during neoplastic progression. These results suggest that the absence of endogenous TIMP-1 alone is insufficient to alter the development and progression of epithelial cancers initiated by HPV16 oncogenes in K14-HPV16 transgenic mice.

MATERIALS AND METHODS

Animal husbandry, genotype and histopathologic grading analyses

The K14-HPV16 transgenic mice [6], the preparation of tissue sections for histologic examination and the characterization of neoplastic stages based on hematoxylin-eosin histopathology and on keratin intermediate filament expression have been described previously [1,7,8]. Tissue samples were fixed and analyzed as described in Chapter 3.

The TIMP-1-homozygous null mice ($T1^{-/-}$) have been described previously [9,10]. Briefly, these mice contain a nonsense mutation carried on an insertion vector, introduced originally by targeted mutagenesis in murine embryonic stem cells. To minimize the effect of background strain differences in susceptibility to carcinogenesis, $T1^{-/-}$ mice (originally generated in 129SvJae) were backcrossed a minimum of six generations into the FVB/n strain prior to intercrossing with K14-HPV16 mice (FVB/n, N15). The TIMP-$1^{-/-}$ insertion vector was followed by PCR genotyping of tail DNA using oligonucleotide primers (5'-ATG ATT GAA CAA CAG GGA TTG CAC-3' and 5'-TTC GTC CAG ATC ATC CTG ATC GAC-3') and amplification for 30 cycles at 95°C 60 seconds, 55°C 30 seconds, and 72°C 120 seconds, to generate a 477-bp product corresponding to a region within the neomycin cassette in the insertion vector. HPV16 mice lacking TIMP-1 (HPV16/TIMP-$1^{-/-}$) were compared to littermates (HPV16/ TIMP-$1^{+/-}$) as negative controls.

RNA analysis

In situ hybridization was performed as described previously [7] and in Chapter 3, using ^{35}S-labelled riboprobes generated from cDNA containing plasmid templates for mouse

TIMP-1 [11], mouse TIMP-2 [12], mouse TIMP-3 [13] and mouse TIMP-4 [14]. As negative controls, hybridization using sense probes was performed and showed no signal (data not shown)

Substrate zymography

Gelatin zymography was performed essentially as described previously [2,15] and in Chapter 3. Tissue samples from negative littermate or neoplastically-staged transgenic mice were homogenized in lysis buffer containing 50 mM Tris-HCl (pH 8.0), 150 mM NaCl, 0.1% NP-40, 0.5% deoxycholate, 0.1% SDS. Soluble and insoluble extracts were separated by centrifugation and subsequently stored at –80°C. Equivalent amounts of soluble extract were analyzed by gelatin zymography [16] on 10% SDS-polyacrylamide gels copolymerized with substrate (1 mg/ml of gelatin) in sample buffer (2% SDS, 50 mM Tris-HCl, 10% Glycerol, 0.1% Bromphenol Blue, pH 6.8). After electrophoresis, gels were washed, incubated overnight at 37°C in 50 mM Tris-HCl, 10 mM $CaCl_2$ (pH 8.2), and then stained in 0.5% Coomassie Blue and destained in 20% methanol, 10% acetic acid. Negative staining indicates the location of active protease bands. Exposure of proenzymes within tissue extracts to SDS during gel separation procedure leads to activation without proteolytic cleavage [17]. Assays were performed in duplicate.

Gelatinase solution assay

Assays were performed as described in Chapter 3. Protein lysates were prepared from fresh-frozen tissue samples of ears or tumors as described for gelatin zymography. 3 μg of protein lysate were incubated at 37°C in reaction buffer (50 mM Tris, pH 7.6, 150 mM

NaCl, 5 mM $CaCl_2$, 0.2 mM NaAzide, 0.05% Brij-35) with 400 ng DQ-gelatin (Molecular Probes) in a total volume of 200 µl/well in a 96-well, black tissue culture plate (Falcon). Reactions were incubated for up to five hours at 37°C and fluorescence measured (excitation 485 nm, emission 530 nm) every three minutes on a SpectraMax Gemini™ spectrophotometer (Molecular Devices) operated by SoftMax Pro 4.3 software (Molecular Devices). Tissue lysates from four mice were assayed per category.

Immunohistochemistry

Immunohistochemical detection of keratin-5 and bromodeoxyuridine (BrdU) was performed as described previously [7] and in Chapter 3. Mice received intraperitoneal injections of bromodeoxyuridine (BrdU;Roche) dissolved in phosphate-buffered saline (PBS) at 50 µg/g total body weight, 90 minutes before sacrifice and preparation of tissue samples. 5-µm-thick paraffin sections were processed using the BrdU Labelling Kit II™ (Roche), developing by the Vector Red Alkaline Phosphatase Kit™ (Vector), and counterstaining by hematoxylin and eosin. Five fields per mouse were analyzed at high-magnification (40X) on a Leica DM-RXA microscope attached to a Leica digital camera operated by OpenLab software™ (Improvision). Proliferative index was quantified for five mice per category as the percentage of the BrdU-positive nuclei in keratin-5-positive keratinocytes over the total number of keratin-5-positive keratinocytes.

Apoptotic frequency was measured as described previously in Chapter 3, using the Fluorescein-FragEL DNA fragmentation detection kit (Oncogene Research Products) by the manufacturer's recommendations. Five fields per mouse were captured as described above, and apoptotic index was quantified for four mice per category as the

percentage of the TUNEL-positive keratinocytes over the total number of DAPI-stained keratinocytes.

Immunohistochemical detection of neutrophils was performed as described previously [1,18] and in Chapter 3. 5-μm-thick paraffin sections were deparaffinized in xylenes, rehydrated in graded ethanol and PBS, digested for three minutes in Proteinase K (DAKO), washed in PBS, blocked in 1X Blocking buffer (5% normal goat serum/2.5% bovine serum albumin/PBS), and incubated in a 1:1,000 dilution of a rat monoclonal antibody against mouse neutrophils (Cedarlane) in 0.5X blocking buffer for two hours. This was followed by a series of PBS washes, incubation of slides with a biotinylated secondary antibody against rat (Vector), conjugation by ABC-AP™ (Vector) and development in NTB/X-phosphate substrate (Roche). Slides were counterstained in eosin, dehydrated by graded ethanol and xylenes, and mounted in Cytoseal 60™ (Richard-Allan Scientific). Five fields per mouse were analyzed at high-magnification (40X) on a Leica DM-RXA microscope attached to a Leica digital camera operated by OpenLab software™ (Improvision). Neutrophil density was quantified for five mice per category as the number of neutrophils per unit stromal area of 1,000 μm^2.

Neutrophil elastase assay

Assays were performed as described previously [19,20]. Protein lysates were prepared by grinding fresh-frozen tissue samples from ears or tumors in liquid nitrogen and vortexing in a detergent-based buffer (0.1% Triton-X100/PBS). After centrifugation at 13,000xg at 4°C for 30 minutes, pellets were vortexed in high-salt buffer (10 mM Tris-HCL pH 6.1 with 2 M NaCl). After centrifugation, supernatants from the high-salt buffer preparation,

into which the elastase activity was extracted (E. Hansell, unpublished observations) were measured for protein concentration by the DC protein assay™ (Bio-Rad) and subjected to enzyme solution assays for neutrophil elastase activity.

Enzyme solution assays were performed on 10 μg of the protein lysate in the high-salt buffer. Enzymatic activity was measured in the reaction buffer (0.1 M HEPES pH 7.5 with 0.5 M NaCl) containing 0.2 mM methoxysuccinyl-Ala-Ala-Pro-Val-4-amidomethylcoumarin (Sigma) in a total volume of 200 μl/well in a 96-well, black tissue culture plate (Falcon). Reactions were incubated for up to three hours at 37°C and fluorescence measured (excitation 380 nm, emission 460 nm) every thirty seconds on a SpectraMax Gemini™ spectrophotometer (Molecular Devices) operated by SoftMax Pro 4.3 software (Molecular Devices). Neutrophil elastase activity was inhibited by preincubation of the reaction assay in 1 μM α1-antitrypsin (Calbiochem) at 4°C for two hours, and tested for linearity with human sputum leukocyte elastase (Elastin Products). Samples were assayed from three mice per category.

RESULTS

Loss of endogenous TIMP-1 expression does not alter tumorigenesis in HPV16 transgenic mice.

To test the hypothesis that endogenous TIMP-1 mRNA expression is a functionally significant modifier of epithelial neoplastic progression, we took a genetic approach and utilized mice that were homozygous for a mutant TIMP-1 allele ($T1^{-/-}$), previously shown to have a reduction in TIMP-1 mRNA levels and a complete loss of functional protein [9,10]. K14-HPV16 transgenic mice were intercrossed with $T1^{-/-}$ mice (n5/FVB/n) to obtain HPV16 transgenic mice lacking a functional TIMP-1 gene (HPV16/$T1^{-/-}$). To verify the complete loss of endogenous expression of TIMP-1 in HPV16/$T1^{-/-}$, *in situ* hybridization analysis was performed for mouse TIMP-1 mRNA on neoplastically staged paraffin-embedded tissue sections (Fig 1). As shown previously (Chapter 3), in HPV16 mice endogenous TIMP-1 mRNA expression is weakly diffuse in the epidermis of premalignant lesions (Fig 1A, B), and reaches a maximum abundance in the invasive front of Grade I SCCs (Fig 1C) and throughout Grade III SCCs (Fig 1D). In contrast, hybridization of a probe for mouse TIMP-1 mRNA on HPV16/$T1^{-/-}$ mice failed to show any corresponding expression (Fig 1E-H), suggesting that expression of endogenous TIMP-1 mRNA was lost or below detectable limits in HPV16/$T1^{-/-}$ mice.

Studies of human cancer, documenting increased expression of human TIMP-1 mRNA correlating with more severe clinical outcome [21,22], have suggested that TIMP-1 expression may contribute to neoplastic progression. To test the hypothesis that the loss of endogenous TIMP-1 expression would be sufficient to alter carcinogenesis in the K14-HPV16 model, we compared a cohort of the HPV16/$T1^{-/-}$ mice (n = 109) against a cohort

of littermate controls (HPV16/T1$^{+/-}$, n = 51) for tumor-free survival, defined as survival without the development of papillomas, sebaceous adenomas, squamous cell carcinomas (SCCs), or microcystic adnexal carcinomas (MACs) (Fig 2A). Quantitative analysis showed that tumor-free survival was similar between the two cohorts (50.5% for HPV16/T1$^{-/-}$ vs. 45.1% for HPV16/T1$^{+/-}$, p = 0.9448 by Log-rank analysis; Fig 2A). Histopathological analysis demonstrated that both cohorts exhibited a similar incidence and latency of premalignant lesions, papillomas (p = 0.6510 by Log-rank analysis; Fig 2B), SCCs, (p = 0.4526), and MACs (p = 0.3525), as well as similar profiles for SCC grade (Fig 2C). Furthermore, the loss of endogenous TIMP-1 in the HPV16/T1$^{-/-}$ mice vs. the control HPV16/T1$^{+/-}$ mice did not alter the incidence of SCC metastasis to lymph nodes (21.1% vs. 13.8%, p = 0.4764, two-tailed Fisher's exact test: Fig 2B), or the anatomic location (ear: 17.9% vs. 21.6%; trunk: 57.1% vs. 56.8%; appendages: 25% vs. 21.6%) or multiplicity of SCCs (1.12 vs. 1.18 per mouse). In combination, these data suggested that loss of endogenous TIMP-1 expression was by itself insufficient to alter tumorigenesis in K14-HPV16 transgenic mice.

Loss of endogenous TIMP-1 expression does not alter proliferation, apoptosis, or gelatinolytic activity in the skin of HPV16 transgenic mice.

Prior work using the K14-HPV16 model has identified distinct biological mechanisms of neoplastic progression that precede and contribute to skin tumor development, such as the proliferation of initiated keratinocytes (Chapter 3) and the activity of gelatin-cleaving MMPs[2]. Therefore, to test the hypothesis that endogenous TIMP-1 expression could be regulating some of these intermediary processes leading to tumor formation, we assessed

the effect of the loss of endogenous TIMP-1 expression on multiple biological pathways (Fig 3).

Consistent with hyperproliferation being an intrinsic property of many neoplastic tissues [23], we have previously reported that keratinocyte hyperproliferation incrementally increases during neoplastic progression in HPV16 mice and, in part, characterizes progression between premalignant stages [6,7]. In addition, we have shown that keratinocyte hyperproliferation can be attenuated by ablating MMP-9 activity in HPV16 mice, and in so doing decreases the incidence of SCCs [2]. Since TIMP-1 is known to regulate MMP-9 activity *in vivo* and *in vitro* [5], one possibility was that loss of endogenous TIMP-1 would result in augmented proliferation possibly due to unchecked MMP-9 activity. Alternatively, many studies have documented the mitogenic activity of TIMP-1 towards keratinocytes *in vitro* [24,25] (Chapter 3), suggesting that loss of TIMP-1 might reciprocally lead to decreases in proliferation. To distinguish between these two possibilities, we assessed keratinocyte proliferation index during neoplastic progression in HPV16/TIMP-1–deficient mice compared to littermate controls (Fig 3A). Quantification demonstrated no significant differences at any histopathological stage of neoplastic progression between HPV16 mice with or without endogenous TIMP-1 (Fig 3A), suggesting that loss of endogenous TIMP-1 does not alter hyperproliferation of keratinocytes in the K14-HPV16 model.

In addition to proliferation, apoptosis has been described as another hallmark of neoplastic progression that is subject to regulation by TIMP-1 *in vitro*[26,27], Furthermore, the ability of TIMP-1 to protect malignant cells against apoptosis *in vivo* has been suggested as one of the mechanisms by which TIMP-1 can contribute to the

growth of transplanted tumors [28]. Therefore, we asked if loss of endogenous TIMP-1 altered apoptotic frequency during neoplastic progression in the HPV16 mice (Fig 3B). Accordingly, keratinocyte apoptotic index was quantified utilizing the TUNEL assay on staged neoplastic tissue sections adjacent to those previously utilized to assess proliferation, and revealed that apoptotic indices were similar between HPV16/T1$^{-/-}$ mice compared to control mice at all stages of neoplastic development in histopathologically-matched sections (Fig 3B), suggesting that loss of TIMP-1 does not alter apoptotic death pathways in K14-HPV16 keratinocytes.

The activity of gelatin-cleaving MMPs, such as MMP-9, has been identified as a critical contributor to K14-HPV16 carcinogenesis, exhibiting progressive increases in the levels of their precursor and mature forms during tumorigenesis [2,15]. Net proteolytic activity *in vivo*, however, is regulated not only by MMP synthesis and activation but also by direct inhibition of activated MMP by TIMPs and other endogenous inhibitors. Functional assays designed to measure net activity in solution have shown that MMP activity, detected as proteolysis of the substrate gelatin, increases incrementally throughout neoplastic progression in the HPV16 mice, in which activity is most prominent in the SCCs and can be inhibited by constitutive levels of transgenic TIMP-1 (Chapter 3). Therefore, to test the hypothesis that loss of endogenous TIMP-1 expression altered gelatinolytic activity in tissue lysates during neoplastic progression, tissue extracts from HPV16/T1$^{-/-}$ mice were compared to littermate controls by gelatin zymography to detect MMP levels and activation status (Fig 3C) and by enzyme solution assays to measure net activity of gelatinolytic MMPs (Fig 3D). As indicated by the clear zones of lysis corresponding to the presence of gelatinases, zymography of tissue lysates from

mice lacking TIMP-1 expression showed incremental increases in precursor and mature forms of MMP-9 and of MMP-2 (Fig 3C), comparable to what has been previously shown for HPV16 mice with normal TIMP-1 [2,15]. Furthermore, enzyme solution assays demonstrated that loss of endogenous TIMP-1 expression did not alter net gelatinolytic activity within tissue (Fig 3D). These results suggest that levels of endogenous TIMP-1 were not sufficient to contribute significantly to inhibition of gelatinolytic activity during neoplastic progression in the HPV16 mice.

Loss of endogenous TIMP-1 expression does not alter the expression patterns of other TIMPs.

The lack of any alterations in net in vitro gelatinolytic activity in the HPV16/T1$^{-/-}$ mice compared to controls (Fig 3D), even in the SCC stage at which endogenous TIMP-1 expression has been shown to be the highest (Chapter 3), suggested the possibility that functional redundancy was compensating for the loss of endogenous TIMP-1 during progression. The other members of the TIMP family, i.e. TIMP-2, -3, and –4, are known to inhibit MMPs with gelatinase activity [29,30], and with even greater potency than TIMP-1 in some situations [31]. Furthermore, concurrent expression of other TIMPs has been observed in TIMP-1-sufficient mice during K14-HPV16 progression (Chapter 3). Therefore, we hypothesized that the observed lack of changes in the gelatinolytic activity and the tumorgenicity observed for the HPV16/T1$^{-/-}$ mice might be the consequence of functional redundancy from concurrent or enhanced expression of the other TIMPs. To determine if other TIMP family members were concurrently or increasingly expressed in the absence of TIMP-1, *in situ* hybridization analysis for TIMP-2, -3, and -4 was

performed on staged neoplastic tissue sections from HPV16/T1$^{-/-}$ mice (Fig 4A-L). The expression pattern for TIMP-2 in the HPV16/T1$^{-/-}$ mice (Fig 4A-D) was similar to what had been shown for HPV16 mice with normal TIMP-1 expression (Chapter 3), i.e. TIMP-2 mRNA was observed in the superficial differentiating layers of hyperplastic and dysplastic ears (Fig 4A, B) and in the cells near keratin pearls of SCCs Grade I (Fig 4C), with a more limited expression pattern in SCCs Grade III (Fig 4D). Similarly, the pattern for TIMP-3 expression (Fig 4E-H) was not altered by the loss of endogenous TIMP-1, expression of TIMP-3 being limited to keratinocytes near follicles in hyperplastic and dysplastic ears (Fig 4E, F) and malignant cells of SCCs Grade III (Fig 4H) but not Grade I (Fig 4G). Finally, no expression of TIMP-4 could be detected in any of the tissues assayed from HPV16/T1$^{-/-}$ mice (Fig 4I-L). Hence, in HPV16/T1$^{-/-}$ mice, TIMP-2 and –3 were expressed throughout neoplastic progression, in patterns similar to what had been observed for HPV16 mice with typical TIMP-1 mRNA expression patterns.

Neutrophil infiltration and activity of neutrophil elastase is increased throughout neoplastic progression.

Infiltration of early hyperplastic tissue by various types of inflammatory cells is a characteristic of neoplastic progression in K14-HPV16 mice [1,15]. It has been hypothesized that infiltrating inflammatory cells contribute to neoplastic progression by delivering potent mediators of cellular proliferation, angiogenesis and invasion [15]. Since several serine proteases, e.g., mast cell chymase and neutrophil elastase, expressed by mast cells and neutrophils are known to target TIMP-1 for degradation [32,33], we hypothesized that the contribution of endogenous TIMP-1 might be attenuated by the

activity of TIMP-1-degrading enzymes present at distinct stages of neoplastic progression. Whereas infiltration of mast cells and activity of mast-cell chymase have been detected in abundance during the early stages of the K14-HPV16 model, both are noticeably reduced in the SCCs [1,15]. Therefore, to determine if neutrophils could potentially represent the source of proteolytic enzymes for degradation of TIMP-1, especially in the SCCs, we profiled neutrophil presence in staged neoplastic tissue sections in K14-HPV16 mice (Fig 5A-E). These analyses revealed that neutrophils were extremely rare in negative-littermate skin (Fig 5A) and in contrast, were progressively increased in hyperplastic and dysplastic tissue (Fig 5B, C), and reached a maximum in SCCs (Fig 5D). Given the abundance of infiltrating neutrophils detected in SCCs (Fig 5E), we speculated that activity of neutrophil elastase (NE) would similarly be increased and might be functionally inactivating high levels of TIMP-1. To assess this, enzyme solution assays using a specific peptide substrate of NE were performed on tissue extracts prepared from K14-HPV16 mice at different stages of neoplastic progression (Fig 5F). These analyses suggested that neutrophil elastase activity was indeed present throughout progression, reaching a maximum level in SCCs, and was specifically inhibited by addition of the specific inhibitor α1-antitrypsin. Therefore, enzymatic activity was present in K14-HPV16 mice and represented a possible mechanism for negative regulation of TIMP-1 inhibitory activity.

DISCUSSION

The present study demonstrates that the loss of endogenous TIMP-1 expression was not sufficient to alter characterisitics of neoplastic progression (e.g., tumor incidence, metastasis, hyperproliferation, orgelatinase activity) in the K14-HPV16 mouse model of epithelial carcinogenesis. Furthermore, expression of TIMP-2 and –3 during progression was preserved in HPV16/TIMP-1-deficient mice, suggesting that loss of endogenous TIMP-1 expression could potentially be compensated by concurrent expression of other TIMP family members. Finally, the activity of neutrophil-derived proteases, capable of degrading TIMP-1, was observed throughout progression and was maximal at the malignant stages in which expression of endogenous TIMP-1 is the highest, suggesting that the contribution of endogenous TIMP-1 to carcinogenesis could potentially be attenuated by degradation. In combination, these results suggest that the loss of endogenous TIMP-1 is by itself not sufficient to alter carcinogenesis in the K14-HPV16 model, perhaps due to functional redundancy from other TIMP family members and to degradation from inflammatory-derived proteases.

Multiplicity of pathways in K14-HPV16 carcinogenesis

The findings in this study of HPV16/TIMP-1-deficient mice represent paradoxical data as compared to the analysis of K14-HPV16 mice modified by constitutive expression of a human TIMP-1 transgene (HPV16/βA-hT1$^+$ mice). In these HPV16/βA-hT1$^+$ mice, transgenic TIMP-1 expression led to elevated proliferation and an enhanced propensity to undergo malignant conversion into invasive lesions (Chapter 3). We hypothesize that in combination, these two studies of both the TIMP-1-transgenic and the TIMP-1-deficient

HPV16 mice suggest that TIMP-1 is a modifier of carcinogenesis that is sufficient, but is not necessary for promoting the multiplicity of changes occurring during tumor development in K14-HPV16 mice.

In contrast to the findings with the TIMP-1 deficient HPV16 mice, loss-of-function studies with other potential modifiers of carcinogenesis have identified MMP-9 as an example of a factor that is critically necessary for promoting this multiplicity of neoplastic changes during K14-HPV16 tumorigenesis [2]. To test the hypothesis that MMP-9 is functionally-significant for tumorigenesis, Coussens and colleagues constructed HPV16 mice in which the endogenous MMP-9 gene had been deleted, and observed that these MMP-9-deficient mice exhibited a decreased incidence of SCCs compared to littermate controls [2]. These data support a model in which multiple, discrete pathways must be altered and/or activated for full progression to the tumor state, and furthermore, a minimal number or combination of these pathways must be compromised in order to exert a detectable attenuation in tumorigenesis. One implication, therefore, is that factors such as MMP-9 would participate in multiple pathways whereas TIMP-1 exerts regulatory pressure on fewer pathways necessary for manifesting a tumor. Consistent with this interpretation, loss of MMP-9 in the K14-HPV16 model has been shown to exert pleiotropic effects on neoplastic progression, resulting not only in reductions in proliferation [2], but delays in angiogenesis as well (Chapter 5) [1], both of which may be responsible for the observed decrease in carcinoma incidence [2].

In addition to the role of individual genetic modifiers such as TIMP-1 and MMP-9, the complexity of K14-HPV16-induced carcinogenesis is compounded by the effect varying genetic backgrounds of inbred mouse strains: different strains of inbred mice

have been shown to exhibit different susceptibilities to tumorigenesis induced by the K14-HPV16 transgene [34], as previously demonstrated for chemical carcinogenesis [35]. To normalize for these strain-specific differences, mice in which endogenous TIMP-1 gene had originally been mutated were backcrossed for a minimum of six generations into the FVB/n strain before crossing into the K14-HPV16-transgene-bearing animals. Furthermore, experimental cohorts were compared against HPV16 littermate controls with normal TIMP-1 expression. Nevertheless, the persistence of some background genetic loci may account for the differences in SCC incidence observed between the HPV16/T1$^{+/-}$ littermate controls (37.3%; Fig 2B) and the historic HPV16 controls (47.0%; Chapter 5).

The potency of the HPV16 early region as an oncogenic stimulus, derived in part from this multiplicity of pathways involved in the K14-HPV16 model, may help explain the context-specific effects observed for TIMP-1 in comparison to other models of tumorigenesis. For example, a protective effect of TIMP-1 was observed by Sternlicht and colleagues using a spontaneous mammary carcinoma model, based upon the whey-acidic protein promoter (WAP) driving breast specific expression of MMP-3 [36,37]. WAP-MMP-3 mice, in which hyperplastic lesions and mammary carcinomas develop spontaneously, were protected against the development of mammary lessions by the concurrent expression of human TIMP-1. This inhibitory effect of TIMP-1 on WAP-MMP-3-induced carcinogeneis was consistent with the primary stimulus for tumorigenesis being MMP-3 activity, one mechanism of which is believed to be cleavage of E-cadherin and subsequent alteration of the β-catenin signalling pathway [37]. In contrast to the WAP-MMP-3 mechanism of carcinogenesis, oncogenic stmulation by the

HPV16 transgene [7] is derived from the activities of the high-risk HPV type 16 oncoproteins E6 and E7 in mediating degradation of the tumor suppressor proteins p53 [38] and pRb [39], regulation of cyclin-dependent-kinases and their inhibitors [40], interaction with the AP-1 family of transcription factors [41], and multiple other processes [42]. Thus, one possible interpretation for the lack of any changes in the HPV16/T1$^{-/-}$ mice is that the potency of the K14-HPV16 oncogenic stimulus, in comparison to other mouse models, is overwhelming the contribution of endogenous TIMP-1 during neoplastic progression.

Functional redundancy from other TIMP family members

In addition to suggesting the multiplicity of pathways involved in K14-HPV16-induced carcinogenesis, the lack of any alterations in tumorigenesis observed in the HPV16/T1$^{-/-}$ mice may reflect the consequence of functional redundancy from concurrent expression of other TIMP family members during neoplastic progression. Despite differences in primary amino acid sequences among the TIMPs, which show ~30-40% identity among family members [1443], similarities in biological activities have been suggested from *in vitro* studies [3444]. TIMP-2, -3, and –4 have been shown to inhibit many of the same MMPs inhibitied by TIMP-1 [2930]. Furthermore, like TIMP-1, the other TIMP family members have been found to have proliferation-inducing activity, with TIMP-2 demonstrating erythroid potentiating activity as well [4]. TIMP-3, however, has been singular for its ability to induce apoptosis instead of inhibit it [45]. These and other distinguishing features among the TIMP family members indicate that the possibility of functional redundancy, suggested by *in vitro* characterization, still requires verification with *in vivo* models.

Recently, an *in vivo* model studying another protease inhibitor, the plasminogen activator inhibitor-1 (PAI-1), has provided a precedence for the possibility of functional redundancy during mammary tumorigenesis [46]. To test the functional significance of PAI-1 in a spontaneous model of breast tumorigenesis induced by the polymoavirus middle T antigen, Almholt and colleagues constructed tumorigenic mice lacking endogenous PAI-1 expression. Though PAI-1 is normally expressed in abundance in the mammary lesions of tumor-prone mice, loss of endogenous PAI-1 expression altered neither the growth of primary tumors nor the rate of metastasis [46]. The authors attributed these findings to the possibility of functional redundancy from the presence of other protease inhibitors, and consistent with this interpretation, expression of the closely-related PAI-2 was observed in the mammary tumors of PAI-1-deficient mice.

Thus, from our study of the K14-HPV16 mice, we conclude that the loss of endogenous TIMP-1 was not sufficient to alter the characteristics of carcinogenesis, possibly due to the multiplicity of pathways involved in neoplastic progression, the potency of the K14-HPV16 oncogenic stimulus, or the potential for functional redundancy from concurrent expression of other TIMP family members. The effects of concurrent expression from the other TIMPs in the HPV16/T1$^{-/-}$ mice could potentially be pursued, given the availability and viability of mice lacking functional TIMP-2 [36,47] or TIMP-3 [37] expression, as a possible future direction.

ACKNOWLEDGEMENTS

We would like to thank Paul Soloway and Zena Werb for the TIMP-1 homozygous null mice; Lidiya Korets, Jake Lee, and Andre Whitkin for technical assistance; and Elizabeth Hansell and members of the Coussens laboratory for discussion and critical comments.

REFERENCES

1. van Kempen, L.C.L. *et al.* Epithelial carcinogenesis: dynamic interplay between neoplastic cells and their microenvironment. *Differentiation* **70**, 501-623 (2002).

2. Coussens, L.M., Tinkle, C.L., Hanahan, D. & Werb, Z. MMP-9 supplied by bone marrow-derived cells contributes to skin carcinogenesis. *Cell* **103**, 481-490 (2000).

3. Fassina, G. *et al.* Tissue inhibitors of metalloproteases: regulation and biological activities. *Clin Exp Metastasis* **18**, 111-120 (2000).

4. Baker, A.H., Edwards, D.R. & Murphy, G. Metalloproteinase inhibitors: biological actions and therapeutic opportunities. *J Cell Sci* **115**, 3719-3727 (2002).

5. Woessner, J.F. & Nagase, H. *Matrix metalloproteinases and TIMPs*, (Oxford University Press, Oxford, UK, 2000).

6. Arbeit, J.M., Munger, K., Howley, P.M. & Hanahan, D. Progressive squamous epithelial neoplasia in K14-human papillomavirus type 16 transgenic mice. *J Virol* **68**, 4358-4368 (1994).

7. Coussens, L.M., Hanahan, D. & Arbeit, J. Genetic predisposition and parameters of malignant progression in K14-HPV16 transgenic mice. *Am J Path* **149**, 1899-1917 (1996).

8. Daniel, D. *et al.* Immune enhancement of skin carcinogenesis by CD4+ T cells. *J Exp Med* **197**(2003).

9. Soloway, P.D., Alexander, C.M., Werb, Z. & Jaenisch, R. Targeted mutagenesis of Timp-1 reveals that lung tumor invasion is influenced by Timp-1 genotype of the tumor but not by that of the host. *Oncogene* **13**, 2307-2314. (1996).

10. Osiewicz, K., McGarry, M. & Soloway, P.D. Hyper-resistance to infection in TIMP-1-deficient mice is neutrophil dependent but not immune cell autonomous. *Ann N Y Acad Sci* **878**, 494-496. (1999).

11. Edwards, D.R. The tissue inhibitors of metalloproteinases (TIMPs). in *Matrix Metalloproteinase Inhibitors in Cancer Therapy* (eds. Clendeninn, N.J. & Appelt, K.) 67-84 (Humana Press, Totowa, New Jersy, 2000).

12. Shimizu, S. *et al.* Cloning and sequencing of the cDNA encoding a mouse tissue inhibitor of metalloproteinase-2. *Gene* **114**, 291-292. (1992).

13. Apte, S.S. *et al.* Gene encoding a novel murine tissue inhibitor of metalloproteinases (TIMP), TIMP-3, is expressed in developing mouse epithelia, cartilage, and muscle, and is located on mouse chromosome 10. *Dev Dyn* **200**, 177-197 (1994).

14. Leco, K.J. *et al.* Murine tissue inhibitor of metalloproteinases-4 (Timp-4): cDNA isolation and expression in adult mouse tissues. *FEBS Lett* **401**, 213-217. (1997).

15. Coussens, L.M. *et al.* Inflammatory mast cells up-regulate angiogenesis during squamous epithelial carcinogenesis. *Genes Dev* **13**, 1382-1397 (1999).

16. Herron, G.S., Werb, Z., Dwyer, K. & Banda, M.J. Secretion of metalloproteinases by stimulated capillary endothelial cells. I. Production of procollagenase and prostromelysin exceeds expression of proteolytic activity. *J Biol Chem* **261**, 2810-2813 (1986).

17. Herron, G.S., Banda, M.J., Clark, E.J., Gavrilovic, J. & Werb, Z. Secretion of metalloproteinases by stimulated capillary endothelial cells. II. Expression of collagenase

and stromelysin activities is regulated by endogenous inhibitors. *J Biol Chem* **261**, 2814-2818. (1986).

18. Ducharme, A. *et al.* Targeted deletion of matrix metalloproteinase-9 attenuates left ventricular enlargement and collagen accumulation after experimental myocardial infarction. *J Clin Invest* **106**, 55-62 (2000).

19. Liu, Z. *et al.* The serpin alpha1-proteinase inhibitor is a critical substrate for gelatinase B/MMP-9 in vivo. *Cell* **102**, 647-655. (2000).

20. Nakajima, K., Powers, J.C., Ashe, B.M. & Zimmerman, M. Mapping the extended substrate binding site of cathepsin G and human leukocyte elastase. Studies with peptide substrates related to the alpha 1-protease inhibitor reactive site. *J Biol Chem* **254**, 4027-4032. (1979).

21. Curran, S. & Murray, G.I. Matrix metalloproteinases in tumour invasion and metastasis. *J Pathol* **189**, 300-308 (1999).

22. Egeblad, M. & Werb, Z. New functions for the matrix metalloproteinases in cancer progression. *Nat Rev Cancer* **2**, 161-174 (2002).

23. Hanahan, D. & Weinberg, R.A. The hallmarks of cancer. *Cell* **100**, 57-70 (2000).

24. Bertaux, B., Hornebeck, W., Eisen, A.Z. & Dubertret, L. Growth stimulation of human keratinocytes by tissue inhibitor of metalloproteinases. *J Invest Dermatol* **97**, 679-685. (1991).

25. Buisson-Legendre, N., Emonard, H., Bernard, P. & Hornebeck, W. Relationship between cell-associated matrix metalloproteinase 9 and psoriatic keratinocyte growth. *Journal of Investigative Dermatology* **115**, 213-218 (2000).

26. Guedez, L. *et al.* In vitro suppression of programmed cell death of B cells by tissue inhibitor of metalloproteinases-1. *J Clin Invest* **102**, 2002-2010 (1998).

27. Li, G., Fridman, R. & Kim, H.R. Tissue inhibitor of metalloproteinase-1 inhibits apoptosis of human breast epithelial cells. *Cancer Res* **59**, 6267-6275 (1999).

28. Guedez, L. *et al.* Tissue inhibitor of metalloproteinase-1 alters the tumorigenicity of Burkitt's lymphoma via divergent effects on tumor growth and angiogenesis. *Am J Pathol* **158**, 1207-1215. (2001).

29. Apte, S.S., Olsen, B.R. & Murphy, G. The gene structure of tissue inhibitor of metalloproteinases (TIMP)-3 and its inhibitory activities define the distinct TIMP gene family. *J Biol Chem* **270**, 14313-14318 (1995).

30. Liu, Y.E. *et al.* Preparation and characterization of recombinant tissue inhibitor of metalloproteinase 4 (TIMP-4). *J Biol Chem* **272**, 20479-20483. (1997).

31. Howard, E.W., Bullen, E.C. & Banda, M.J. Preferential inhibition of 72- and 92-kDa gelatinases by tissue inhibitor of metalloproteinases-2. *J Biol Chem* **266**, 13070-13075. (1991).

32. Frank, B.T., Rossall, J.C., Caughey, G.H. & Fang, K.C. Mast cell tissue inhibitor of metalloproteinase-1 is cleaved and inactivated extracellularly by alpha-chymase. *J Immunol* **166**, 2783-2792 (2001).

33. Itoh, Y. & Nagase, H. Preferential inactivation of tissue inhibitor of metalloproteinases-1 that is bound to the precursor of matrix metalloproteinase 9 (progelatinase B) by human neutrophil elastase. *J Biol Chem* **270**, 16518-16521. (1995).

34. Coussens, L.M., Hanahan, D. & Arbeit, J.M. Genetic predisposition and parameters of malignant progression in K14- HPV16 transgenic mice. *Am J Path* **149**, 1899-1917 (1996).

35. Hennings, H. *et al.* FVB/N mice: an inbred strain sensitive to the chemical induction of squamous cell carcinomas in the skin. *Carcinogenesis* **14**, 2353-2358. (1993).

36. Sternlicht, M.D. *et al.* The stromal proteinase MMP3/stromelysin-1 promotes mammary carcinogenesis. *Cell* **98**, 137-146 (1999).

37. Sternlicht, M.D., Bissell, M.J. & Werb, Z. The matrix metalloproteinase stromelysin-1 acts as a natural mammary tumor promoter. *Oncogene* **19**, 1102-1113 (2000).

38. Scheffner, M. Ubiquitin, E6-AP, and their role in p53 inactivation. *Pharmacol Ther* **78**, 129-139. (1998).

39. Munger, K. *et al.* Biological activities and molecular targets of the human papillomavirus E7 oncoprotein. *Oncogene* **20**, 7888-7898. (2001).

40. McMurray, H.R., Nguyen, D., Westbrook, T.F. & McAnce, D.J. Biology of human papillomaviruses. *Int J Exp Pathol* **82**, 15-33 (2001).

41. Antinore, M.J., Birrer, M.J., Patel, D., Nader, L. & McCance, D.J. The human papillomavirus type 16 E7 gene product interacts with and trans-activates the AP1 family of transcription factors. *Embo J* **15**, 1950-1960. (1996).

42. von Knebel Doeberitz, M. New markers for cervical dysplasia to visualise the genomic chaos created by aberrant oncogenic papillomavirus infections. *Eur J Cancer* **38**, 2229-2242 (2002).

43. Gomez, D.E., Alonso, D.F., Yoshiji, H. & Thorgeirsson, U.P. Tissue inhibitors of metalloproteinases: structure, regulation and biological functions. *Eur J Cell Biol* **74**, 111-122. (1997).

44. Brew, K., Dinakarpandian, D. & Nagase, H. Tissue inhibitors of metalloproteinases: evolution, structure and function. *Biochim.Biophys.Acta* **1477**, 267-283 (2000).

45. Woessner, J.F., Jr. That impish TIMP: the tissue inhibitor of metalloproteinases-3. *J Clin Invest* **108**, 799-800. (2001).

46. Almholt, K. *et al.* Metastasis of transgenic breast cancer in plasminogen activator inhibitor-1 gene-deficient mice. *Oncogene* **22**, 4389-4397 (2003).

47. Buck, T.B., Yoshiji, H., Harris, S.R., Bunce, O.R. & Thorgeirsson, U.P. The effects of sustained elevated levels of circulating tissue inhibitor of metalloproteinases-1 on the development of breast cancer in mice. *Ann N Y Acad Sci* **878**, 732-735 (1999).

FIGURE LEGENDS

Figure 1: Characterization of HPV16/TIMP1-deficient mice.

In situ hybridization for mouse TIMP-1. An antisense riboprobe specific for mouse TIMP-1 mRNA was hybridized to paraffin-embedded staged tissue sections from HPV16/mT1$^{+/+}$ (A-C) and HPV16/mT1$^{-/-}$ mice (D-F) with dysplastic ears (A, D) and SCC pathologies Grade I (B, E) and Grade III (C, F) from HPV16/mT1$^{+/+}$ and HPV16/mT1$^{-/-}$. Arrows indicate silver grains corresponding to TIMP-1 mRNA presence, most abundantly in the SCCs Grade I and Grade III, dashed lines denote the epidermal-dermal or keratinocyte-stromal boundaries, "e" epidermis, "d" dermis, "t" tumor, "s" stroma, and "*" keratin pearl. Scale bar: 100 μm.

Figure 2: Tumorigenicity in HPV16/TIMP1-null mice.

(A) Tumor-free survival of TIMP-1 knockout mice. Cohorts of HPV16/ TIMP-1$^{+/-}$ (n = 51) and HPV16/TIMP-1$^{-/-}$ mice (n = 109) were aged for the incidence of epidermal tumors, as found by gross examination. Curves reflect the percentage of tumor-free survival at each age in months ($p = 0.9448$, log-rank analysis).

(B) Incidence of specific epidermal lesions by category. Tissue sections from the two cohorts were analyzed by hematoxylin-eosin histopathology and immunohistochemistry to determine the incidence of hyperplasia by one month of age ("Hyp") and of dysplasia by six months ("Dys"); the lifetime incidence of papilloma, SCC, and microcystic adnexal carcinoma ("MAC"); and the incidence of lymph node metastasis ("LN mets")

among SCC-bearing mice. Values represent percentage of mice (LN mets: $p = 0.4764$, Fisher's exact test).

(C) Distribution of SCCs by Grade. Tissue sections of SCCs from the two cohorts were analyzed by hematoxylin-eosin histopathology and immunohistochemistry to determine the grade of each lesion. Values represent the percentage for each grade over the total number of SCC lesions within each cohort.

Figure 3: Proliferation, apoptosis, and proteolytic activity in HPV16/TIMP1-null mice.

(A) Proliferation of keratinocytes during carcinogenesis. Negative-littermate, HPV16/ TIMP-$1^{+/+}$ and HPV16/TIMP-$1^{-/-}$ mice were injected with the nucleotide analog bromodeoxyuridine (BrdU), incorporation of which was assessed in the ears of negative-littermate mice ("(-) LM"), premalignant ears with hyperplasia ("Hyp") or dysplasia ("Dys"), and SCC tumors ("SCC"). Proliferative index was quantified from dual-color immunohistochemistry as the percentage of BrdU-positive keratinocytes over total keratinocytes ("% BrdU(+) keratinocytes"), averaged from five high-power fields per mouse, and five mice per category. Error bars represent standard error of the mean.

(B) Apoptosis of keratinocytes during carcinogenesis. The TUNEL reaction was performed on adjacent tissue sections to those used in p(A) to determine the percentage of TUNEL-positive keratinocytes at distinct stages of neoplastic development in the two cohorts of mice. Apoptotic index was quantified as the percentage of TUNEL-positive keratinocytes over total keratinocytes, averaged from five high-power fields per mouse, and four mice per category. Error bars represent standard error of the mean.

(C) Gelatin substrate zymography of neoplastic tissue lysates. Tissue lysates were prepared from the same animals as in p(A), with distinct neoplastic development, and assessed for relative differences in levels of pro and/or active molecular weight forms of MMP-2 and MMP-9, which were not found to vary between the two genotypes. Hyperplasia (Hyp); dysplasia (Dys); SCC (SCC).

(D) Proteolytic activity against gelatin during carcinogenesis. Enzymatic solution assays were performed on tissue extracts from ears of negative-littermate mice ("(-) LM"), premalignant ears with hyperplasia ("Hyp") or dysplasia ("Dys"), and SCC tumors ("SCC"). Proteolytic activity in the extracts was measured by incubation with fluorescein-conjugated gelatin as the substrate. Values represent the change in relative fluorescence units (RFU) per minute per μg tissue protein, averaged for four mice per time-point. Error bars represent standard error of the mean.

Figure 4: Spatial-temporal expression patterns of TIMP-2, -3, and –4 in HPV16/TIMP-1-null mice.

(A-L) In situ hybridization for mouse TIMP-2 (A-D), TIMP-3 (E-H), and TIMP-4 (I-L) in HPV16/TIMP-1$^{-/-}$ mice. Antisense riboprobes specific for mouse TIMP-2, -3, and-4 mRNA were hybridized to paraffin-embedded staged tissue sections of ears with hyperplasia (A, E, I) or dysplasia (B, F, J), and SCC pathologies Grade I (C, G, K) and Grade III (D, H, L). Arrows indicate silver grains corresponding to mRNA presence, dashed lines denote the epidermal-dermal or keratinocyte-stromal boundaries, "e" epidermis, "d" dermis, "f" follicle, "t" tumor, "s" stroma, and "*" keratin pearl. Scale bar: 100 μm

Figure 5: Neutrophil infiltration and neutrophil elastase activity in HPV16 mice.

(A-E) Neutrophil infiltration during carcinogenesis. Immunohistochemistry for neutrophils (in blue) was performed on sections from ears of negative-littermate mice (A; "(-)LM"), premalignant ears with hyperplasia (B; "Hyp") or dysplasia (C; "Dys"), and SCCs (D) from HPV16 mice. Green arrows indicate neutrophils, dashed lines denote the epidermal-dermal boundaries, "e" epidermis, "d" dermis, and "c" cartilage. Scale bar: 100 μm. Neutrophil density (E) was quantified as the number of neutrophils per unit stromal area of 1,000 μm^2, averaged from five high-power fields per mouse, and five mice per category. Error bars represent standard error of the mean.

(F) Neutrophil elastase activity during carcinogenesis. Enzymatic solution assays were performed on tissue extracts prepared from HPV16 mice. Proteolytic activity in the extracts was measured by incubation with a fluorescence-quenched peptide (methoxysuccinyl-Ala-Ala-Pro-Val-amidomethylcoumarin) as the substrate. Values represent the change in relative fluorescence units (RFU) per minute per μg tissue protein, averaged for three mice per time-point. Error bars represent standard error of the mean.

Figure 1

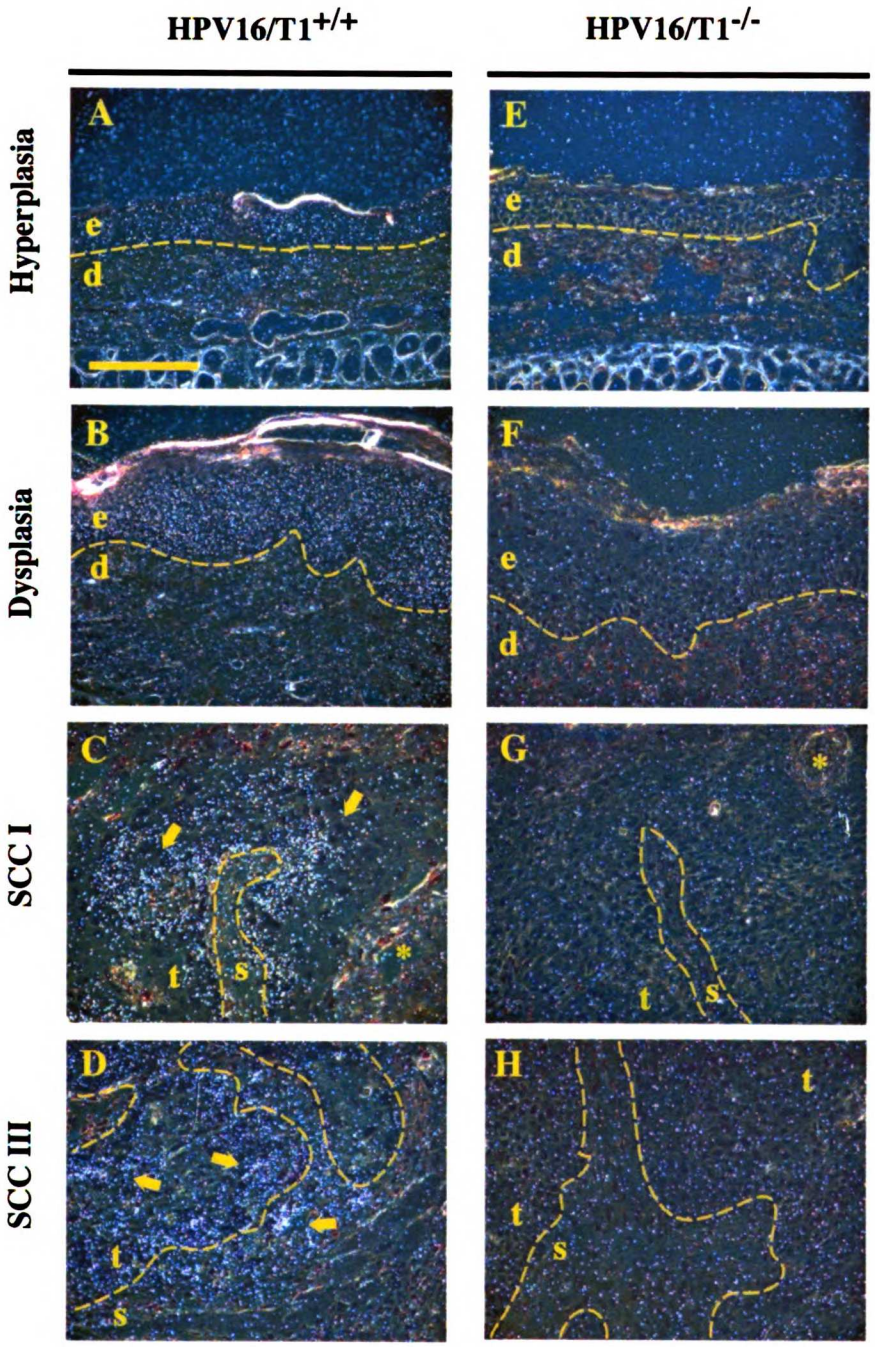
HPV16/T1+/+
HPV16/T1-/-
Hyperplasia
Dysplasia
SCC I
SCC III
A
B
C
D
E
F
G
H
e
d
t
s
*

A

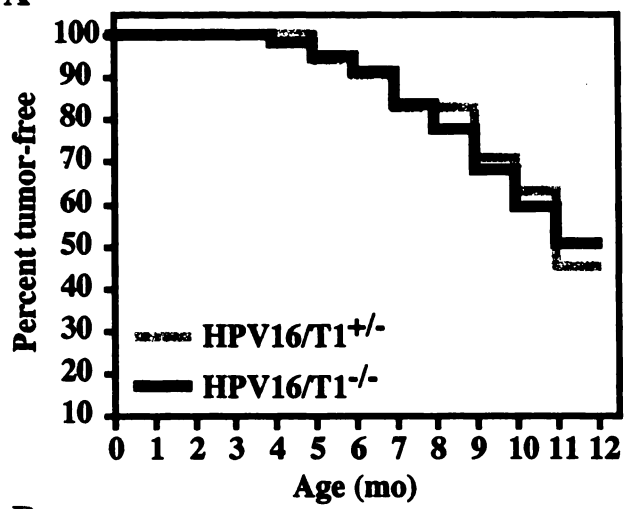

B

Histopathology	HPV16/T1$^{+/-}$ n = 51	HPV16/T1$^{-/-}$ n = 109
Hyp (by 1-mo)	100	100
Dys (by 6-mo)	100	100
Papilloma	11.8	11.0
SCC	37.3	27.8
MAC	11.8	5.7
LN mets	21.1	13.8

C

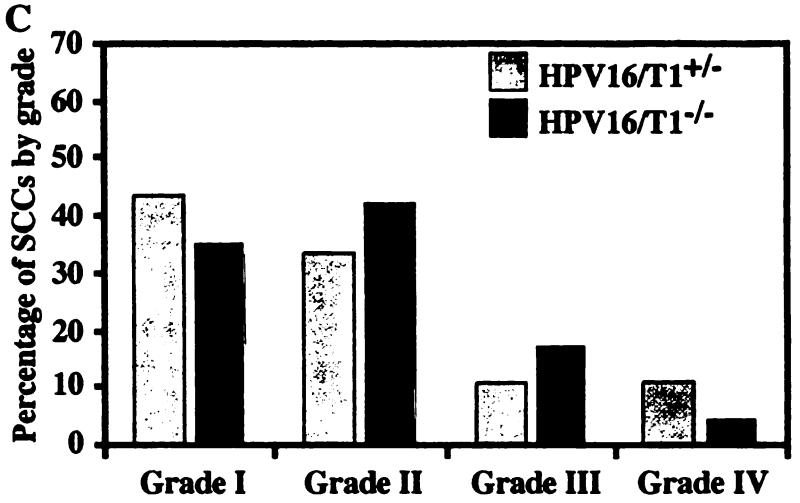

Figure 3

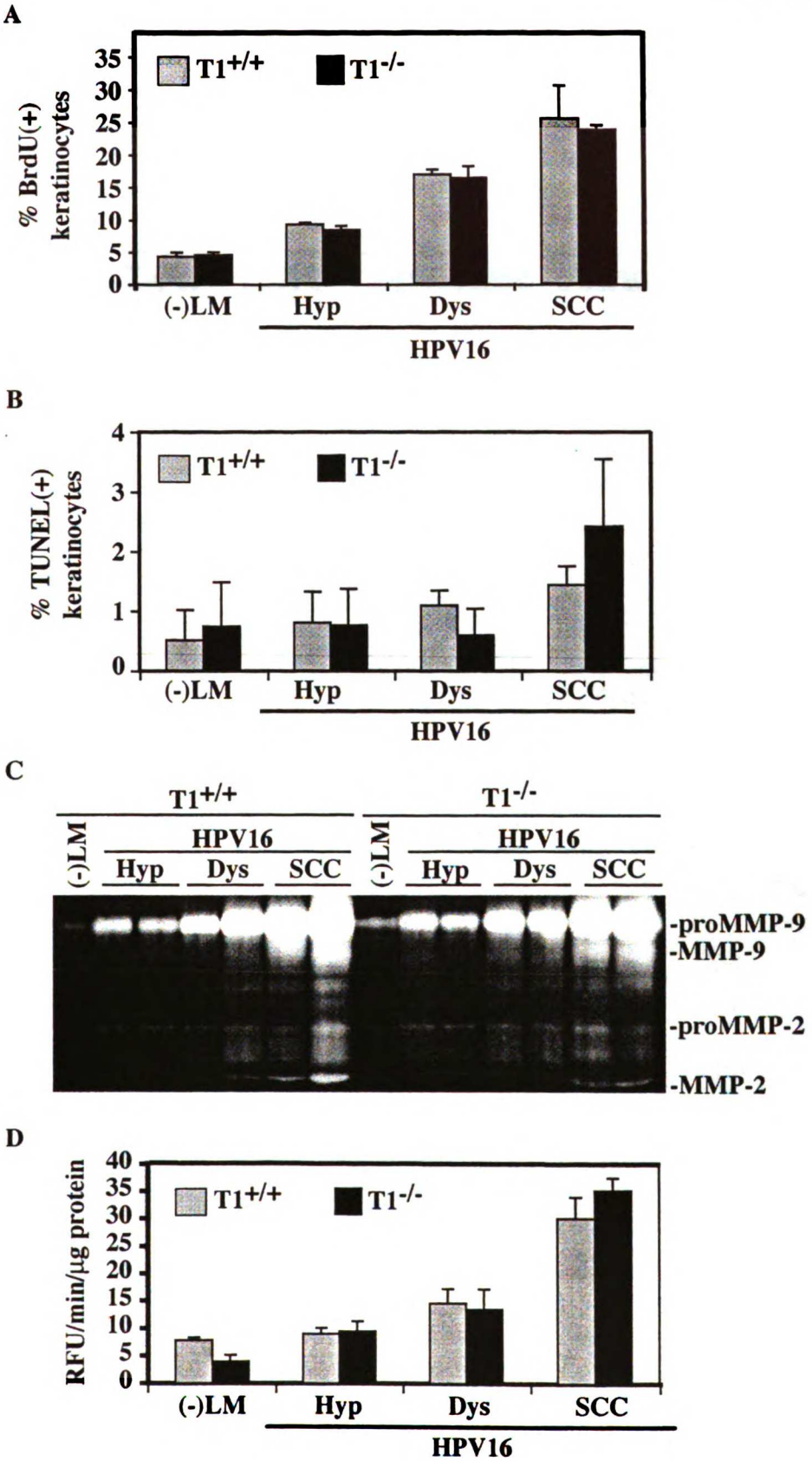
A
% BrdU(+) keratinocytes
T1+/+
T1-/-
(-)LM
Hyp
Dys
SCC
HPV16
B
% TUNEL(+) keratinocytes
C
T1+/+
T1-/-
HPV16
-proMMP-9
-MMP-9
-proMMP-2
-MMP-2
D
RFU/min/µg protein

Figure 4

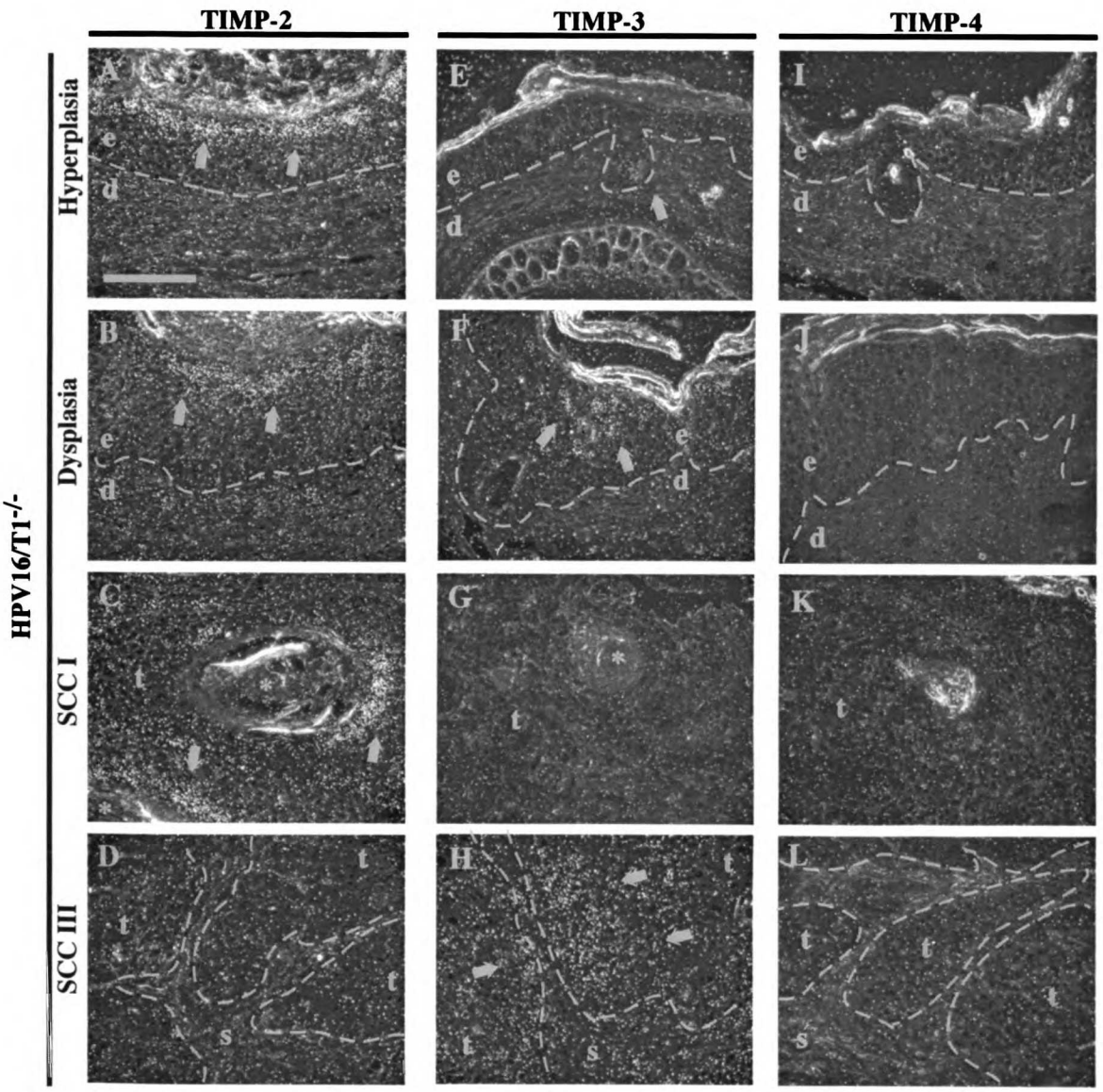
TIMP-2
TIMP-3
TIMP-4
HPV16/T1-/-
Hyperplasia
Dysplasia
SCC I
SCC III
A
B
C
D
E
F
G
H
I
J
K
L
e
d
t
s

Figure 5

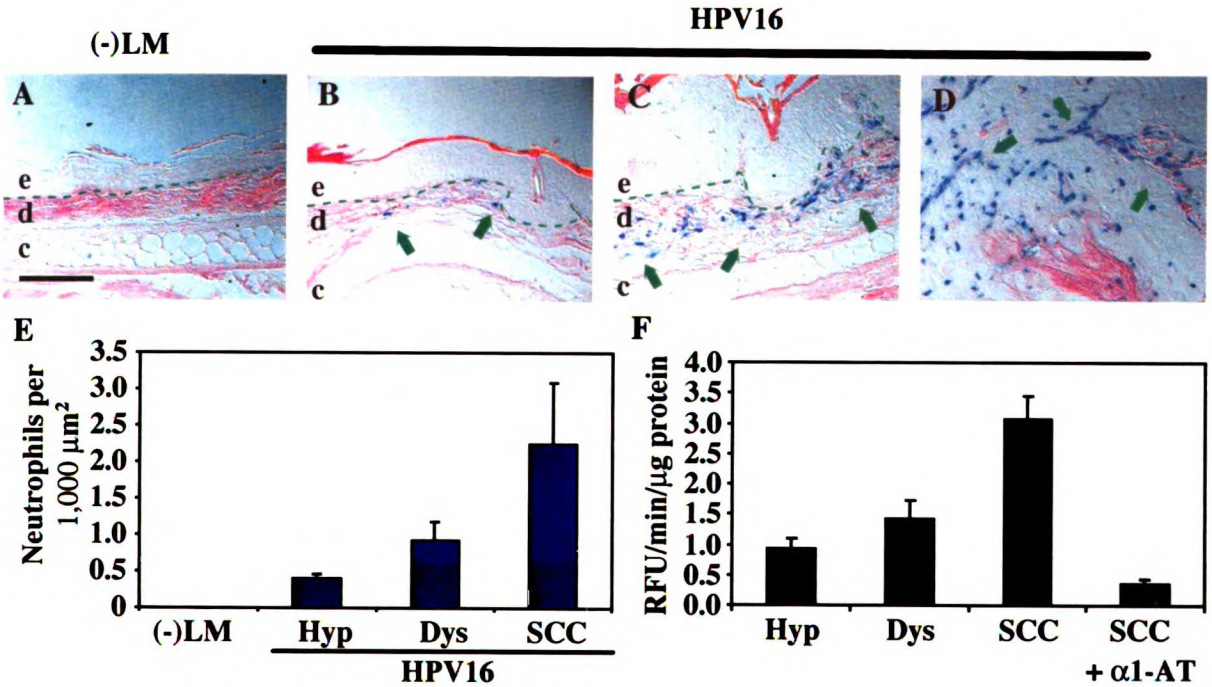
(-)LM
HPV16
A
B
C
D
e
d
c
E
Neutrophils per 1,000 µm²
3.5
3.0
2.5
2.0
1.5
1.0
0.5
0
(-)LM
Hyp
Dys
SCC
HPV16
F
RFU/min/µg protein
4.0
3.5
3.0
2.5
2.0
1.5
1.0
0.5
0.0
Hyp
Dys
SCC
SCC
+ α1-AT

Chapter 5

Epithelial Carcinogenesis: Dynamic Interplay Between Neoplastic Cells and Their Microenvironment

PROLOGUE

This chapter describes studies assessing the significance of epithelial-stromal interactions in the context of K14-HPV16 epithelial carcinogenesis. It represents a collaborative effort with other members of the Coussens lab, with the histopathological analysis performed by Lisa Coussens (Fig 1, 2, Table 1), the vascular architecture analyses by Lisa Coussens, Jake Lee, and myself (Fig 3), inflammatory cell profiling was performed by myself (Fig 4), and gelatin substrate zymography by Christopher Tinkle (Fig 5). This chapter was published in the journal *Differentiation.*

ABSTRACT

Matrix metalloproteinases (MMPs) have long been thought of as critical factors regulating matrix degradation associated with cell invasion into ectopic tissue compartments during primary tumor growth and metastasis. One member of the MMP family historically linked to these invasive processes is MMP-9/gelatinase B. By studying a transgenic mouse model of *de novo* epithelial carcinogenesis, new roles for MMP-9 have emerged that broaden the view of its functional contribution to malignant progression. The combined implication of these studies suggest that MMP-9 functionally contributes to cancer development; however, its major regulatory role may be in its ability to activate poorly diffusible and/or matrix-sequestered growth factors that regulate epithelial and/or endothelial cell growth as opposed to regulating cellular invasion across basement membranes.

INTRODUCTION

It is well established that cancer is a progressive disease, occurring in a series of well-defined stages, typically arising in proliferating cells harboring activating and/or inactivating mutations in critical 'sentinel' genes. From studies exploiting cultured tumor cells, two-stage carcinogenesis protocols in mice, and transgenic mouse models of human cancer, it is now evident that single mutagenic events do not result in the formation of malignant tumors. Instead, additional genetic and epigenetic events are necessary for progression to the tumor state. Initiated cells require alterations rendering them self-sufficient for growth, insensitive to growth-inhibitory signals, resistant to programs of terminal differentiation, senescence, or apoptosis – as well as endowing them with unlimited self-renewal capacity, the ability to orchestrate and direct sustained angiogenesis, and the ability to invade and thrive in ectopic tissue environments [1]. Acquiring these hallmarks of tumor progression and metastasis is most likely not solely dependent on the neoplastic cells themselves, but also dependent upon environmental cues.

In 1982, Bissell and co-workers [2] proposed that the cellular microenvironment directly modulated cell fate. Indeed, cell morphology and even tissue architecture largely depends on the nature of the pericellular environment [3]. The functional association of neoplastic cells with their extracellular matrix (ECM) and 'normal' cells within a 'tumor' can be regarded as a unique organ that undergoes dynamic change as malignancy ensues [3]. Homeostasis within an organ is maintained by complex growth factor signaling within the ECM that is, in part, regulated by expression and bioavailabilty of mitogenic and angiogenic molecules. The dynamic microenvironment resulting from extensive matrix

remodeling would therefore potentially alter the status quo of growth factor bioavailability and subsequently affect neoplastic progression.

A clear goal in the past several decades has been to identify classes of molecules regulating post-initiation, rate-limiting biologic events critical for cancer evolution. ECM remodeling enzymes of the matrixin gene family, *i.e.* matrix metalloproteinases (MMPs), have been at the forefront of these investigations due to their abundant expression in neoplastic tissues and their *in vitro* capacity to degrade virtually all ECM components [4,5]. MMPs are, therefore, potentially critical modulators of the pericellular environment that may evoke a response of (tumor) cells to a changing milieu, *e.g.* enabling tissue expansion and/or cell migration. Like many other classes of proteolytic enzymes, MMPs are first synthesized as inactive proenzymes or zymogens. They are found as either secreted or cell surface enzymes sharing several highly conserved domains, including a pre- and pro-peptide domain, a catalytic domain containing a zinc atom binding site, as well as several other structural domains believed to facilitate specific interactions with substrates and/or other target molecules [6,7]. Strict control over MMP activity occurs at both the transcriptional and post-transcriptional levels resulting in spatially and temporally controlled proteolytic activity [5]. A further level of MMP regulation results from specific interactions with naturally occurring tissue inhibitors of MMPs (TIMPs 1-4) [8], the μ2-macroglobulin plasma protein that facilitates irreversible clearance of MMPs via scavenger receptor-mediated endocytosis [9], as well as a newly described membrane-associated MMP inhibitor, RECK [10]. Disruption or alteration of proteolytic activity at any one of these regulatory steps can result in varied cellular responses towards the microenvironment.

Degradation of ECM by proteinases has long been viewed as being essential for tumor progression since focal destruction of ECM barriers theoretically permits invasion of malignant cells into the surrounding tissue, entry and exit from venous and lymphatic vasculature, and metastasis. While many lines of investigation have implicated the importance of MMPs during neoplastic growth, mouse models of *de novo* cancer development harboring homozygous null mutations in MMP genes has revealed new, previously unappreciated, regulatory roles for this important multi-gene family. This article focuses on the role of one member of the MMP-family, MMP-9/gelatinase B, and its role during squamous carcinogenesis of the skin.

METHODS AND MATERIALS

Histopathology and Immuno- and enzyme histochemistry

Generation and husbandry of K14-HPV16 and MMP9$^{-/-}$ mice, intercrossing, generation and husbandry of HPV16/MMP9$^{-/-}$ mice has been reported elsewhere [11]. Tissue pieces from transgenic and control animals were immersion-fixed in 3.75% paraformaldehyde and phosphate buffered saline (PBS) followed by dehydration through graded alcohol's and xylene, and embedded in paraffin. 5-μm-thick paraffin sections were cut using a Leica 2135 microtome. Sections were deparaffinized and subjected to immunohistochemical staining as previously described [11]. Dilutions of the primary antibodies: pan-Keratin, 1:200 (pAb 071P, BioGenex), CD45, 1:500 (Leukocyte Common Antigen, Ly-5, Pharmingen), and neutrophil-specific primary antibody 1:1000, (CL8993AP Cedarlane Labs). Epitopes were visualized by NBT/X-phosphate substrate (Roche) or 3,3'-diaminobenzidine (DAB; Sigma,) and counterstained with either Gils Hematoxylin #3, 1% Methyl Green or Eosin Y. All immunolocalization experiments were repeated three times on multiple tissue sections and included negative controls for determination of background staining, which was negligible. Chloroacetate esterase histochemistry was performed to visualize serine esterase activity in mast cells as described previously [12]. Neutrophils and mast cells were counted in five high-power (40X) fields per staged tissue section from five mice per neoplastic stage (time point). Data presented reflect the total cell count per area (μm^2) from the ventral ears leaflet and the peripheral area of Grade II squamous cell carcinomas (SCCs). All tissues were histopathologically staged based on Hematoxylin and Eosin and keratin intermediate filament expression as previously described [11]. Images were visualized with a Leica

DMRXA brightfield microscope equipped with a Leica DC500 digital camera. Images were captured and analyzed using Improvision, Inc., OpenLab Imaging Analysis Software.

Confocal fluorescent angiography

Mice were tail vein injected with 100 µl fluorecein isothiocyanate conjugated *Lycopersicon esculentum* (tomato) lectin (2 mg/ml, Vector Laboratories, FL-1171) followed by cardiac perfusion through the aorta with 30 ml PBS-buffered 4% paraformaldehyde (pH 7.4) [13]. Ears were harvested and the ventral aspect of the ear separated from cartilage, immersion fixed in PBS-buffered 4% paraformaldehyde (pH 7.4) for 4 hr at 4°C, rinsed briefly in PBS and whole mounted in Vectashield mounting medium (Vector Laboratories) for fluorescence visualization using a Laser scanning confocal Zeiss LSM510 META microscope and analyzed with a Zeiss LSM Image Examiner.

MMP expression profiling

RNA was isolated from histologically staged tissues pieces with Trizol (GibcoBRL) according to the manufacturer. Following DNAse treatment (RQ1 DNAse, Promega), 1µg total RNA was reverse transcribed (RT Superscript II, Invitrogen) according to manufactures specifications. The reaction mixture for the subsequent polymerase chain reaction amplifications contained dATP, dGTP, dCTP, dTTP (200 mM each), 0.5 pmol 5' forward and 3' reverse primer in buffer (10 mM Tris pH 8.3, 50 mM KCL and 2.5mM $MgCl_2$). Taq polymerase was added during the initial denaturing step at 95°C. Samples

were amplified in 30 cycles (95°C 1 minute, TM 45 seconds, 72°C 45 seconds) and a final extension at 72°C for 10 minutes. Control reactions contained either control cDNA for specific primer sets or minus-RT RNA control. Sequences for the oligonucleotide primers, annealing temperatures and expected amplimer lengths for RT-PCR were: mCol1A: 5' primer CCT AAC TAT AAG CTT GCT CAC A, 3' primer GAA TAC CTA TTA AAT TGA GCT C, 60°C, 430 bp [14]; mCol1B: 5' primer TTG ATC GAT GTG ATA GAC CTT A, 3' primer AGC AGT TGA ACC AAG TAT TAA T, 60°C, 470 bp [14]; mMMP-2: 5' primer TTG AGA AGG ATG GCA AGT ATG G, 3' primer ACA CCT TGC CAT CGT TGC, 55°C, 326 bp; mMMP-3: 5' primer GAC AAT TCT GGA GGT TTG ATG AGA, 3' primer ACC AGC TGT TGC TCT TCA ATA TGT G, 65°C, 3mM $MgCl_2$, 207 bp; MMP-9: 5' primer GGC GTG TCT GGA GAT, 3' primer AGG GTC CAC CTT GTT CAC C, 55°C, 190 bp; mMMP-8: 5' primer TGA CTC TGG TGA TTT CTT GCT AA, 3' primer GTG AAG GTC AGG GGC GAT GC, 65°C, 164 bp (Balbin *et al*, 1998); mMMP-10: 5' primer TTC TCC ACA AGC CCA GCT AAC, 3' primer TGA CTG AAT CGA AGG ACA AAG C, 55°C, 171 bp; mMMP-11: 5' primer ATC TCA TTA CCA ACA CCA CTC C, 3' primer CTA TGC CTA CTT CCT TCG TGC, 68°C, 5mM $MgCl_2$, 527 bp; mMMP-12: 5' primer CTG CCT GTG GGG CTG CTC CCA T, 3' primer ATC CTC ACG CTT CAT GTC CG, 65°C, 329bp; MMP-13: 5' primer GAC ATT CTG GAA CGT TAT CC, 3' primer ACT CTC ACA ATG CGA TTA CTC C, 55°C, 304 bp; mMMP-14: 5' primer CTC TCT TCT GGA TGC CCA ATG, 3' primer CAC CTC AAT GAT GAT CAC CTC, 55°C, 343 bp.

Substrate Zymography

Tissue samples representing distinct histological stages of neoplastic progression, as verified by histological analysis of paraffin-embedded sections from adjacent skin, were weighed and then homogenized (1:4 weight to volume) in lysis buffer containing 50 mM Tris-HCl (pH 8.0), 150 mM NaCl, 1% NP-40, 0.5% deoxycholate, 0.1% SDS. Soluble and insoluble extracts were separated by centrifugation and subsequently stored at -20°C. Equivalent amounts of soluble extract were analyzed by gelatin zymography on 10% SDS-polyacrylamide gels copolymerized with substrate (1 mg/ml of gelatin) in sample buffer (10% SDS, 0.25 M Tris-HCl, 0.1% Bromphenol Blue, pH 6.8). After electrophoresis, gels were washed twice for 15 min in 2.5% Triton X-100, incubated for 16 hrs at 37°C in 50 mM Tris-HCl, 10 mM $CaCl_2$ (pH 7.6), and then stained in 0.5% Coomassie Blue and destained in 50% methanol. Negative staining indicates the location of active protease bands. Exposure of proenzymes within tissue extracts to SDS during gel separation procedure leads to activation without proteolytic cleavage. For inhibition of MMP proteolytic activities, substrate gels were incubated in substrate buffer with 4 mM 1,10-phenanthroline (Sigma), 5 mM phenylmethylsulfonylfluoride (PMSF), or 2 mM N-ethylmaleimide (Sigma). Data shown in Figure 5 is representative of results obtained following examination of ~200 tissue pieces representing various stages of neoplastic progression.

Lethal irradiation and bone marrow transplantation.

HPV16/MMP-9 +/- and HPV16/MMP-9 -/- mice were lethally X-irradiated with 7.5 Gray (Gy). 24 hours later, bone marrow-derived cells from either wild-type MMP-9-

sufficient (+/+) mouse or MMP-9-deficient (-/-) mice were obtained by flushing the cavity of freshly dissected syngeneic femurs and tibias with PBS. Flushed cells were dispersed by pipetting, washed, and resuspended in PBS. Nucleated cells ($1x10^6$) in 50 µl were transplanted retro-orbitally into lethally irradiated animals, 10 - 12 animals per cohort. Neomycin at 2 mg/ml was added to the water of the irradiated mice. To verify engraftment, small (~ 1 mm^2) punch biopsies were removed from ear skin at 3 and 5 months of age and cut in half. One half of each punch biopsy was subjected to gelatin zymographic analysis to test for MMP-9 activity. The other half of each punch biopsy was embedded in paraffin (see above) and used for histopathology.

RESULTS

The skin as a model organ to study microenvironmental signaling

The skin is composed of a variety of cells and structures, *e.g.* keratinocytes, fibroblasts, inflammatory cells, vascular endothelial cells, dendritic cells and epithelial cells making up the hair follicles and sebaceous glands. Moreover, skin constitutes the largest mammalian organ. Although sebaceous glands, hair follicles and the epidermis are different structures within skin (Fig. 1A), they share a common origin - the epithelial stem cell. These pluripotent cells reside in the bulge region of the hair follicle [15] and differentiate into, 1) transient amplifying cells that constitute the epidermis, 2) cells that differentiate into sebatocytes that subsequently form the sebaceous gland, and 3) cells that form the hair follicle [16,17]. The environmental clues regulating these cell fate decisions are still the subject of great debate. It is clear however, that during embryonic development, skin differentiation is regulated by varying spatial cues emanating from the stroma; thus, skin is an excellent and easily accessible organ system in which to study the role of the local micro- and macro-environment in regulating differentiation decisions during normal developmental processes as well as during neoplastic progression of cutaneous structures towards malignant tumors.

K14-HPV16 mice display a spectrum of epithelial malignancies.

In a transgenic mouse model of epithelial carcinogenesis, keratin 14 driven expression of the human papillomavirus type 16 (HPV16) early region genes, including the E6 and E7 oncogenes, results in reproducible multistage development of invasive squamous cell carcinoma of the epidermis [18]. In addition, since the keratin 14 promoter is also active in

the epithelial stem cell compartment and cells that give rise to the sebaceous gland and hair follicles, neoplasms with sebaceous and follicular differentiation are also observed in HPV16 transgenic mice, albeit to a lesser degree (Fig. 1B and C; Table 1).

Tumors of squamous origin. HPV16 transgenic animals are born phenotypically normal; by one month of age, with 100% penetrance, epidermal hyperplasias appear (Fig. 1C, 2B; Table 1), and advance focally into angiogenic dysplasias between 3 and 6 months (Fig. 1C, 2C; Table 1) and sporadically into papillomas (10% lifetime risk, Fig. 1C, 2D; Table 1). Angiogenic dysplasias are characterized by increased density and altered architecture of capillaries (Fig. 3A-D) and intense leukocyte infiltration of the reactive stroma (Fig. 4A-E) [12,19]. Premalignant epidermal lesions in HPV16 mice are characterized by a progressively increasing keratinocyte proliferation index (Table 1) [11]. Accompanying increased proliferation, is an alteration in the repertoire of keratin intermediate filament proteins that correlates with loss of terminal differentiation [18]. By one year of age, 50% of transgenic mice (maintained in the FVB/n strain background) develop invasive squamous cell carcinomas (SCCs, Fig. 1C, 2E-G; Table 1), of which ~20% metastasize to regional lymph nodes (Fig. 2H) [18]. Tumors emerge out of dysplastic skin lesions and develop most frequently on ear (25%) and truncal (72%) skin, and, less frequently, on the head (2%) and appendages (1%).

Tumors of sebaceous origin. Neoplastic lesions of sebaceous origin, including sebaceous hyperplasias (3.5% lifetime risk; Fig. 1C; Table 1), consist of a greatly enlarged sebaceous gland composed of numerous lobules around a centrally located, wide

sebaceous duct (Fig. 2I). Large lesions may consist of several enlarged glands and contain several ducts, with sebaceous lobules grouped around each of them. Although some lobules appear fully mature, others show more than one peripheral row of undifferentiated cells. These lesions can progress into sebaceous adenomas (3.4% lifetime risk, Fig. 1C, 2J; Table 1) that are characterized by incompletely differentiated irregular sebaceous lobules consisting of mature sebaceous cells and undifferentiated keratin-positive basaloid epithelial cells at the periphery of the sebaceous glands (Fig. 2K).

Tumors of follicular origin. The follicular neoplasms observed in HPV16 mice arise from the infundibular region of the upper permanent segment of the hair follicle. Trichofolliculoma (9.2% lifetime risk; Fig. 1C; Table 1) consists of one to three large follicular cysts lined by squamous epithelium containing horny material and frequently hair shafts. In cases where a central pore is present, the large cystic space is continuous with the epidermis, indicating that it represents an enlarged distorted hair follicle (Fig. 2L). Small and usually well-differentiated "secondary" hair follicles radiate from the wall of these "primary" hair follicles and remain connected by epithelial strands. These lesions may progress into trichoadenomas (10% lifetime risk; Fig. 1C; Table 1) that are characterized by numerous keratin-positive cystic structures linked to one another via merger of the epithelial lining or small columns of squamous epithelium (Fig. 2M). In contrast to the benign neoplasms, trichofolliculoma and trichoadenoma, malignant microcystic adnexel carcinomas (MACs; 3.1% lifetime risk; Fig. 1C; Table 1) are characterized by numerous single or clusters of differentiated wholly solid keratin-

positive cells, typically found in the dermis in cystic structures that invade widely and deeply (Fig. 2N-P). Similar to human MAC, these lesions fail to develop detectable metastases.

Inflammation potentiates angiogenesis in the skin

Neoplastic progression is characterized by the formation of new blood vessels at the tumor-host interface and often coincides with increased infiltration of inflammatory cells [1]. Induction of an angiogenic program is essential for sustaining growth of tumorigenic cells beyond the limit of growth for which passive diffusion of nutrients from preexisting blood vessels is sufficient [1]. HPV16 mice display vascular as well as inflammatory changes consistent with the activation of an angiogenic switch during neoplastic progression from hyperplasia to dysplasia (Fig. 3 and 4). The stroma underlying hyperplastic lesions evidences a modest increase in the density and dilation of capillaries as compared to the dermal vasculature of wildtype skin, as visualized by immunolocalization of platelet endothelial cell adhesion molecule PECAM-1/CD31 or by fluorescent angiography (Fig. 3A, B, E and F, respectively). In contrast, dysplastic lesions display dilated and enlarged capillaries in close proximity to the dermal-epidermal interface (Fig. 3C), in a tortuous, dense organization (Fig. 3G). These changes are indicative of an angiogenic switch from vascular quiescence to modest neovascularization in early low-grade lesions (hyperplasias) to a striking upregulation of vascularization in high-grade dysplasias. SCCs are highly vascularized containing a combination of small and dilated vessels (Fig. 3D and H).

Initial investigation into angiogenic factors that may have been responsible for

these characteristic changes in vascular architecture and physiology revealed that the bulk of transcriptional induction of notable angiogenic growth factors, *i.e.* basic fibroblast growth factor (bFGF) and vascular endothelial growth factor (VEGF), occurred after the apparent angiogenic switch [20]. This data suggested that the early induction of angiogenesis in the skin of HPV16 mice was likely potentiated by the activation of factors resident within the ECM or delivered to lesional skin focally by the degranulation of infiltrating leukocytes. To test this hypothesis, leukocytes were profiled in HPV16 mice by immunodetection of CD45 (leukocyte common antigen) in staged neoplastic tissues (Fig. 4). This data suggested that accompanying epithelial neoplastic progression in HPV16 mice, there was an incremental increase in the number of CD45-positive leukocytes in the successive neoplastic stages (Fig. 4A-E) paralleling the induction and activation of the angiogenic vasculature (Fig. 3). A more detailed analysis of the specific granulocyte populations present in discrete neoplastic stages revealed an early increase in the number of mast cells and neutrophils in the premalignant lesions, while in frank carcinomas, the presence of neutrophils was found both within SCCs and at their invasive borders where mast cells were also localized (Fig. 4F).

Mast cells are bone marrow derived inflammatory cells of hematopoeitic origin that are often associated with immune responses towards experimentally induced rodent tumors as well as a variety of human neoplasms [21]. In angiogenic dysplasias, degranulation of mast cells likely alters the local balance of pro- and anti-angiogenic factors, likely via the release of diverse proteases, *e.g.*, chymase, tryptase, and matrix metalloproteinases. Proteolysis of the ECM facilitates endothelial cell migration and proliferation and results in a release of matrix sequestered latent mitogenic and

angiogenic molecules [22]. In addition, mast cells contain proMMP-9 in granules [23] that is released into the ECM upon mast cell degranulation; thus, mast cells are an important source of MMP-9 while also directly participating in the activation of latent proMMP-9 by mast cell-derived chymase [12,23]. In addition, mast cell derived tryptase is a mitogen for both keratinocytes and dermal fibroblasts and induces expression of type I collagen mRNAs [12,24].

The accumulation of mast cells at the leading edge of carcinomas where tumor cells invade into ectopic stroma, suggest that mast cells may regulate conversion of the cellular environment into a neoplastic stroma permissive for angiogenic activity. To test the hypothesis that mast cells contribute to squamous carcinogenesis, mast cell deficient/HPV16 transgenic mice were generated by introduction of $KIT^{W}/KIT^{W^{v}}$ alleles [12]. Mast cell-deficient/HPV16 transgenic mice demonstrated an attenuated early neoplastic phenotype characterized by reduced epithelial thickness, keratinocyte proliferation and vascularization [12], suggesting a role for mast cell-derived factors during premalignant progression.

MMP expression in HPV16 neoplastic skin

MMPs have long been viewed as critical regulators of neoplastic progression, owing largely to their *in vitro* biochemical properties of degrading ECM proteins and their expression adjacent to migrating cells *in vivo* [5,7,25]. To assess the relative contribution of MMP mRNA expression to neoplastic-associated ECM remodeling in HPV16 mice, MMP mRNAs and protease activities were assessed in biopsies of staged neoplastic tissues by *in situ* hybridization, real-time and/or RT-PCR analysis and gelatin substrate

zymography (Table 2). The combined expression profile of this diverse protease family suggests that MMP-14, -15 and –17 mRNAs are expressed in normal wildtype murine skin. It is notable that these family members represent a subset of the membrane-type MMPs as opposed to soluble family members. In neoplastic tissues, mRNAs encoding MMP-2, -3 –9, -11, -12 -14 –15 and -17 were found in tissues representing all stages of progression. In contrast, MMP-8, -10, -16 and –19 were identified in dysplastic tissues as well in SCCs, whereas mRNAs encoding MMP-7 and MMP-13 were only found in tissues derived from frank carcinomas.

In situ hybridization analysis further revealed that expression of MMPs-2, -3 and –11 mRNA was restricted to activated stromal fibroblasts in close association with neoplastic epithelium. In hyperplastic skin, MMP-9 mRNA was detected in isolated basal keratinocytes abutting skin abrasions and in some hair follicles, but primarily in cells localized around capillaries and in a subset of tumor associated fibroblasts [11]. Expression of MMP-13 was observed emanating from both stromal cells and neoplastic keratinocytes only within carcinomas (van Kempen *et al*, manuscript in preparation). These varied patterns of MMP mRNA expression suggest that while some MMPs are present at all stages of neoplastic progression, others are restricted to a particular cell type or to a particular neoplastic stage suggesting that multiple, non-redundant cell signaling pathways are activated during neoplastic progression, each possibly regulating a unique subset of MMP mRNAs, the functional consequences of which are of as yet undetermined.

While mRNA expression profiling is informative, it likely reflects an underestimation of MMP presence as these molecules are also delivered to lesional tissue

by a variety of granulocytes, *e.g.* neutrophils, mast cells and macrophages. To address the total gelatinolytic activity present in neoplastic tissue, we employed gelatin substrate zymography to reveal temporal changes in proteolytic activities as compared to negative littermate normal skin (Fig. 5A). This analysis revealed that the proenzyme form of MMP-9 was barely detectable in normal skin, and was incrementally upregulated in hyperplasias, dysplasias and SCCs. Active MMP-9 was detected at low levels in some hyperplasias and increased in 100% of dysplastic and tumor tissue lysates. In contrast, MMP-2 (latent and active) changed only modestly with progression. With the exception of an ~ 90kDa gelatinase, the majority of gelatinolytic activity in neoplastic lysates was MMP-derived as suggested by its inhibition with 1,10-phelantrolin (1,10 Phe: Fig 5A panel *b*), whereas the gelatinolytic profile was unchanged by incubation of substrate gels with phenylmethylsulfonylfluoride (PMSF; Fig. 5A, panel *c*) or N-ethylmaleimide (NEM; Fig. 5A, panel *d*), serine and cysteine protease inhibitors, respectively.

Premalignant progression in HPV16/MMP-9$^{-/-}$ mice

To determine the functional significance of MMP-9 during epithelial carcinogensis, HPV16 transgenic mice harboring a homozygous disruption in the MMP-9 gene [26] were generated [11]. In contrast to HPV16 and HPV/MMP-9$^{+/-}$ control cohorts, total loss of MMP-9 expression induced a marked delay in development of the characteristic hyperplastic and dysplastic phenotypes. By 2 months of age, 100% of HPV16/MMP-9$^{-/-}$ mice showed a mildly hyperplastic epidermis characterized by keratinocyte expansion (a 2-fold increase in all keratinocyte layers) with retention of complete terminal differentiation capacity, minimal stromal remodeling and inflammatory cell infiltration,

typical of 3-4-week-old HPV16 controls (Table 1). At 4 months, HPV16/MMP-9$^{-/-}$ skin remained largely hyperplastic, whereas HPV16/MMP-9$^{+/-}$ skin had rapidly progressed to characteristic broad dysplastic lesions in 100% of the animals by comparison (data not shown). Dysplastic lesions were evident in 20% of HPV16/MMP-9$^{-/-}$ mice at 4 months and ~90% at 6 months of age (Table 1). In addition, an approximate 50% reduction in SCC incidence was observed in MMP-9-deficient/HPV16 mice (Table 1) [11]. Surprisingly, MMP-9-deficient SCCs represented more poorly differentiated carcinomas compared to characteristic SCCs as determined by keratin expression profiling, thus representing a higher malignant grade of SCC. However, absence of MMP-9 did not affect the incidence or histopathology of sebaceous or follicular neoplasms (Table 1), nor did its absence alter the presence or activation of MMP-2 at any neoplastic stage as measured by gelatin-zymography (Fig. 5B). Taken together, these data indicate that MMP-9 functionally contributes to epithelial carcinogenesis.

MMP-9 accelerates activation of angiogenesis in HPV16 transgenic mice

To define the underlying mechanism by which MMP-9 deficiency attenuates the incidence of SCCs in HPV16 transgenic mice, we assessed the angiogenic and inflammatory responses during neoplastic progression in HPV16/MMP9$^{-/-}$ mice as compared to HPV16/MMP9-proficient controls. Whereas absence of MMP-9 did not result in varied stromal infiltration of CD45 positive leukocytes, mast cells or neutrophils into lesional tissue (Fig. 4F), confocal fluorescent angiography revealed a modestly delayed and diminished angiogenic response in the MMP-9 deficient background (Fig. 3I-K). Vascular architecture in 1-month-old HPV16/MMP9$^{-/-}$ transgenic mice was less

dilated than age-matched HPV16 animals and more resembled the vasculature of the HPV16 negative littermate controls. By six months of age, vessel dilation observed in HPV16/MMP9$^{-/-}$ resembled that of 1-month-old HPV16 mice, suggesting an attenuated angiogenic response, that was confirmed by immunostaining for CD31. The vascular architecture characteristic of angiogenic dysplasias, fully penetrant by 4-5 months in HPV16/MMP-9-proficient mice, was not observed in HPV16/MMP-9$^{-/-}$ tissue until much later (~11-mo of age) where 90% of mice demonstrated dysplastic lesions showing chaotic organization of vascular trees, and close apposition of capillaries to epithelial basement membrane, thus representing a 5-month delay as compared to HPV16 controls (Fig. 3).

MMP-9 has similarly been implicated as an important mediator of angiogenic activation in a model of multi-stage pancreatic islet carcinogenesis (RIP1-Tag2) [27]. In this model, mice develop insulomas by 12–14 weeks of age as a result of SV40 large-T antigen (Tag) expression driven by the rat the insulin promoter. Tumor incidence in RIP1-Tag2 mice in an MMP-9 deficient background is decreased with a similar attenuation of angiogenesis [28]. The delayed activation of the angiogenic switch in RIP-Tag mice is the result of a diminished ability to mobilize VEGF due to lack of MMP-9 [28]. The observation that angiogenesis is delayed but not ablated in a MMP-9 deficient background of the HPV16 and RIP1-Tag2 carcinogenesis models, indicates the acquisition of an alternative yet unidentified compensatory mechanism regulating angiogenesis in these models.

Host-derived MMP-9 regulates epithelial proliferation

In addition to an attenuated vascular response during premalignant progression in MMP-9-deficient/HPV16 transgenic mice, a reduced premalignant epidermal expansion is observed compared to HPV16 controls, suggesting a role for MMP-9 in regulating epithelial proliferation. Premalignant lesions in MMP-9-deficient/HPV16 mice display a reduced keratinocyte cell proliferation index as assessed by the S-phase frequency by immunodetection of bromodeoxyuridine (BrdU) incorporated into proliferating keratinocytes (Table 1). Whereas angiogenesis and development of the vasculature was merely delayed ~5 months by the absence of MMP-9, keratinocytes never fully attain characteristic stage-specific proliferation indices, even when histologically similar tissues were compared (albeit at different ages), *e.g.* hyperplasia versus hyperplasia, dysplasia versus dysplasia, or in similarly graded SCCs. In addition, SCCs that arise in HPV16/MMP-$9^{-/-}$ mice contained fewer proliferating malignant cells (Table 1), and were less differentiated. Despite the propensity toward a higher malignant grade, keratinocyte proliferation within MMP-9-deficient SCCs remained suppressed compared to controls. In addition to reduced proliferation rate, the SCCs in the HPV16/MMP-$9^{-/-}$ mice showed a provocative difference in their pattern of proliferation. Whereas proliferating keratinocytes in SCCs of HPV16 and HPV16/MMP-$9^{+/-}$ mice were found throughout malignant clusters, proliferating keratinocytes in SCCs from MMP-9 deficient/HPV16 transgenic mice were restricted to layers of epithelia in close apposition to stroma. The broader pattern of keratinocyte proliferation was restored in HPV16/MMP-$9^{-/-}$ mice by transplantation of wildtype bone marrow derived cells, but not by transplantation of MMP-9 deficient bone marrow derived cells (Table 1). These data suggest that the availability of poorly diffusible matrix-sequestered mitogenic factor(s) is reduced in the

absence of MMP-9 and that this deficiency likely accounts for the reduced and altered proliferation index and tumor incidence in MMP-9-deficient neoplastic skin. To address whether the altered proliferation index in HPV16/MMP-9$^{-/-}$ skin was the result of a varied apoptotic response resulting from MMP-9 deficiency, the percentage of TUNEL-positive apoptotic cells was assessed in both dysplastic and carcinoma tissues (Table 1). These results suggests that absence of MMP-9 does not significantly alter the incidence of TUNEL-positive apoptotic cells as no significant difference in age-matched HPV16 versus HPV16/MMP9$^{-/-}$ derived tissue was observed (Table 1). The combined implication of these data is that keratinocyte hyperproliferation is not solely controlled by intrinsic mechanisms, *e.g.* E6/E7 oncogene expression, but is also regulated by extrinsic factors emanating from the stroma, under the control of MMP-9.

DISCUSSION

Old players, a different game

Tumor progression has classically been regarded as a multistep process involving initiation, promotion, and malignant conversion – neoplastic events focused on intrinsic mechanisms. However, it is now clear that extrinsic factors present in the local microenvironment are also influential parameters of the tumorigenic program [5,29]. Proteinases, including MMPs, play pivotal roles in altering the local microenvironment during physiologic and pathologic processes [5,7] by not only disrupting extracellular matrix barriers, but also by affecting cellular signaling pathways [25,30]. The ability of MMPs to digest virtually all components of the ECM and the invasion promoting abilities

of MMPs in *in vitro* invasion assays [5] suggested a role for these enzymes in enabling tumor cell invasion into their surrounding tissue. However, study of *de novo* mouse models of multi-stage tumorigenesis, now reveal additional regulatory functions for MMPs during neoplastic progression. Ectopic expression of MMP-3 in the mammary gland enables initial tumor growth whereas its expression is dispensable once a tumor is established, a classic example of a 'hit-and-run' mechanism [31]. In a model for intestinal tumorigenesis, tumor incidence and burden is reduced in the absence of MMP-7 [32], suggesting a role for MMP-7 early in neoplastic evolution. MMP-11, on the other hand, expressed by stromal cells [33], contributes to xenograft growth of colon carcinoma cells *in vivo*, most likely by preventing apoptosis via a yet unidentified mechanism [34]. Whereas MMP-2 expression is generally associated with increased invasion in *in vitro* models and enhanced metastatic capacity of tumor cell lines in nude mice, the invasive capacity of pancreatic tumors was not affected by the absence of MMP-2 [28]. Likewise, MMP-9 does not exert its major activity on invasion [11,28]. The combined implications of these studies is that inhibition of MMP activity may best be directed at early neoplastic disease as opposed to late-stage progression.

Our study of squamous carcinogenesis in the absence of MMP-9 adds to this growing body of literature, and has further revealed new regulatory properties of MMP-9. MMP-9 is selectively involved in squamous carcinogenesis, its primary effects are on angiogenesis and keratinocyte proliferation, while not altering cell signaling pathways regulating cell death (apoptotic) programs. While the reduced tumor incidence resulting from MMP-9-deficiency in HPV16 mice might have been anticipated, the more aggressive phenotype of invasive cancers that managed to develop was unexpected, as

was the clear role of MMP-9 in facilitating tumor cell proliferation. Most surprising of all was the observation that although MMP-9 can be expressed by both epithelial cells and stromal cells, bone marrow-derived cells restore the wild-type phenotype [11]. In line with these observations, depletion of mast cells, a known source of MMP-9 and chymase, which can convert pro-MMP-9 into its active form, attenuates premalignant progression. A pertinent question for the future is the nature of the alternative mechanism(s) regulating angiogenesis, proliferation, and malignancy revealed by the absence of MMP-9, and whether it too is manifested by inflammatory cells. If so, then anti-inflammatory agents should be seriously considered as frontline anti-cancer drugs in squamous cancer, since blocking the conscripted cell type would impact both the MMP-9-dependent mechanisms, as well as the compensatory pathway that together appear critical for carcinogenesis in this mouse model.

ACKNOWLEDGEMENTS

The authors would like to thank Dr. M. Balbin for providing the plasmids encoding mColA, mColB and mouse MMP-8, Lidiya Korets for assistance with animal husbandry, William Huyn and the UCSF Comprehensive Cancer Center Laboratory for Cell Analysis, and Drs, Zena Werb, Douglas Hanahan, Jeffrey Arbeit, Gabriele Bergers, and Matthias Schmuth for insightful comments. This work and LMC were supported by the American Cancer Society, The V foundation for Cancer Research, The Hallman Family, The Edward J. Mallinckrodt Foundation, and the National Institutes of Health, LCLvK was supported by the Dutch Cancer Society.

REFERENCES

1. Hanahan, D. & Weinberg, R.A. The hallmarks of cancer. *Cell* **100**, 57-70 (2000).

2. Bissell, M.J., Hall, H.G. & Parry, G. How does the extracellular matrix direct gene expression? *J Theor Biol* **99**, 31-68 (1982).

3. Radisky, D., Hagios, C. & Bissell, M.J. Tumors are unique organs defined by abnormal signaling and context. *Semin Cancer Biol* **11**, 87-95 (2001).

4. Stamenkovic, I. Matrix metalloproteinases in tumor invasion and metastasis. *Semin Cancer Biol* **10**, 415-433 (2000).

5. Egeblad, M. & Werb, Z. New functions for the matrix metalloproteinases in cancer progression. *Nat Rev Cancer* **2**, 161-174 (2002).

6. Bergers, G. & Coussens, L.M. Extrinsic regulators of epithelial tumor progression: metalloproteinases. *Curr Opin Genet Dev* **10**, 120-127 (2000).

7. Sternlicht, M.D. & Werb, Z. How matrix metalloproteinases regulate cell behavior. *Annu Rev Cell Dev Biol* **17**, 463-516 (2001).

8. Woessner, J.F. & Nagase, H. *Matrix metalloproteinases and TIMPs*, (Oxford University Press, Oxford, UK, 2000).

9. Woessner, J.F., Jr. Matrix metalloproteinase inhibition. From the Jurassic to the third millennium. *Ann.N.Y.Acad.Sci.* **878**, 388-403 (1999).

10. Oh, J. *et al.* Membrane-anchored MMP inhibitor RECK is a key regulator of extracellular matrix integrity and angiogenesis. *Cell* **107**, 789-800. (2001).

11. Coussens, L.M., Tinkle, C.L., Hanahan, D. & Werb, Z. MMP-9 supplied by bone marrow-derived cells contributes to skin carcinogenesis. *Cell* **103**, 481-490 (2000).

12. Coussens, L.M. *et al.* Inflammatory mast cells up-regulate angiogenesis during squamous epithelial carcinogenesis. *Genes Dev* **13**, 1382-1397 (1999).

13. Thurston, G., Baluk, P., Hirata, A. & McDonald, D.M. Permeability-related changes revealed at endothelial cell borders in inflamed venules by lectin binding. *Am J Physiol* **271**, 2547-2562 (1996).

14. Balbin, M. *et al.* Identification and enzymatic characterization of two diverging murine counterparts of human interstitial collagenase (MMP-1) expressed at sites of embryo implantation. *J Biol Chem* **276**, 10253-10262 (2001).

15. Taylor, G., Lehrer, M.S., Jensen, P.J., Sun, T.T. & Lavker, R.M. Involvement of follicular stem cells in forming not only the follicle but also the epidermis. *Cell* **102**, 451-461 (2000).

16. Lavker, R.M. & Sun, T.T. Epidermal stem cells: properties, markers, and location. *Proc Natl Acad Sci U S A* **97**, 13473-13475 (2000).

17. Merrill, B.J., Gat, U., DasGupta, R. & Fuchs, E. Tcf3 and Lef1 regulate lineage differentiation of multipotent stem cells in skin. *Genes Dev* **15**, 1688-1705. (2001).

18. Coussens, L.M., Hanahan, D. & Arbeit, J. Genetic predisposition and parameters of malignant progression in K14-HPV16 transgenic mice. *Am J Path* **149**, 1899-1917 (1996).

19. Smith-McCune, K., Zhu, Y.-H., Hanahan, D. & Arbeit, J. Angiogenesis and VEGF mRNA upregulation in progressive squamous carcinogenesis: Cross-species comparison of human cervix and K14-HPV16 transgenic mice. *Cancer Research* **57**, 1294-1300 (1997).

20. Arbeit, J.M., Olson, D.C. & Hanahan, D. Upregulation of fibroblast growth factors and their receptors during multi-stage epidermal carcinogenesis in K14-HPV16 transgenic mice. *Oncogene* **13**, 1847-1857 (1996).

21. Ribatti, D. *et al.* The role of mast cells in tumour angiogenesis. *Br J Haematol* **115**, 514-521 (2001).

22. Friedl, A., Chang, Z., Tierney, A. & Rapraeger, A.C. Differential binding of fibroblast growth factor-2 and -7 to basement membrane heparan sulfate: comparison of normal and abnormal human tissues. *Am J Pathol* **150**, 1443-1455. (1997).

23. Fang, K.C., Raymond, W.W., Blount, J.L. & Caughey, G.H. Dog mast cell alpha-chymase activates progelatinase B by cleaving the Phe88-Gln89 and Phe91-Glu92 bonds of the catalytic domain. *J Biol Chem* **272**, 25628-25635. (1997).

24. Cairns, J.A. & Walls, A.F. Mast cell tryptase stimulates the synthesis of type I collagen in human lung fibroblasts. *J Clin Invest* **99**, 1313-1321 (1997).

25. Lukashev, M.E. & Werb, Z. ECM signalling: orchestrating cell behaviour and misbehaviour. *Trends Cell Biol* **8**, 437-441. (1998).

26. Vu, T.H. *et al.* MMP-9/gelatinase B is a key regulator of growth plate angiogenesis and apoptosis of hypertrophic chondrocytes. *Cell* **93**, 411-422 (1998).

27. Hanahan, D. Heritable formation of pancreatic ß-cell tumors in transgenic mice harboring recombinant insulin/simian virus 40 oncogenes. *Nature* **315**, 115-122 (1985).

28. Bergers, G. *et al.* Matrix metalloproteinase-9 triggers the angiogenic switch during carcinogenesis. *Nat Cell Biol* **2**, 737-744 (2000).

29. Tlsty, T.D. & Hein, P.W. Know thy neighbor: stromal cells can contribute oncogenic signals. *Curr Opin Genet Dev* **11**, 54-59 (2001).

30. Werb, Z. ECM and cell surface proteolysis: regulating cellular ecology. *Cell* **91**, 439-442. (1997).

31. Sternlicht, M.D. *et al.* The stromal proteinase MMP3/stromelysin-1 promotes mammary carcinogenesis. *Cell* **98**, 137-146 (1999).

32. Wilson, C.L., Heppner, K.J., Labosky, P.A., Hogan, B.L. & Matrisian, L.M. Intestinal tumorigenesis is suppressed in mice lacking the metalloproteinase matrilysin. *Proc Natl Acad Sci U S A* **94**, 1402-1407. (1997).

33. Masson, R. *et al.* In vivo evidence that the stromelysin-3 metalloproteinase contributes in a paracrine manner to epithelial cell malignancy. *Journal of Cell Biology* **140**, 1535-1541 (1998).

34. Boulay, A. *et al.* High cancer cell death in syngeneic tumors developed in host mice deficient for the stromelysin-3 matrix metalloproteinase. *Cancer Res* **61**, 2189-2193 (2001).

FIGURE LEGENDS

Figure 1. Spectrum of neoplastic lesions developing in HPV16 transgenic mice.

(A) Schematic representation of skin including hair follicle, sebaceous gland and epidermis. (B) Neoplastic lesions that develop in HPV16 transgenic mice. (C) Incidence of neoplastic lesions in K14-HPV16 mice (n = 292; FVB/n N25-28).

Figure 2. Characteristic histopathology of neoplastic lesions in K14-HPV16 transgenic mice.

Hematoxylin and Eosin (H & E; panels A-E, G-J, L-N) staining and keratin immunoreactivity (panels F, K, O, P) of paraffin-embedded tissue sections reveals histopathologic differences between control (HPV16-negative) littermate ear skin (A) with that of HPV16 transgenic mice (B-P). (A) normal ear skin, (B) hyperplastic ear skin, (C) dysplastic ear skin, (D) truncal papiloma and (E) squamous cell carcinoma, grade I (SCCI). (F) High magnification view of the boxed area shown in panel E, from an adjacent tissue section where immunoreactivity of keratin filaments (brown staining) reveals characteristic keratin pearls (asterisk, *) and clustering of malignant keratinocytes residing in the dermis. (G) SCC Grade III showing characteristic anaplastic cells residing in malignant clusters of keratinocytes with notable mitotic figures (arrowheads), and (H) axillary lymph node from the animal in panel G showing metastatic keratinocytes (e) residing adjacent to resident lymphocytes (l). (I-K) A low incidence of neoplasms is also observed in sebaceous glands of HPV16 mice. In sebaceous hyperplasias (I), the enlarged well-differentiated gland is composed of numerous lobules (asterisk, *), whereas

in sebaceous adenomas (J) the enlarged incompletely differentiated and irregular gland containing sebaceous lobules consists of mature sebaceous cells. The boxed area in panel J is shown in panel K at higher magnification where immunodetection of keratin filaments on an adjacent tissue section reveals an expanded population of basal keratinocytes (brown staining) differentiating into sebocytes with prominent nuclei (asterisks). The spectrum of follicular infundibullar neoplasms observed in HPV16 transgenic mice include characteristic trichofolliculomas (L) displaying a large cyst with a central pore (asterisk, *) continuous with the epidermis. These hyperproliferative lesions progress into trichoadenoma (M) composed of discontinuous large cysts (asterisk, *). Benign lesions further progress into malignant microcystic adnexel carcinomas (MAC, panel N). These carcinomas are distinct from trichoadenomas, and from SCCs, in that they demonstrate invasive growth of keratin-positive cells (brown staining) emanating from cystic structures proliferating in the dermis (O). The boxed area in panel O is shown at higher magnification in panel P. This view illustrates the invasive nature of MACs (brown stained cells; arrows) where malignant keratinocytes invade tissue as solitary cells or small nests of cells, a characteristic difference from that observed with SCCs. e, epidermal keratinocytes; d, dermis; l, lymphocytes, f, hair follicle; sg, sebaceous gland. Bar: 50 μm (A-E, I, J, L-O); 100 μm (F-H, K, P)

Figure 3. Vascular architecture in HPV16 transgenic mice.

Immunolocalization of CD31/PECAM-1 (A-D; red staining) reveals a modest increase in the density and dilation of capillaries in hyperplastic lesions (B) as compared to wildtype skin (A). Dysplastic lesions display dilated and enlarged capillaries in close proximity to

the dermal-epidermal interface (C). SCCs are highly vascularized containing a combination of small and dilated vessels (D). Fluorescent angiography (E-K; green) reveals increased dilation and branching during malignant progression from normal (E) to development of hyperplastic (F) and dysplastic (G) lesions. SCCs (H) display a tortuous and dense vascular architecture. By comparison, the vascular response in MMP-9-deficient/HPV16 mice (I-K) is modestly attenuated in age-matched animals. Vascular architecture in 1-month-old HPV16/MMP9$^{-/-}$ transgenic mice (J) is less dilated than age-matched HPV16 animals (F). By six months of age, vessel dilation observed in HPV16/MMP9$^{-/-}$ (K) resembled that of 1-month-old HPV16 animals (F). e, epidermal keratinocytes; d, dermis. Bar (A): 100 μm (A-D); Bar (E) 200 μm (E-K).

Figure 4. Inflammatory cell infiltration in HPV16 transgenic skin.

Immunodetection of CD45-positive leukocytes (brown staining) in paraffin-embedded sections of staged neoplastic tissue (A-E) reveals incremental increases in the number of CD45-positive leukocytes in the successive neoplastic stages (A: negative littermate control tissue [wt, wildtype]; B: hyperplasia; C: dysplasia; D, center of SCCII; E, invasive edge of an SCCII). F. Profile analysis on paraffin-embedded tissue sections revealed presence of mast cells (red bars) and neutrophils (blue bars) in successive neoplastic stages (1-month and 6-month of age, and in SCCs in K14-HPV16, MMP9$^{-/-}$ and K14-HPV16/MMP9$^{-/-}$ mice. Few mast cells are detected in frank carcinomas and neutrophils were not detected in "normal" skin. Absence of MMP-9 during neoplastic progression in HPV16 mice neither alters the abundance or location of CD45-positive leukocytes (data not shown), nor does its absence alter the profile of mast cells or

neutrophils in neoplastic tissues. Data shown represent the mean (± SEM) from 5 animals per time point, where cell populations were determined in five 40X fields per mouse. e, epidermal keratinocytes; d, dermis; dashed line, invasive edge of SCC with arrow indicating direction of invasion. Bar: 100 μm (A-E)

Figure 5. Gelatinolytic activity during neoplastic progression in HPV16 mice.

Tissue extracts of staged biopsies of neoplastic tissue were analyzed for gelatinolytic activity by gelatin substrate zymography. (A) Low proMMP-9 activity was detected in HPV16-negative littermates (-LM), whereas in neoplastic tissues, proMMP-9 activity is detected in all stages of tumor progression (hyp., hyperplasia; dys., dysplasia). Active MMP-9 is observed in dysplasias and SCCII only. No significant changes in latent proMMP-2 expression was detected in premalignant tissue of transgenic mice as compared to that of HPV16-negative littermates. Increased presence of active MMP-2 was only observed in SCCs. The gelatinolytic activity in tissue lysates, with the exception of a 90kDa protein (*), was inhibited by 1,10-phenanthroline (1,10 Phe; panel b), but not by inhibition of serine and cysteine proteinease with phenylmethylsulfonylfluoride (PMSF; panel c) or N-ethylmaleimide (NEM; panel d), respectively. (B) Absence of MMP9 in K14-HPV16/MMP9 deficient neoplastic tissues is without apparent consequence regarding the presence or activation status of MMP-2.

Figure 1,

A

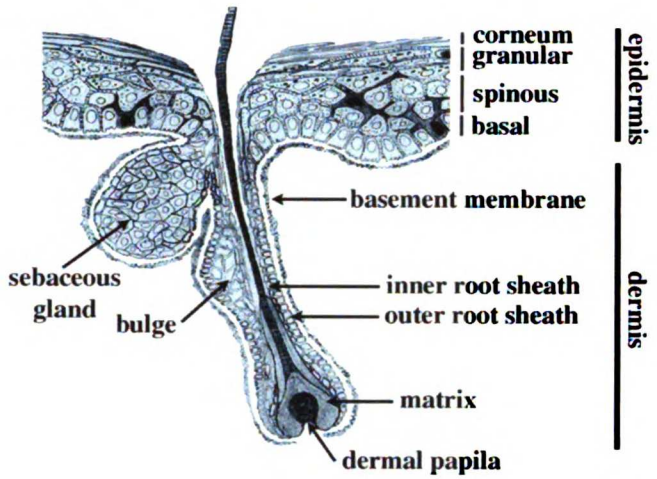
corneum
granular
spinous
basal
epidermis
basement membrane
sebaceous gland
bulge
inner root sheath
outer root sheath
dermis
matrix
dermal papila

B

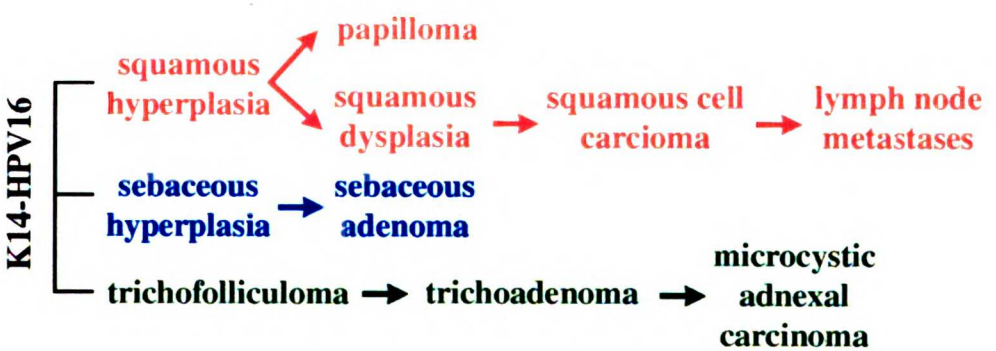
K14-HPV16
squamous hyperplasia
papilloma
squamous dysplasia
squamous cell carcioma
lymph node metastases
sebaceous hyperplasia
sebaceous adenoma
trichofolliculoma
trichoadenoma
microcystic adnexal carcinoma

C

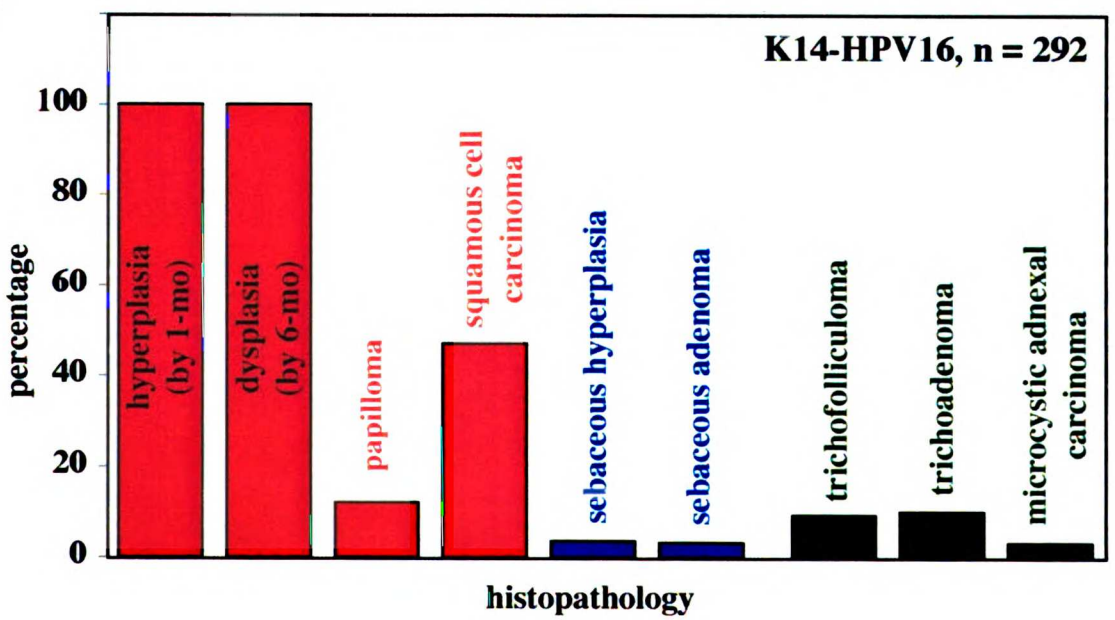
K14-HPV16, n = 292
percentage
100
80
60
40
20
0
hyperplasia (by 1-mo)
dysplasia (by 6-mo)
papilloma
squamous cell carcinoma
sebaceous hyperplasia
sebaceous adenoma
trichofolliculoma
trichoadenoma
microcystic adnexal carcinoma
histopathology

Figure 2

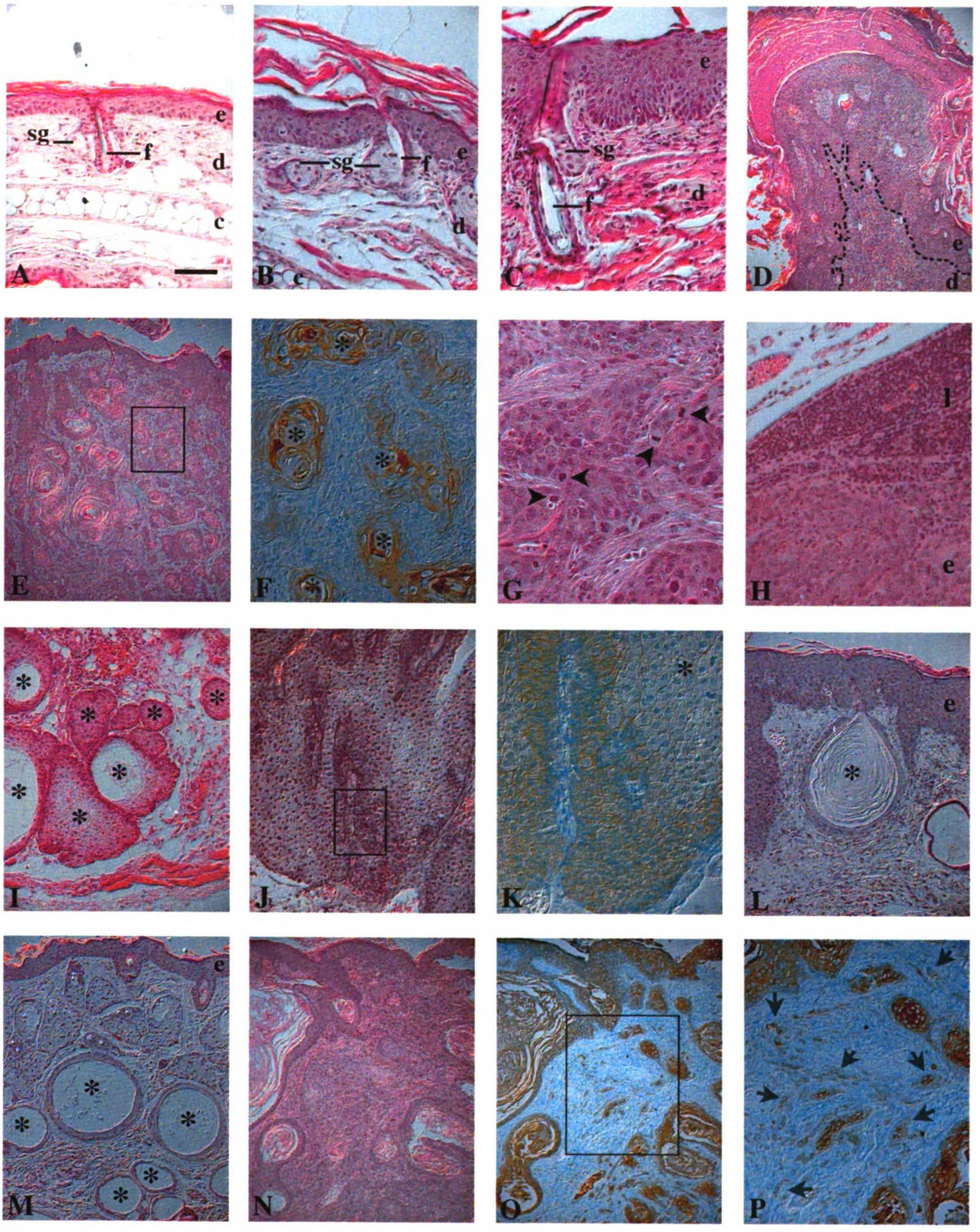

Figure 3

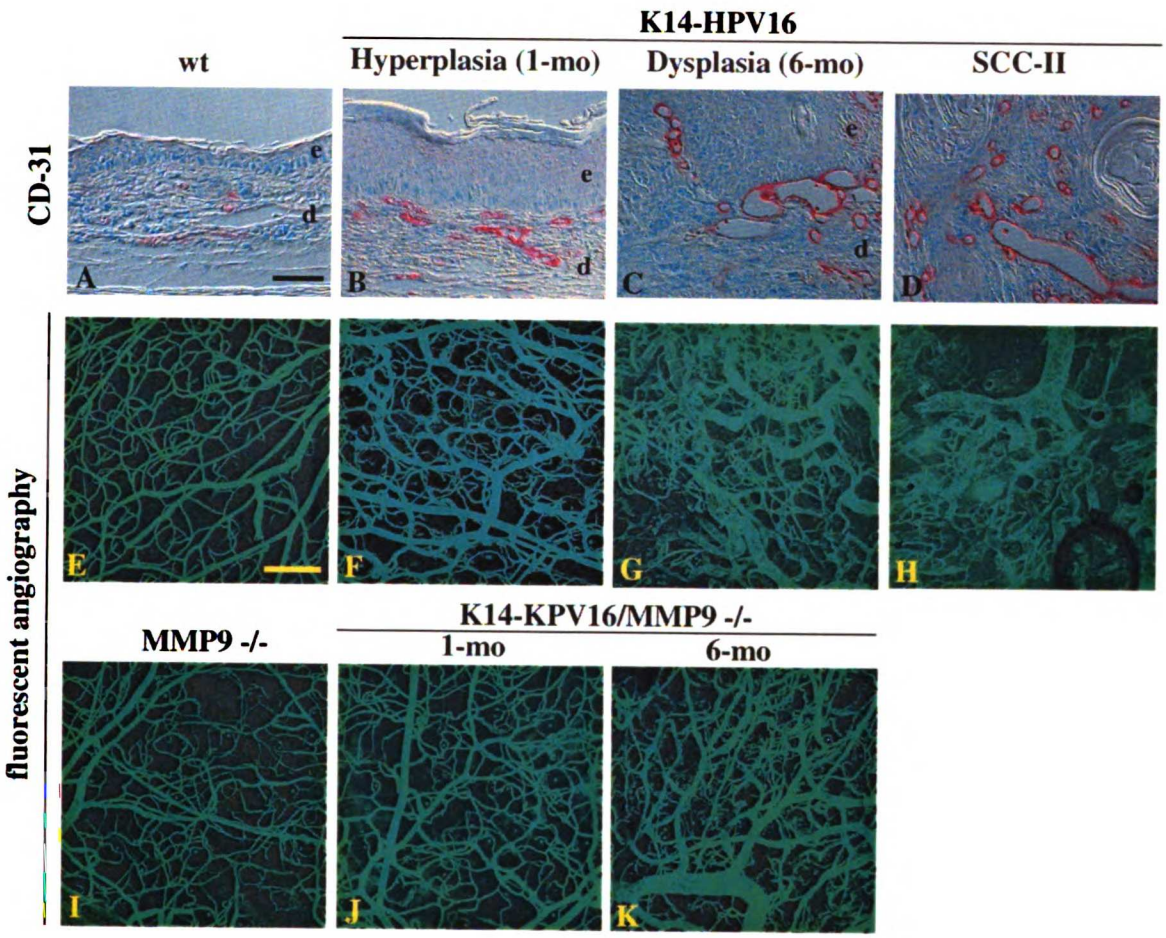
K14-HPV16
wt
Hyperplasia (1-mo)
Dysplasia (6-mo)
SCC-II
CD-31
e
d
A
B
C
D
fluorescent angiography
E
F
G
H
MMP9 -/-
K14-KPV16/MMP9 -/-
1-mo
6-mo
I
J
K

Figure 4

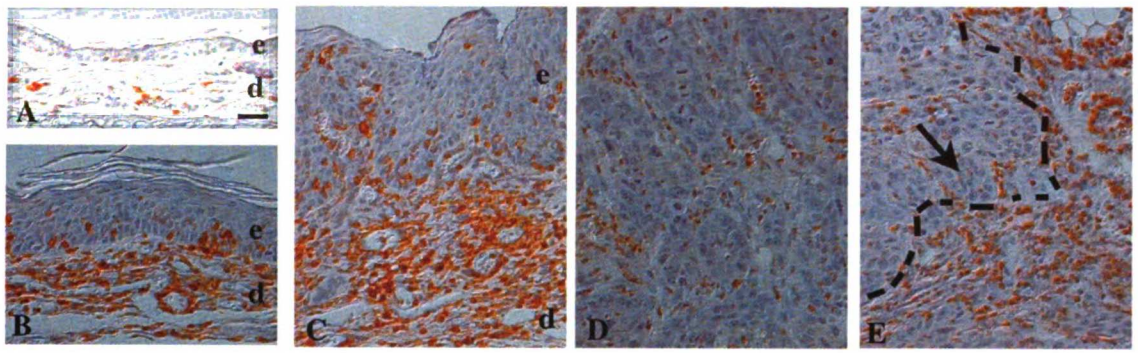
A
B
C
D
E
e
d

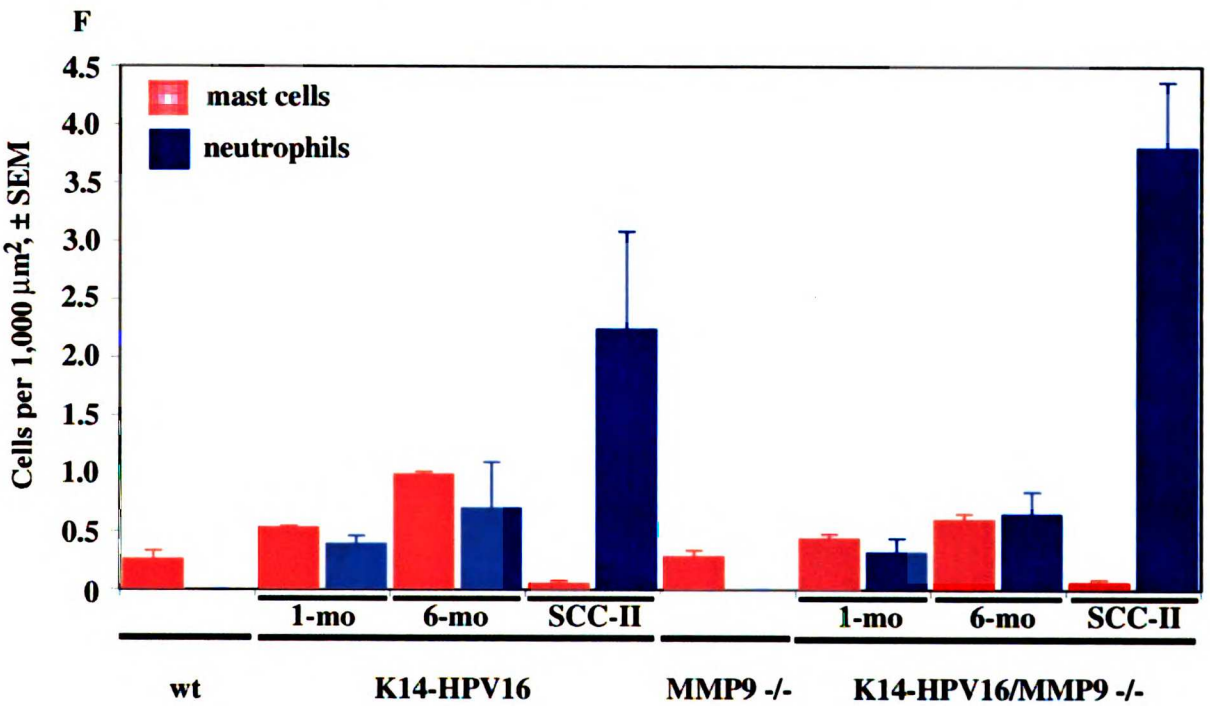
F
mast cells
neutrophils
Cells per 1,000 μm², ± SEM
4.5
4.0
3.5
3.0
2.5
2.0
1.5
1.0
0.5
0
1-mo
6-mo
SCC-II
1-mo
6-mo
SCC-II
wt
K14-HPV16
MMP9 -/-
K14-HPV16/MMP9 -/-

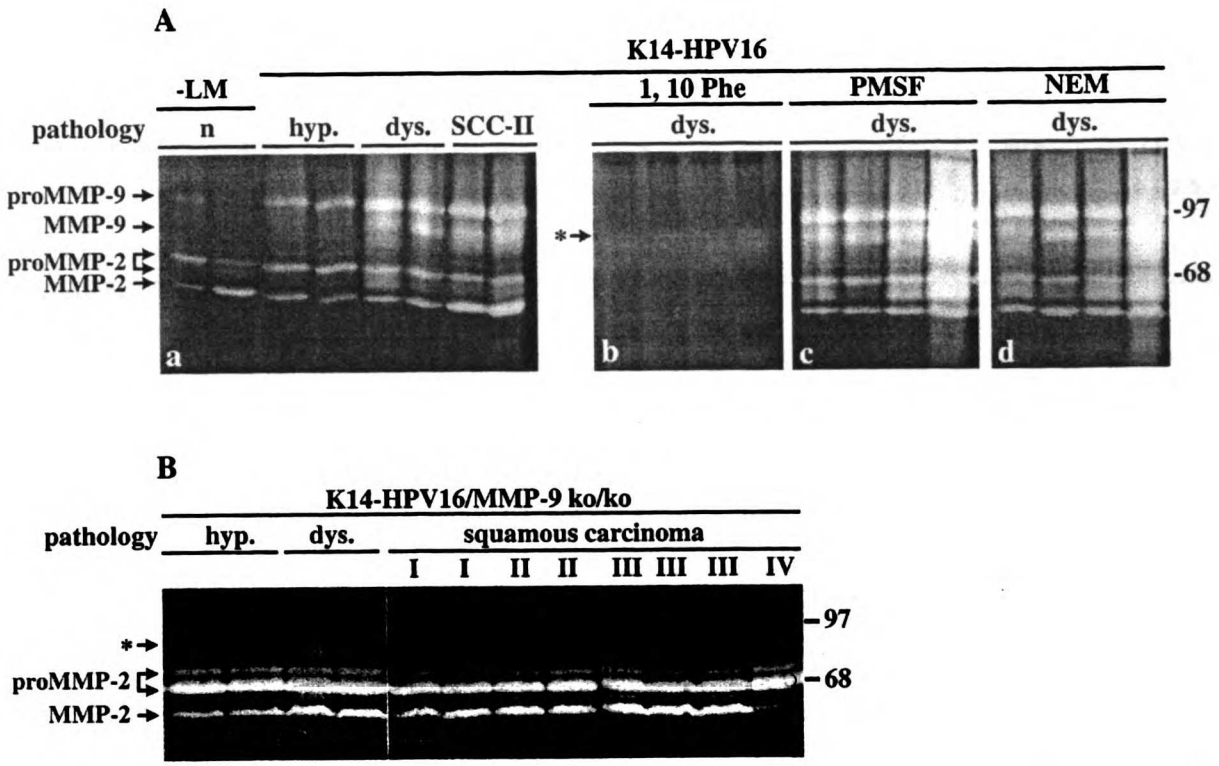
A
K14-HPV16
-LM
1, 10 Phe
PMSF
NEM
pathology
n
hyp.
dys.
SCC-II
dys.
dys.
dys.
proMMP-9
MMP-9
proMMP-2
MMP-2
*
-97
-68
a
b
c
d
B
K14-HPV16/MMP-9 ko/ko
pathology
hyp.
dys.
squamous carcinoma
I I II II III III III IV
*
proMMP-2
MMP-2
97
68

Table 1. Summary of Characteristic Differences in K14-HPV16 vs. K14-HPV16/MMP9-deficient mice.

	HPV16/MMP9$^{+/+}$ n = 292			HPV16/MMP9$^{-/-}$ n = 137			HPV16/MMP9$^{-/-}$, BMT +/+[d], n= 10	
HISTOLOGIC STAGE	Incidence[a] (%)	Prolif. Index[b] (mean±SEM)	Apop. Index[c] (mean ±SEM)	Incidence[e] (%)	Prolif. Index[b] (mean±SEM)	Apop. Index[c] (mean ±SEM)	Incidence[a] (%)	Prolif. Index[b] (mean±SEM)
EPIDERMIS:								
hyperplasia	100 (by 1-mo)	19.73 ± 0.11	(-)	100 (by 2-mo)	10.13 ± 3.69[h]	(-)	(-)	(-)
dysplasia (by 6-mo.)	100	20.6 ± 5.11	1.74 ± 0.80	90.0	13.83 ± 1.99[i]	2.00 ± 0.61[k]	100	21.2 ± 2.02
SCC (lifetime)	47.0[f]			27.0[f]			50.0[g]	
SCC-I	43.6	(-)	(-)	21.5	(-)	(-)	60.0	(-)
SCC-II	39.2	26.3 ± 3.3	1.70 ± 0.60	42.8	16.4 ± 2.4[j]	1.64 ± 0.01[l]	40.0	25.4 ± 2.6
SCC-III	14.9	(-)	(-)	28.5	(-)	(-)	0	
SCC-IV	2.2	(-)	(-)	7.1	(-)	(-)	0	
SEBACEOUS:								
Seb. hyperplasia	3.5	(-)	(-)	2.1	(-)	(-)	0	
Seb. adenoma	3.4	(-)	(-)	1.5	(-)	(-)	0	
FOLLICULAR:								
Tricho-folliculoma	9.2	(-)	(-)	7.2	(-)	(-)	0	
trichoadenoma	10.0	(-)	(-)	2.2	(-)	(-)	0	
MAC	3.1	(-)	(-)	0			0	

(-), data point not determined

a, incidence determined as a percentage of animals reflecting characteristic pathology

b, percentage of bromodeoxyuridine-positive (BrdU) keratinocytes

c, percentage of TUNEL-positive keratinocytes

d, see Materials and Methods section for details of bone marrow transplantation

e, 292 K14-HPV mice in cohort, 137 mice with SCCs, 181 SCCs total in cohort

f, 137 K14-HPV16/MMP9$^{-/-}$ mice in cohort, 37 mice with SCCs, 42 SCCs total in cohort; p = 0.0001 (Wilcoxan score for variable grade)

g, 10 K14-HPV16/MMP9$^{-/-}$, +/+BMT mice in cohort, 5 mice with SCC, 5 SCCs total

h, p = 0.11 (unpaired, nonparametric Mann-Whitney)

i, p = 0.03 (unpaired, nonparametric Mann-Whitney)

j, p = 0.06 (unpaired, nonparametric Mann-Whitney)

k, p = 0.66 (student's T test)

l, p = 0.96 (student's T test)

SCC, squamous cell carcinoma, MAC, microcystic adnexal carcinoma, prolif., proliferation, apop., apoptosis

2. MMP mRNA Expression in K14-HPV16 Neoplastic Skin

Table 2. MMP mRNA expression in K14-HPV16 neoplastic skin.

matrix metalloproteinase	normal	K14-HPV16		
		hyperplastic	dysplastic	carcinoma
MColA	-	-	-	-
MColB	-	-	-	-
MMP-2/gelatinase A	-	+	+	+
MMP-3/stromelysin-1	-	+	+	+
MMP-7/matrilysin	-	-	-	+/-
MMP-8/collagenase-2	-	-	+	+
MMP-9/gelatinase B	-	+	+	+
MMP-10/stromelysin-2	-	-	+	+
MMP-11/stromelysin-3	-	+	+	+
MMP-12/metalloelastase	-	+/-	+	+
MMP-13/collagenase-3	-	-	-	+
MMP-14/MT1-MMP	+	+	+	+
MMP-15/MT2-MMP	+	+	+	+
MMP-16/MT3-MMP	-	-	+	+
MMP-17/MT4-MMP	+	+	+	+
MMP-19/RASI-1	-	-	+	+/-
MMP-26/matrilysin-2	nd	nd	nd	nd
MMP-28/epilysin	nd	nd	nd	nd

(-), no detectable mRNA expression
(+), mRNA expression detected by either RT-PCR, TAQ-MAN, or in situ hybridization analysis
(+/-), mRNA expression found in some, but not all, representative tissues
nd, not done

Concluding Remarks and Future Directions

Concluding Remarks

As endogenous inhibitors of MMPs, the TIMPs have been studied extensively with the intent of identifying possible therapeutic applications in the treatment of cancer, as reviewed in Chapter 1. Initial optimism for therapeutic utility, however, was undermined by technical difficulties involving the manufacturing of sufficient quantities of recombinant TIMP protein [1] and the administration of high levels required for therapeutic effect [2]. Nevertheless, recent advances in the development of viral vectors for gene therapy, that bypass problems with synthesis and delivery of recombinant protein, have renewed interest in the possibility of using TIMPs in the treatment of cancer [3,4]. In this context of the possible therapeutic applications against cancer, the implications of our studies described here would argue against the use of TIMPs, specifically TIMP-1, given our findings regarding (1) the timing of MMP inhibition and (2) the potential for pro-cancer effects exerted by TIMP-1.

The timing of MMP inhibition during neoplastic progression represents a critical variable for carcinogenesis, as revealed by our studies in the K14-HPV16 model, as well as those of Bergers and colleagues [5]. The contribution of MMP activity has been substantiated by the studies of MMP-9 deficient mice: HPV16 mice lacking MMP-9 throughout neoplastic progression exhibited a reduced incidence of carcinomas [6] (Chapter 5). Inhibition of MMP solely during the carcinoma stage, however, failed to reduce the number of carcinomas in the HPV16 mice bearing the human TIMP-1 transgene (Chapter 3), suggesting that MMP inhibition during the earlier, premalignant stages is necessary to exert a negative effect on tumorigenesis. This hypothesis has been born out by the work of Bergers and colleagues, who reported that treatment of

established pancreatic islet carcinomas with batimastat failed to cause regression of malignant tumors, whereas treatment of precursor hyperplastic lesions reduced their progression into more advanced angiogenic dysplasias [5]. Furthermore, results from human clinical trials, in which treatment with synthetic MMP inhibitors generally failed to show efficacy in patients with late-stage disease, have reinforced the conclusion that the timing of MMP inhibition is a critical variable for therapy against cancer [1,7,8] (Chapter 1). In combination, these studies suggest that targeting inhibition of MMP activity during the later stages of carcinogenesis will be of limited therapeutic utility.

In the case of TIMP-1, therapeutic applications targeting MMP inhibition may actually have the opposite effect from what is intended for cancer treatment, given the pro-cancer effects observed from transgenic TIMP-1 expression in the HPV16 mice (HPV16/βA-hT1$^+$; Chapter 3). Not only did transgenic TIMP-1 expression fail to attenuate neoplastic progression in these HPV16/βA-hT1$^+$ mice, it instead led to an increase in the incidence of carcinomas, possibly due to mitogenic effects of TIMP-1 on initiated epidermal keratinocytes. Other studies have revealed the ability of TIMP-1 to induce proliferation on a wide range of cells *in vitro* [9-12], including cultures of hyperproliferative psoriatic keratinocytes [13]. The finding of elevated proliferation in the premalignant keratinocytes of the HPV16/βA-hT1$^+$ mice verifies this mitogenic function for TIMP-1 *in vivo* (Chapter 3). How this induction of proliferation is translated into an increased incidence of carcinomas may potentially be explained by the observation of accelerated aneuploidy in the premalignant skin of HPV16/βA-hT1$^+$ mice, as a possible intermediary mechanism by which TIMP-1 can exert pro-cancer effects (Chapter 3).

In light of these findings demonstrating how TIMP-1 can contribute to carcinogenesis via non-MMP-inhibitory mechanisms, a more appealing candidate for a therapeutic factor is an MMP inhibitor that lacks any mitogenic or other potentially-deleterious effects besides activity against MMPs. One possible candidate that has been identified is RECK (reviewed in Chapter 2)—an endogenous inhibitor that appears to negatively regulate MMPs at the levels of transcription, post-translational activation, and substrate proteolysis. RECK has been shown to have efficacy in inhibiting MMPs *in vivo* and in regulating the process of angiogenesis, which may make it an efficacious treatment against cancer if administered at the appropriate stage of neoplastic progression.

Future Directions

The studies described here reveal additional questions, especially addressing the role of TIMP-1 in contributing to carcinogenesis, that can potentially pursued as future directions.

First, is there a receptor for TIMP-1 that mediates the observed induction of hyperproliferation? As discussed previously, a 32 kDa receptor for TIMP-1 has been found on erythroid cells [10], and some cell-surface binding has been hypothesized as the initial, prerequisite step in translocation to the nuclei of mammary carcinoma cells in S-phase [14]. To date, however, no further identification or characterization has been reported. One possible approach to identifying candidate receptors can be derived from the observation that the N-terminal domains of TIMPs are homologous to the netrins [15], which are a family of signalling molecules involved in axonal guidance [16]. Interestingly, receptors for netrins are widely distributed within the body and include *d*eleted-in-*c*olon-

carcinoma (DCC) [17]—a putative tumor suppressor which has been found in many of the same tissues that are receptive to TIMP-1-induced proliferation, including mammary and skin epithelium [18]. Based upon these homologies, screening approaches for candidate receptors may be able to identify possible cell-surface receptors mediating the proliferative effects of TIMP-1 in the HPV16 mice.

Second, is the ability of TIMP-1 to accelerate aneuploidy independent of its MMP-inhibitory activity? Our studies strongly suggest that the acceleration of chromosomal changes—which represents a novel function revealed in our studies for TIMP-1 *in vivo*—is a consequence of the induction of proliferation and not of the inhibition of MMPs (Chapter 3). Previously, Chelser and colleagues have identified single-amino-acid mutants of TIMP-1 that have lost MMP inhibitory activity but have retained the ability to induce proliferation [19]. Incorporation of these mutations in the context of K14-HPV16 carcinogenesis could determine if transgenically-expressed TIMP-1 requires MMP inhibitory activity in order to induce hyperproliferation and to mediate the observed acceleration of aneuploidy. The prediction would be that both hyperproliferative induction and aneuploidy acceleration would be preserved in these HPV16 mice with mutant TIMP-1 transgenic expression—an outcome which would verify that hyperproliferation mediates and is sufficient for promoting the appearance of chromosomal aberrations.

Thus, in conclusion, the studies described here provide further evidence that contrary to initial characterizations as an endogenous inhibitor of MMPs, TIMP-1 can actually be sufficient for positive modulation of epithelial carcinogenesis.

REFERENCES

1. Whittaker, M., Floyd, C.D., Brown, P. & Gearing, A.J. Design and therapeutic application of matrix metalloproteinase inhibitors. *Chem Rev* **99**, 2735-2776 (1999).

2. Blavier, L., Henriet, P., Imren, S. & Declerck, Y.A. Tissue inhibitors of matrix metalloproteinases in cancer. *Ann.N.Y.Acad.Sci.* **878**, 108-119 (1999).

3. Baker, A.H., Ahonen, M. & Kahari, V.M. Potential applications of tissue inhibitor of metalloproteinase (TIMP) overexpression for cancer gene therapy. *Adv Exp Med Biol* **465**, 469-483 (2000).

4. Fassina, G. *et al.* Tissue inhibitors of metalloproteases: regulation and biological activities. *Clin Exp Metastasis* **18**, 111-120 (2000).

5. Bergers, G., Javaherian, K., Lo, K.M., Folkman, J. & Hanahan, D. Effects of angiogenesis inhibitors on multistage carcinogenesis in mice. *Science* **284**, 808-812 (1999).

6. Coussens, L.M., Tinkle, C.L., Hanahan, D. & Werb, Z. MMP-9 supplied by bone marrow-derived cells contributes to skin carcinogenesis. *Cell* **103**, 481-490 (2000).

7. Hidalgo, M. & Eckhardt, S.G. Development of matrix metalloproteinase inhibitors in cancer therapy. *J Natl Cancer Inst* **93**, 178-193 (2001).

8. Coussens, L.M., B. Fingleton, B. & Matrisian, L.M. Matrix metalloproteinase inhibitors and cancer: trials and tribulations. *Science* **295**, 2387-2392 (2002).

9. Docherty, A.J. *et al.* Sequence of human tissue inhibitor of metalloproteinases and its identity to erythroid-potentiating activity. *Nature* **318**, 66-69. (1985).

10. Avalos, B.R. *et al.* K562 cells produce and respond to human erythroid-potentiating activity. *Blood* **71**, 1720-1725 (1988).

11. Bertaux, B., Hornebeck, W., Eisen, A.Z. & Dubertret, L. Growth stimulation of human keratinocytes by tissue inhibitor of metalloproteinases. *J Invest Dermatol* **97**, 679-685 (1991).

12. Hayakawa, T., Yamashita, K., Tanzawa, K., Uchijima, E. & Iwata, K. Growth-promoting activity of tissue inhibitor of metalloproteinases-1 (TIMP-1) for a wide range of cells. A possible new growth factor in serum. *FEBS Lett* **298**, 29-32. (1992).

13. Buisson-Legendre, N., Emonard, H., Bernard, P. & Hornebeck, W. Relationship between cell-associated matrix metalloproteinase 9 and psoriatic keratinocyte growth. *J Invest Dermatol* **115**, 213-218 (2000).

14. Ritter, L.M., Garfield, S.H. & Thorgeirsson, U.P. Tissue inhibitor of metalloproteinases-1 (TIMP-1) binds to the cell surface and translocates to the nucleus of human MCF-7 breast carcinoma cells. *Biochem Biophys Res Commun* **257**, 494-499. (1999).

15. Banyai, L. & Patthy, L. The NTR module: domains of netrins, secreted frizzled related proteins, and type I procollagen C-proteinase enhancer protein are homologous with tissue inhibitors of metalloproteases. *Protein Sci* **8**, 1636-1642 (1999).

16. Oster, S.F. & Sretavan, D.W. Connecting the eye to the brain: the molecular basis of ganglion cell axon guidance. *Br J Ophthalmol* **87**, 639-645. (2003).

17. Livesey, F.J. Netrins and netrin receptors. *Cell Mol Life Sci* **56**, 62-68. (1999).

18. Hsu, Y.H., Shaw, C.K. & Chuong, C.M. Immunohistochemical localization of deleted-in-colon-cancer (DCC) protein in human epithelial, neural, and neuro-endocrine tissues in paraffin sections with antigen retrieval. *Kaohsiung J Med Sci* **17**, 351-357. (2001).

19. Chesler, L., Golde, D.W., Bersch, N. & Johnson, M.D. Metalloproteinase inhibition and erythroid potentiation are independent activities of tissue inhibitor of metalloproteinases-1. *Blood* **86**, 4506-45015 (1995).